Strongly coupled plasmas: high-density classical plasmas and degenerate electron liquids

Setsuo Ichimaru

Department of Physics, University of Tokyo, Bunkyo-ku, Tokyo 113, Japan

Classical and degenerate, strongly coupled plasmas are approached by computer simulations, analytic theories, and variational methods. Thermodynamic properties predicted in those various approaches are compared and examined; possibilities of Wigner crystallization and other instabilities are investigated. Salient features in the static and dynamic correlations are reviewed. Screening effects are analyzed and applied to calculations of the enhancement factor of the thermonuclear reaction rate and the electric resistivity in dense plasmas. Theoretical predictions on the dynamic properties are compared with the x ray and electron scattering data for the metallic electrons.

CONTENTS

I. INTRODUCTION

A. What is a strongly coupled plasma?

The plasma is a statistical system of mobile charged particles. The charged particles interact with each other via the electromagnetic forces. To answer what a strongly coupled plasma is, we might as well begin with a specification of the strong-coupling concept in the plasma.

For simplicity, we consider a spatially homogeneous *one-component plasma* (OCP). It is a system consisting of a single species of charged particles embedded in a uniform background of neutralizing charges. Such an OCP is a substantially idealized model for real plasmas; some plasmas in nature, as we shall see, do indeed satisfy the conditions for such idealization.

Let us define the coupling constant of the plasma as the ratio of the average Coulomb energy to the average kinetic energy. One is thus concerned with the strength of coupling due to the Coulomb interaction. Those plasmas with values of the coupling constant greater than unity may be called the *strongly coupled plasmas.*

For a system of charged particles obeying the classical statistics, the kinetic energy per particle may be estimated approximately as $k_B T$, the temperature T in energy units (k_B is the Boltzmann constant). For a degenerate electron system with the number density n, one instead uses the Fermi energy,

$$E_F = \frac{\hbar^2}{2m}(3\pi^2 n)^{2/3} , \tag{1.1}$$

where m is the mass of an electron.

The Coulomb energy per particle of an OCP containing N particles with electric charge Ze in a volume V may also be estimated as $(Ze)^2/a$, where

$$a=(3V/4\pi N)^{1/3} \tag{1.2}$$

is the radius of a sphere with the characteristic volume V/N; this radius is usually referred to as the *ion-sphere radius* or the *Wigner-Seitz radius.*

For the system of degenerate electrons the coupling constant may be calculated as

$$\frac{e^2/a}{E_F}=0.543r_s\ , \tag{1.3}$$

where

$$r_s=\left[\frac{3}{4\pi n}\right]^{1/3}\frac{me^2}{\hbar^2} \tag{1.4}$$

is the Wigner-Seitz radius of the electrons in units of the Bohr radius. For the valence electrons in metals $r_s=2-6$, so that the coupling constant (1.3) is greater than unity. The system of valence electrons in the metal is a typical example of a degenerate, strongly coupled plasma.

The coupling constant of a plasma obeying the classical statistics is

$$\Gamma\equiv\frac{(Ze)^2}{ak_BT}$$
$$=2.69\times10^{-5}Z^2\left[\frac{n}{10^{12}\ \mathrm{cm}^{-3}}\right]^{1/3}\left[\frac{T}{10^6\ \mathrm{K}}\right]^{-1}. \tag{1.5}$$

This expression indicates that for a plasma with $Z\simeq1$ and $T\simeq10^6$ K, the density n $(=N/V)$ must become as high as $\sim10^{26}$ cm^{-3} to make $\Gamma\simeq1$.

Most of the classical plasmas that we ordinarily encounter are, however, characterized by $\Gamma\ll1$. For example, we may assume $n\simeq10^{11}$ cm^{-3}, $T\simeq10^4$ K for a gaseous-discharge plasma in laboratory, $n\simeq10^{16}$ cm^{-3}, $T\simeq10^8$ K for a plasma in a controlled thermonuclear experiment, and $n\simeq10^6$ cm^{-3}, $T\simeq10^6$ K for a plasma in the solar corona. For those plasmas, respectively, we find $\Gamma\simeq10^{-3}$, 10^{-5}, and 10^{-7}. They are thus weakly coupled plasmas, so to speak; their thermodynamic properties are analogous to those of an ideal gas.

A most typical example of a strongly coupled classical plasma may be seen in the system of ions inside a highly evolved star (e.g., Salpeter and Van Horn, 1969; Schatzman, 1978, 1980). The interior of such a star is in a compressed, high-density state. The Fermi energy of the electron system takes on a value much greater than the binding energy of an electron around an atomic nucleus; all the atoms are thus in ionized states (pressure ionization). The electron system constitutes a weakly coupled ($r_s\ll1$) degenerate plasma with an immensely large Fermi energy ($E_F\simeq mc^2$). It makes an ideal neutralizing background of negative charges to the ion system; since $r_s\ll1$, the polarizability of the background may be negligible. Those atomic nuclei stripped of the electrons form an ion plasma obeying the classical statistics; their de Broglie wavelengths are much smaller on the average than the interparticle spacing; that is, $\hbar(Mk_BT)^{-1/2}\ll a$, where M is the ionic mass. In the interior of a highly evolved star, the coupling constant Γ for such an ion plasma is usually greater than unity; in a white dwarf one estimates that $\Gamma=10-200$ (e.g., Schatzman, 1958; Van Horn, 1980).

As an example of a strongly coupled plasma closer to the earth, we may take the Jovian interior (e.g., Salpeter, 1973; Graboske, Pollack, Grossman, and Olness, 1975; Stevenson and Salpeter, 1977; Stevenson, 1980) which consists mostly of hydrogen and a small fraction of helium. Its electron system is characterized by $r_s=0.6-1$; its ion system, $\Gamma=20-50$. The Jovian interior thus appears to offer a complex system of a strongly coupled classical plasma immersed in a *polarizable* background of degenerate electrons. In addition, the ion plasma may have to be looked upon as a *binary ion mixture* of hydrogen and helium.

As the example of a strongly coupled plasma in laboratory, one may think of the plasmas produced in the laser implosion experiments (e.g., Brueckner and Jorna, 1974; Grandey, 1978), whose densities will eventually reach a value as high as $\Gamma=1-100$. It has been reported (Ivanov, Mintsev, Fortov, and Dremin, 1976) that $\Gamma=1-5$ has been realized in transient plasmas produced in explosive shock tubes. In addition, as a purest example of the strongly coupled classical OCP realized in the laboratory, we have the two-dimensional system of electrons trapped in the surface states of liquid helium (e.g., Cole and Cohen, 1969; Cole, 1974; Grimes, 1978; Ichimaru, 1978).

B. Approach

As the aforementioned definition of a strongly coupled plasma may suggest, the Coulomb interaction between particles plays the essential role in determining the physical properties of such a plasma. In a theoretical treatment of the strongly coupled plasma, one cannot resort to a usual expansion scheme in which the Coulomb interaction is regarded as a weak perturbation. We may also note that the interaction potential adopted in the OCP problem has a simple and unique character: Among the repulsive potentials expressible as inverse power $r^{-\nu}$ of the distance r, the OCP problem constitutes a typical example ($\nu=1$) of the soft cases, while the hard-core potential corresponds to the other extreme case of $\nu=\infty$. It may therefore be said that we are here faced with a charged liquid problem. It is nevertheless of interest that the strongly coupled plasmas exhibit a remarkable similarity to hard-sphere systems in a number of significant aspects, as we shall see in the subsequent analyses.

The strongly coupled OCP problem has been approached by various methods. Computer experiments based on the Monte Carlo simulation (Metropolis *et al.*, 1953) and the molecular dynamics method (Alder and Wainwright, 1959) have provided certain vital informa-

tion on the static and dynamic properties of the strongly coupled classical plasmas.

Analytic theories are usually directed to derivation of a set of nonlinear integral equations for the correlation functions, which may then be solved numerically. Theoretical schemes developed in the treatment of liquids, such as the hypernetted chain (HNC) equations and the Bogoliubov-Born-Green-Kirkwood-Yvon (BBGKY) hierarchy (e.g., Rice and Gray, 1965; Hansen and McDonald, 1976), provide useful tools in such an analysis.

Dielectric formulation (e.g., Pines and Nozières, 1966) has been pursued extensively to account for the static and dynamic properties of strongly coupled plasmas. It is developed in the general framework of the linear-response formalism in the statistical mechanics, where the strong-coupling effects are taken into consideration through a number of characteristic functions.

Variational methods on the basis of the Gibbs-Bogoliubov inequality (e.g., Feynman, 1972; Hansen and McDonald, 1976) have been used quite successfully when an appropriate choice of the reference system can be made. For the analysis of a degenerate electron system, computer techniques have make it possible to carry out variational calculations in terms of trial wave functions of the Bijl-Dingle-Jastrow type (e.g., Ceperley, 1978). Those variational calculations have been refined recently by incorporating the Fermi hypernetted chain (FHNC) method (Fantoni and Rosati, 1975) or the Green's function Monte Carlo (GFMC) method (Ceperley and Kalos, 1979).

C. Scope

In this article I wish to review the current status of our knowledge on various aspects of the strongly coupled plasmas, which has been accumulated through application of the methods mentioned above. I classify the topics roughly in two groups: the strongly coupled classical plasmas (Sec. II) and the degenerate electron liquids (Sec. III). Certain problems associated with the binary ion mixtures are described in Sec. II.D.3; screening effects of the degenerate electrons on the properties of the high-density two-component (electrons and ions) plasmas are treated in Sec. III.E.

We shall begin with description of basic quantities such as the radial distribution function, the static structure factor, and the local-field correction (Sec. II.A, III.C, and III.D.1). Thermodynamic quantities such as the internal or correlation energy are then calculated (Sec. II.B.1 and III.D.2); conditions for the Wigner crystallization and possibilities of the charge-density wave (CDW) instability are investigated (Sec. II.B.4—II.B.6, III.D.3, and III.D.4). Physical models to account for such static properties are described (Sec. II.B.2 and II.C.2).

Dielectric formulation of strongly coupled plasmas (Sec. II.E.3 and III.A) and analytic treatments of the correlational properties (Sec. II.D, III.B, and III.C) are presented. Applications of the static screening properties to the enhancement of the thermonuclear reaction rate (Sec. II.C.3) and to the modification of the ionic correlations in dense plasmas (Sec. III.E) are described.

Dynamic properties such as the velocity autocorrelation function (Sec. II.E.1), the plasmon dispersion (Sec. II.E.4 and III.F.2) and the spectra of density fluctuation excitations (Sec. II.E.2 and III.F.3—III.F.6) are discussed and compared with experimental data.

The subjects covered in this review are confined, more or less, to those areas where my collaborators and I have been able to make some contact, directly or indirectly, through the course of our study on strongly coupled plasmas. Thus there are a number of important topics on the strongly coupled plasmas that are not adequately treated here; examples include the ionization equilibrium of high-density plasmas (e.g., Norman and Starostin, 1970; Ebeling, Kraeft, and Kremp, 1977) and the spin-dependent properties of the degenerate electron liquids such as a transition into a ferromagnetic state and the possibility of the spin-density-wave (SDW) instability (for example, Overhauser, 1968). The reader is referred also to other review articles on strongly coupled plasmas (e.g., Baus and Hansen, 1980; Raether, 1980; Singwi and Tosi, 1981; Deutsch, Furutani, and Gombert, 1981), which were prepared from somewhat different points of view.

II. CLASSICAL PLASMAS

A. Description of static properties

In their pioneering work, Brush, Sahlin, and Teller (1966) performed numerical experiments on OCP by the Monte Carlo method. A few years later, Hansen (1973) carried out similar experiments with improved accuracy. Recently, Slattery, Doolen, and DeWitt (1980) obtained the Monte Carlo data with further improvement of the accuracy.

Figure 1 shows the *radial distribution function* $g(r)$ computed through these experiments for various values of the OCP coupling constant Γ. The radial distribution function represents the probability of finding another particle at a distance r away from a given particle; it is normalized so that $g(r)$ approaches unity as $r \to \infty$.

The *static structure factor* $S(q)$ is related to the radial

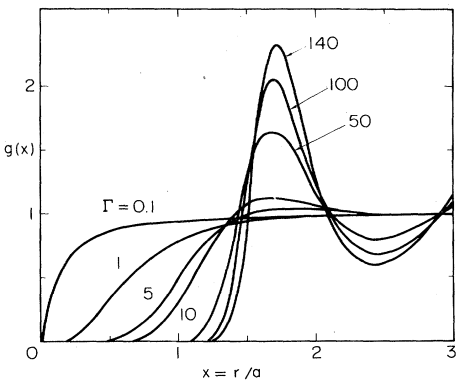

FIG. 1. The radial distribution function at various values of Γ.

distribution function via the Fourier transformation as (e.g., Ichimaru, 1973; Hansen and McDonald, 1976)

$$S(q)-1=n\int d\mathbf{r}[g(r)-1]\exp(-i\mathbf{q}\cdot\mathbf{r})\ . \tag{2.1}$$

In Fig. 2 the values of $S(q)$ as compiled by Galam and Hansen (1976) are plotted for various Γ.

For a weakly coupled OCP ($\Gamma \ll 1$), the linearized Debye-Hückel approximation (Debye and Hückel, 1923) is applicable, so that one finds

$$S_{\rm DH}(q)=\frac{q^2}{q^2+q_D^2}\ , \tag{2.2}$$

where

$$q_D^2=4\pi n(Ze)^2/k_BT \tag{2.3}$$

is the square of the Debye wave number. Since Eq. (2.2) can also be obtained from the linearized Vlasov equation (e.g., Ichimaru, 1973), which is equivalent to application of the random-phase approximation (RPA), it will be referred to as the RPA values of the static structure factor for the OCP.

Departure of the static structure factor from its RPA values is measured by the *local-field correction* $G(q)$; it is defined for the OCP as

$$G(q)=1+\left[1-\frac{1}{S(q)}\right]\frac{q^2}{q_D^2}\ . \tag{2.4}$$

The values of $G(q)$ have been computed (Tago, Utsumi, and Ichimaru, 1981) by substituting the Monte Carlo data of $S(q)$ in (2.4); results are shown in Fig. 3. The long-wavelength behavior of the local-field correction is related to the isothermal compressibility of the OCP as (e.g., Pines and Nozières, 1966)

$$\lim_{q\to 0}\left[\frac{q_D}{q}\right]^2 G(q)=1-\frac{1}{k_BT}\left[\frac{\partial P}{\partial n}\right]_T\ , \tag{2.5}$$

where P is the pressure.

The static dielectric function $\varepsilon(q,0)$ is then given by (e.g., Ichimaru, 1973)

$$\varepsilon(q,0)=\frac{q^2}{q^2-q_D^2S(q)}$$

$$=1+\frac{q_D^2}{q^2-q_D^2G(q)}\ . \tag{2.6}$$

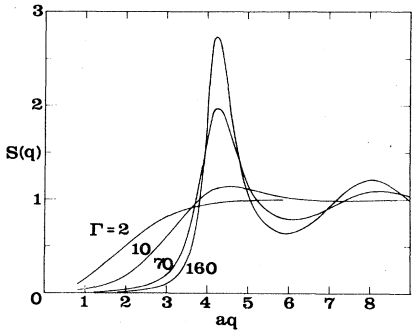

FIG. 2. The static structure factor at various values of Γ.

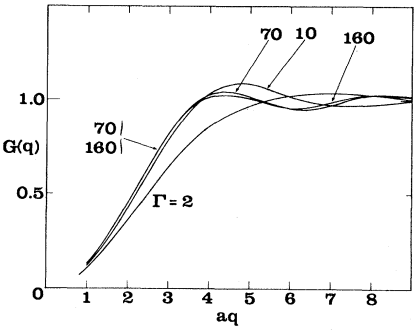

FIG. 3. The local-field correction at various values of Γ.

Monte Carlo values of Eq. (2.6) have been computed (e.g., Fasolino, Parrinello, and Tosi, 1978; Baus and Hansen, 1980; Ichimaru and Tago, 1981); results are shown in Fig. 4.

The classical system of electrons in a two-dimensional surface layer has been studied by using the Monte Carlo simulation (Totsuji, 1978; Gann, Chakravarty, and Chester, 1979) and the molecular dynamics method (Hockney and Brown, 1975; Hansen, Levesque, and Weis, 1979; Morf, 1979; Totsuji and Kakeya, 1980; Kalia, Vashishta, and de Leeuw, 1981).

B. Equation of state

1. Internal energy formula

With the knowledge of the radial distribution function or the static structure factor, the excess internal energy $U_{\rm ex}$ of the OCP is calculated according to

$$\frac{U_{\rm ex}}{Nk_BT}=\frac{n}{2k_BT}\int d\mathbf{r}\frac{(Ze)^2}{r}[g(r)-1]$$

$$=\frac{1}{4\pi^2k_BT}\int d\mathbf{q}\frac{(Ze)^2}{q^2}[S(q)-1]\ . \tag{2.7}$$

Since the total internal energy U of the system is given by

$$U=\tfrac{3}{2}Nk_BT+U_{\rm ex}\ , \tag{2.8}$$

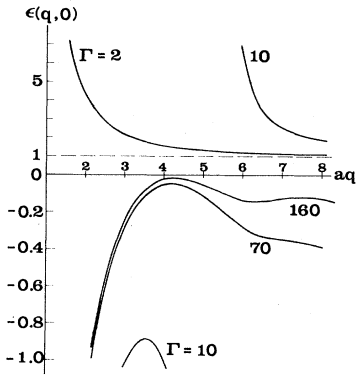

FIG. 4. The static dielectric function at various values of Γ. Note the difference in scales above and below the abscissa.

and the pressure by

$$P=nk_BT+U_{ex}/3V\ , \tag{2.9}$$

various thermodynamic functions of the OCP can be determined once Eq. (2.7) is evaluated as a function of Γ.

Analyzing the Monte Carlo data obtained by Hansen (1973), DeWitt (1976) found that a fitting formula,

$$\begin{aligned} U_{ex}/Nk_BT=&-(0.894\,61\pm0.000\,03)\Gamma \\ &+(0.8165\pm0.0008)\Gamma^{1/4} \\ &-(0.5012\pm0.0016)\ , \end{aligned} \tag{2.10a}$$

reproduced the data with good accuracy in the region, $1\le\Gamma\le40$. He proposed also a slightly modified formula,

$$\begin{aligned} U_{ex}/Nk_BT=&-(0.8966\pm0.0001)\Gamma \\ &+(0.874\pm0.009)\Gamma^{1/4} \\ &-(0.568\pm0.023)\ , \end{aligned} \tag{2.10b}$$

for $50\le\Gamma\le140$; the agreement of this formula with the Monte Carlo data was, however, less accurate than that of Eq. (2.10a). This fact led DeWitt to question the accuracy of Hansen's data for large values of Γ (i.e., $40<\Gamma<160$).

Slattery, Doolen, and DeWitt (1980) fitted their liquid U_{ex}/Nk_BT data ($1\le\Gamma\le160$) for 128 particle Monte Carlo runs to the form

$$U_{ex}/Nk_BT=a\Gamma+b\Gamma^{1/4}+c\Gamma^{-1/4}+d \tag{2.11}$$

by minimizing the sum of the squares of the relative errors using a, b, c, and d as parameters. The values of the parameters so determined were

$$\begin{aligned} &a=-0.897\,52,\quad b=0.945\,44\ , \\ &c=0.179\,54,\quad d=-0.800\,49\ . \end{aligned} \tag{2.12}$$

Accuracy of this fit was excellent; the relative rms error was 3×10^{-5}.

The Helmholtz free energy F of the OCP could then be calculated from the formula

$$\begin{aligned} f(\Gamma)\equiv&\frac{F}{Nk_BT} \\ =&\int_{\Gamma_1}^{\Gamma}\frac{U_{ex}}{Nk_BT}\frac{d\Gamma'}{\Gamma'}+f(\Gamma_1)\ . \end{aligned} \tag{2.13}$$

The normalized free energy $f(\Gamma_1)$ at $\Gamma_1=1$ was evaluated through integration of U_{ex}/Nk_BT with the Abe (1959) formula ($0.0\le\Gamma\le0.1$), the hypernetted chain (HNC) results ($0.1\le\Gamma\le0.6$), and the Monte Carlo values ($0.6\le\Gamma\le1.0$). Slattery, Doolen, and DeWitt (1980) thus found

$$\begin{aligned} f(\Gamma)=&\,a\Gamma+4(b\Gamma^{1/4}-c\Gamma^{-1/4})+(d+3)\ln\Gamma \\ &-(a+4b-4c+1.135)\ . \end{aligned} \tag{2.14}$$

2. Ion-sphere model

The leading term in Eq. (2.11) or (2.14) for $\Gamma>1$ is the first term on its right-hand side. For the interpretation of this term and more generally for the understanding of the properties of the strongly coupled plasma, it is instructive to introduce the *ion-sphere model* as illustrated in Fig. 5. We construct an ion sphere by picking a particle (an ion with the electric charge Ze) in the plasma and by associating with it a sphere of neutralizing charges that would exactly cancel the point charge of the ion. This sphere has the radius as given by Eq. (1.2) and the electric charge density $-3Ze/4\pi a^3$. It is the same as the Wigner-Seitz sphere in solid-state physics (e.g., Pines, 1964).

Let us calculate the electrostatic energy E_{IS} of the ion sphere consisting of the ion and the negative charge sphere. The electrostatic potential produced by the negative charge sphere at r from its center is given by $-(\frac{3}{2})(Ze/a)+(Ze/2a)(r/a)^2$. Since the electrostatic energy of the negative charge sphere itself is $(\frac{3}{5})(Ze)^2/a$, we find

$$\begin{aligned} E_{IS}/k_BT=&-[(3/2)-(3/5)]\Gamma+(\Gamma/2)(r/a)^2 \\ =&-0.9\Gamma+0.5\Gamma(r/a)^2\ . \end{aligned} \tag{2.15}$$

The first term on the right-hand side of Eq. (2.15) represents the electrostatic energy of the ion sphere when the ion is located at the site $r=0$ of the lowest energy. It has been proved by Lieb and Narnhofer (1975, 1976) that this term, -0.9Γ, gives a lower bound to the estimate of the excess internal energy for the OCP.

Since the last term of Eq. (2.15) is proportional to r^2, it may induce a motion of the harmonic-oscillator type to the ion. The potential energy of a harmonic oscillator is $(1/2)k_BT$ per degree of freedom; an average of Eq. (2.15) thus yields

$$\langle E_{IS}\rangle/k_BT=-0.9\Gamma+1.5\ . \tag{2.16}$$

This estimate in fact gives a fairly close approximation to the excess internal energy of the OCP for $\Gamma\gg1$.

On the suggestion of this observation, Itoh and Ichimaru (1980a) proposed an internal energy formula on the basis of a harmonic lattice model. Analyzing the numerical results of Slattery, Doolen, and DeWitt (1980), they found that

$$U_{ex}/Nk_BT=-0.8903\Gamma+1.500\quad(70\le\Gamma\le160) \tag{2.17}$$

adequately represents the Monte Carlo data. The coeffi-

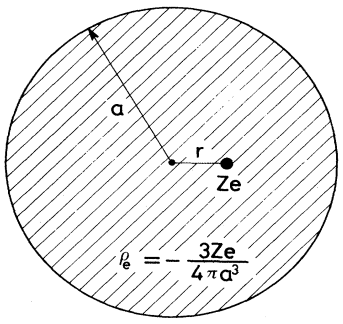

FIG. 5. Ion-sphere model. ρ_e refers to the average charge density in the sphere.

cient of the first term in Eq. (2.17), -0.8903, is greater than both the ion-sphere value (i.e., -0.9) and the Madelung value (i.e., $-0.895\,929$) for the bcc Coulomb lattice. We may interpret the difference as reflecting the extent to which the long-range translational order of the crystalline lattice is destroyed in the strongly coupled OCP fluid.

Analogously, analyzing the Monte Carlo results (Gann *et al.*, 1979) for the two-dimensional classical OCP fluid, Itoh and Ichimaru (1980b) proposed an analyic formula based on the harmonic lattice model

$$U_{\rm ex}/Nk_BT=-1.103\Gamma+1.000 \quad (50\le\Gamma\le 120) \tag{2.18}$$

which accurately represents the numerical data. For such a two-dimensional system the Coulomb coupling constant Γ is given by

$$\Gamma=(Ze)^2(\pi n)^{1/2}/k_BT\ , \tag{2.19}$$

where n is the areal number density of the charged particles. Here again, the coefficient of the first term in Eq. (2.18), -1.103, takes on a value slightly greater than the Madelung value, $-1.106\,103$, for the triangular close-packed Coulomb lattice. The validity and accuracy of Eq. (2.18) have been reconfirmed in a recent molecular-dynamics experiment by Kalia *et al.* (1981).

The existence of the dominant Madelung-like contribution to the internal energy formulas as evidenced in Eqs. (2.11), (2.17), and (2.18) points to applicability of the ion-sphere model for a strongly coupled OCP fluid. The internal structure of such an OCP may be characterized by a latticelike short-range order. We shall return to this consideration later in Sec. II.C.2.

3. Hard-sphere variational calculation

As explained above, the interpretation of the first term of Eq. (2.11) is relatively straightforward in terms of the latticelike short-range order in the strongly coupled OCP fluid. The remaining terms, which are sometimes called the "thermal energy," have yet to be satisfactorily accounted for, however. It remains to be confirmed if the specific form of expansion in powers of $\Gamma^{1/4}$ that those thermal-energy terms assume has any physical significance; in the case of the two-dimensional classical OCP (Totsuji, 1978), such a $\Gamma^{1/4}$ dependence has not yet been confirmed.

An interesting and suggestive argument has been presented by DeWitt and Rosenfeld (1979) on the form of Eq. (2.11). The argument is based on a hard-sphere variational calculation stemming from the Gibbs-Bogoliubov inequality (e.g., Feynman, 1972; Hansen and McDonald, 1976).

The Gibbs-Bogoliubov inequality on the Helmholtz free energy F of the many-particle system with the Hamiltonian H reads

$$F\le F_0+\langle H-H_0\rangle_0\ , \tag{2.20}$$

where F_0 is the free energy of the reference system with the Hamiltonian H_0 and $\langle\cdots\rangle_0$ denotes the statistical average over this reference system. One may thus choose a variational reference system with a well-known solution; an upper bound of F may then be obtained by minimizing the right-hand side of Eq. (2.20) with respect to a variational parameter.

DeWitt and Rosenfeld (1979) chose a hard-sphere system with an effective hard-sphere diameter σ as the reference system and regarded the hard-sphere packing fraction,

$$\eta=(\pi n/6)\sigma^3\ , \tag{2.21}$$

as the variational parameter. As an analytic solution to the hard-sphere problem, they adopted the Percus-Yevick virial equation of state (e.g., Hansen and McDonald, 1976),

$$\frac{p^{(v)}}{nk_BT}=\frac{1+2\eta+3\eta^2}{(1-\eta)^2}\ . \tag{2.22}$$

The minimization of Eq. (2.20) for the OCP then yields the relation

$$\Gamma=2\eta^{1/3}(1+2\eta)^2/(1-\eta)^4\ . \tag{2.23}$$

Expanding the Percus-Yevick internal energy and Eq. (2.23) around $\eta=1$, they finally found a variational expression,

$$\frac{U_{\rm ex}}{Nk_BT}=-\frac{9}{10}\Gamma+\left[\frac{8\Gamma}{9}\right]^{1/4}-\frac{1}{2}+\frac{7}{80}\left[\frac{18}{\Gamma}\right]^{1/4}-\cdots\ . \tag{2.24}$$

The first term on the right-hand side of Eq. (2.24) corresponds to the ion-sphere evaluation (2.16); it agrees well with the first term of Eq. (2.11). The remaining terms in Eq. (2.24) are expanded in powers of $\Gamma^{1/4}$ and are thus consistent with the indication of Eq. (2.11).

Although instructive, the argument cited above does not constitute a rigorous proof on the form of the thermal energy. For one thing, an exact solution for the hard-sphere system is not used in Eq. (2.20), since the Percus-Yevick equation itself is an approximation. As a consequence, equations of state different from Eq. (2.22), such as the compressibility equation of state and the Carnahan-Starling formula (Carnahan and Starling, 1969; Hansen and McDonald, 1976), do exist. Use of such an equation of state would lead to a form of the thermal energy different from Eq. (2.24). Nonetheless, the existence of a correspondence such as Eq. (2.23) suggests the physical relevance of considering a hard-sphere system "equivalent" to the strongly coupled OCP for $\Gamma\gg 1$. It has been noted (Nagano and Ichimaru, 1980) that the values of the friction coefficient $1/\tau_s$ in the strongly coupled OCP evaluated through molecular dynamics experiments (Hansen, 1978) approximately satisfy the Stokes relation (M: the mass of a particle),

$$\frac{1}{\tau_s}=\frac{3\pi\eta_s\sigma}{M}\ , \tag{2.25}$$

with the effective diameter σ as determined from Eqs. (2.21) and (2.23), when the molecular dynamics values of the shear viscosity η_s (Bernu, Vieillefosse, and Hansen, 1977; Bernu and Vieillefosse, 1978) are substituted in Eq. (2.25).

4. Wigner crystallization

Pollock and Hansen (1973) carried out extensive Monte Carlo computations for the OCP in a perfect bcc lattice configuration and found that the numerical data for the excess internal energy are well represented by the formula

$$\frac{U_{\rm ex}}{Nk_BT}=-0.895\,929\Gamma+1.5+\frac{3500}{\Gamma^2}\ . \tag{2.26}$$

Comparing the Helmholtz free energy in this lattice phase and that in the fluid phase (Hansen, 1973), they determined the critical value Γ_m of the Coulomb coupling constant at which the liquid-solid phase transition or the Wigner crystallization takes place to be

$$\Gamma_m=155\pm10\ . \tag{2.27}$$

Subsequently, Slattery, Doolen, and DeWitt (1980) performed improved Monte Carlo computations and fitted their 128-ion bcc lattice data for $160\le\Gamma\le300$ to the form

$$\frac{U_{\rm ex}}{Nk_BT}=-0.895\,929\Gamma+1.5+\frac{2980}{\Gamma^2}\ . \tag{2.28}$$

The normalized Helmholtz free energy [see Eq. (2.13)] was then derived from Eq. (2.28) as

$$f(\Gamma)=-0.895\,929\,256\Gamma+\tfrac{9}{2}\ln\Gamma -1.8856-\frac{1490}{\Gamma^2}\ . \tag{2.29}$$

The transition point determined from the intersection of Eqs. (2.14) and (2.29) was

$$\Gamma_m=168\pm4\ . \tag{2.30}$$

They further added a note that the most recent Γ_m using their new results is 171 ± 3.

Wigner crystallization in a two-dimensional classical OCP has been studied through computer simulations by a number of investigators (Hockney and Brown, 1975; Gann, Chakravarty, and Chester, 1979; Morf, 1979; Kalia, Vashishta, and de Leeuw, 1981). According to Gann *et al.* (1979), the transition occurs at

$$\Gamma_m=125\pm15\ . \tag{2.31}$$

Kalia *et al.* (1981) find that the system undergoes a first-order phase transition between $\Gamma=118-130$, exhibiting hysteresis in the temperature dependence of such a quantity as total energy.

Experimentally, Grimes and Adams (1979) first observed the existence of an electron solid on a liquid-helium surface. Fisher, Halperin, and Platzman (1979) analyzed the experiment and found that the results can be explained on the basis of the electrons forming a triangular lattice below the transition temperature. The transition point found in the experiment was $\Gamma_m=137\pm15$, in good agreement with the simulation results.

5. Stability criterion for the OCP fluid

As an application of the Gibbs-Bogoliubov inequality, one can derive a necessary condition for stability of the homogeneous fluid phase of the OCP (Ichimaru, Iyetomi, and Utsumi, 1982). It is a generalization to a classical OCP of Ferrell's validity criterion (Ferrell, 1958) for testing approximations to the degenerate electron-gas correlation energy.

Let the Hamiltonian of the classical OCP be expressed as a sum of the kinetic energy $\mathscr{K}$ and the interaction energy $\Gamma\mathscr{V}$. We substitute

$$H_0=\mathscr{K}+\Gamma\mathscr{V}\ ,$$

$$H=\mathscr{K}+(\Gamma+\Delta\Gamma)\mathscr{V}\ ,$$

in Eq. (2.20) and expand the result with respect to $\Delta\Gamma$. The zeroth- and first-order terms vanish identically by virtue of Eq. (2.13), or equivalently,

$$\frac{df(\Gamma)}{d\Gamma}=\frac{\langle\mathscr{V}\rangle_0}{Nk_BT}\ . \tag{2.32}$$

The second-order terms of Eq. (2.20) then yield

$$\frac{d^2f(\Gamma)}{d\Gamma^2}\le0\ . \tag{2.33}$$

This condition thus makes a stability criterion for the classical OCP fluid.

Since the excess specific heat $\tilde{c}_v$ per particle at constant volume is given by

$$\tilde{c}_v=-\Gamma^2\frac{d^2f(\Gamma)}{d\Gamma^2}\ , \tag{2.34}$$

the criterion (2.33) may be reexpressed as

$$\tilde{c}_v\ge0\ . \tag{2.35}$$

Thus the condition (2.35) is more restrictive than the ordinary criterion for thermodynamic stability that requires positivity of the total specific heat, $(\frac{3}{2})+\tilde{c}_v$.

One easily finds that the internal energy formulas such as Eqs. (2.14) and (2.17) satisfy the criterion (2.33) or (2.35) in their ranges of validity below the crystallization point at Γ_m. This finding is consistent with the statement that the criterion (2.33) and (2.35) is a necessary condition for stability of the homogeneous liquid state.

6. Possibility of a charge-density-wave instability

In the study of the phase properties of plasmas, it has been conjectured by some investigators (Schneider, Brout, Thomas, and Feder, 1970; Totsuji and Ichimaru, 1974; Sander, Rose, and Shore, 1980) that the onset of a "soft-mode" instability associated with transition into a charge-density-wave (CDW) state (Overhauser, 1968)

might be connected with the Wigner crystallization. The possibility of such a CDW instability rests on the observation that the negative sign of the static dielectric function $\varepsilon(q,0)$ not only is permitted theoretically (Martin, 1967; Dolgov, Kirzhnits, and Maksimov, 1981) but also has been realized in various systems such as a strongly coupled OCP (cf. Fig. 4). The onset condition (see Sec. II.D.1 below for derivation)

$$\varepsilon(q,0)=0 \tag{2.36}$$

for the CDW instability may then be approached from below as the coupling constant Γ is increased; Eq. (2.36) may thus determine the critical values, Γ_c and $q_{\rm cr}$.

For the classical OCP, the use of the fluctuation-dissipation theorem enables one to evaluate $\varepsilon(q,0)$ with the knowledge of $S(q)$ as in Eq. (2.6); Monte Carlo results are shown in Fig. 4. It would appear that with a further increase of Γ, the vertex point, $\varepsilon(q,0)_{\rm max}$, may soon reach zero with $q_{\rm cr}\simeq 4.3/a$.

To see the general trend of approach to the critical condition (2.36), we plot in Fig. 6 the peak value $\varepsilon(q,0)_{\rm max}$ as a function of Γ, both on the logarithmic scales. The triangular points have been obtained by Ichimaru and Tago (1981) on the basis of the static structure factor evaluated by Galam and Hansen (1976). As we here observe, the three points are aligned almost on a straight line. Although not shown in the figure, this trend in fact continues down to $\Gamma=10$. If this trend should also continue into the supercooled domain, $\Gamma>\Gamma_m$, then the plasma would not be able to attain the critical condition (2.36) at a finite value of Γ, although the peak value $\varepsilon(q,0)_{\rm max}$ at $\Gamma=160$ is extremely close to zero. We may therefore conclude tentatively that if an instability of the homogeneous fluid phase should take place at all, its critical Γ value would be much greater than that associated with the first-order Wigner transition, i.e., $\Gamma_c \gg \Gamma_m$.

Recently, Iyetomi and Ichimaru (1982a) developed a theoretical scheme in which the hypernetted-chain approximation is systematically improved for the strongly coupled plasmas (see Sec. II.D.4 for details). It has been confirmed that the correlation functions computed in this improved scheme almost identically reproduce all the published data of the latest Monte Carlo simulations carried out by Slattery *et al.* (1980); the case with $\Gamma=160$ will be shown later in Fig. 13(a). This scheme also enables one to extend the calculation of $S(q)$ into the supercooled domain, $\Gamma>\Gamma_m$; the values of $\varepsilon(q,0)_{\rm max}$ computed from such a calculation are shown in Fig. 6 by filled circles (Iyetomi and Ichimaru, 1982b). We again observe that the points are aligned almost on a straight line. It is thus expected that the metastability of the fluid phase may persist well beyond $\Gamma=500$. Later, in Sec. II.D.5, we shall see a microscopic evidence that such a metastable supercooled OCP fluid may in fact assume an amorphous glassy state.

C. Screening potential

1. Short-range behavior

Since the radial distribution function $g(r)$ describes the spatial correlation between two particles, the potential of average force $w(r)$ may be defined through the equation

$$g(r)=\exp[-w(r)/k_BT]\ . \tag{2.37}$$

In a weakly coupled plasma it is sufficient to take the bare Coulomb interaction, $w(r)=(Ze)^2/r$. In a strongly coupled plasma, however, $w(r)$ deviates significantly away from $(Ze)^2/r$ due to the effects of many-particle correlations. To single out such a deviation, we introduce a function

$$H(r)=[(Ze)^2/r]-w(r)\ , \tag{2.38}$$

which will be referred to as the *screening potential.* This function measures the extent to which the effective potential $w(r)$ between two particles is lowered from the bare Coulomb value $(Ze)^2/r$.

By substituting in Eq. (2.37) the values of $g(r)$ such as shown in Fig. 1 and with the aid of Eq. (2.38), one may compute the screening potential $H(r)$ evaluated on the basis of the Monte Carlo experiments. The result of such a computation has revealed an interesting feature. Figure 7 plots the values of $H(r)/[(Ze)^2/a]$ as a function of r/a

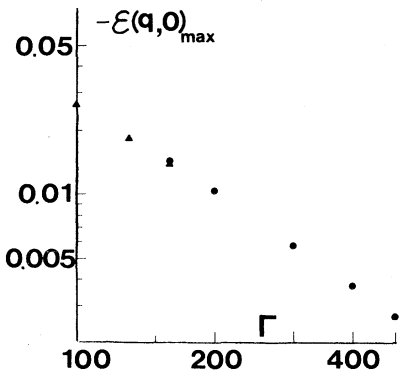

FIG. 6. The peak value $\epsilon(q,0)_{\rm max}$ of the static dielectric function versus the coupling constant Γ. From Iyetomi and Ichimaru (1982b).

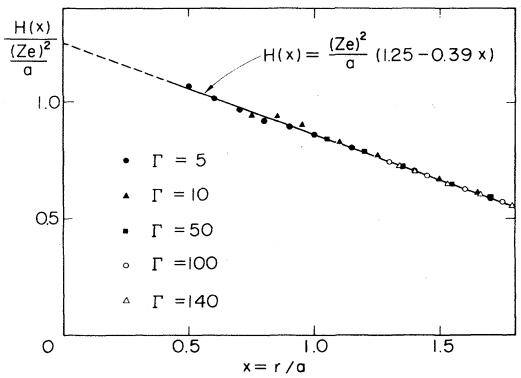

FIG. 7. Linearity of the screening potential derived from the Monte Carlo simulation data.

for various Γ; here we clearly observe that the data follow a straight line in the interval, $0.4<r/a<1.8$. This straight line may be expressed as

$$H(r)=\frac{(Ze)^2}{a}\left[c_0-c_1\left[\frac{r}{a}\right]\right] \tag{2.39}$$

for $4\leq\Gamma\leq 160$. The choice of the coefficients, $c_0=1.25$ and $c_1=0.39$, reproduces the Monte Carlo data of Hansen (1973) within errors less than 4% (Itoh, Totsuji, and Ichimaru, 1977). The coefficients are then mutually connected via

$$c_1=(c_0/2)^2 . \tag{2.40}$$

The linear relationship (2.39) and the connecting formula (2.40) were discovered by DeWitt, Graboske, and Cooper (1973) through the analysis of the Monte Carlo data of Brush *et al.* (1966). Such relations have been found to apply not only in the OCP but also in the binary mixtures of ions (Itoh, Totsuji, Ichimaru, and DeWitt, 1979) and in the two-dimensional electron layers (Itoh, Ichimaru, and Nagano, 1978; Totsuji, 1978). As we shall discuss in the next section, those features are directly related to the existence of a latticelike short-range order in the strongly coupled plasma.

In the vicinity of $r=0$, $(Ze)^2/r$ is predominantly large in $w(r)$ so that $g(r)$ vanishes; one cannot deduce $H(r)$ from the Monte Carlo data. Instead, one may adopt the ion-sphere model to evaluate the screening potential in the following way (Salpeter, 1954): When two ions are close to each other, a complex ion sphere is constructed with a negative charge sphere of radius $2^{1/3}a$ and charge $-2Ze$ (see Fig. 8). The screening potential in the vicinity of $r=0$ is then calculated from the energy difference between such a complex ion sphere and two ion spheres of charge Ze. With the aid of Eq. (2.15), one finds

$$H(r)=(2^{5/3}-2)\times 0.9\frac{(Ze)^2}{a}-2\times 0.5\frac{(Ze)^2}{a}\left[\frac{r}{2a}\right]^2$$
$$=\frac{(Ze)^2}{a}\left[1.057-\frac{1}{4}\left[\frac{r}{a}\right]^2\right] . \tag{2.41}$$

It has been shown (Widom, 1963) that $H(r)$ is expressed in a power series of r^2 near $r=0$; Eq. (2.41) gives the first two terms of such an expansion. Instead of Eq. (2.15), one can alternatively use an expression of the free energy such as Eq. (2.14) for the calculation of $H(r)$ (Jancovici, 1977).

The short-range screening potential in the two-dimensional electron layer has also been computed (Itoh *et al.*, 1978).

2. Lattice model

For a calculation of the screening potential in connection with an estimation of the nuclear reaction rate in a compressed star, Salpeter and Van Horn (1969) introduced the following model: Suppose that the strongly coupled plasma in a liquid state has a short-range order of a crystalline system, so that one may assume a bcc structure with the lattice constant b corresponding to the plasma density n (see Fig. 9). One then picks a pair of adjacent ions (the filled spheres in Fig. 9) and calculates the electrostatic energy as a function of the interparticle separation r with the center of mass fixed. When the interparticle separation is close to the nearest-neighbor distance, d, one assumes that the screening potential is given by this calculation based on what may be called a lattice model.

When the two particles approach close to each other ($r\ll d$), Eq. (2.41) based on the ion-sphere model is assumed to be valid. When the results of those two calculations, valid at $r\simeq d$ and $r\simeq 0$, are fitted by a polynomial, one finds the screening potential according to the lattice model as (Itoh and Ichimaru, 1977, 1979)

$$H_L(r)=[(Ze)^2/b][\,1.1547+1.1547(1-y)$$
$$-0.9935(1-y)^2+4.3385(1-y)^3$$
$$-5.3868(1-y)^4+1.8728(1-y)^5] , \tag{2.42}$$

where $y=r/d$. Figure 10 compares this result with Eq. (2.39), showing that the linearity of the screening potential can be reproduced by taking account of the latticelike order in the vicinity of $r=d$.

Although Eq. (2.42) is successful in reproducing the linearity of the screening potential, it does not accurately predict the magnitudes of the two coefficients, c_0 and c_1,

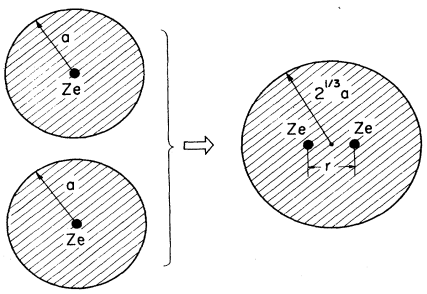

FIG. 8. Calculation scheme of the short-range screening potential based on the ion-sphere model.

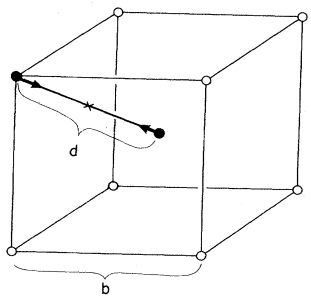

FIG. 9. Calculation of the screening potential on the basis of the bcc lattice model. Distance between the two particles depicted by the filled circles is varied, with their center of mass ($\times$) fixed. $d=0.8660b=1.7589a$.

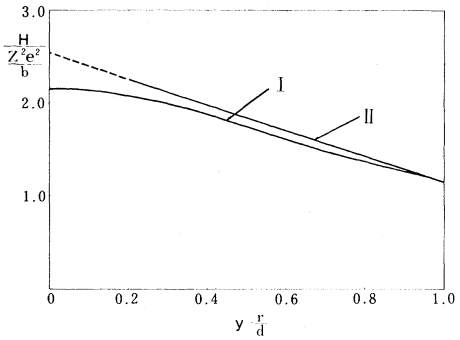

FIG. 10. Screening potential H as functions of y, the interparticle distance r measured in units of the nearest-neighbor distance d for the bcc lattice. I represents the lattice model formula, Eq. (2.42); II, the Monte Carlo result, Eq. (2.39). The dashed line of II for $0 \leq y \leq 0.2$ is an extrapolation.

of Eq. (2.39). To determine those coefficients more accurately in connection with the lattice model, we proceed one step further and assume an effective potential of the harmonic-oscillator type near the nearest-neighbor separation (Itoh and Ichimaru, 1977). That is, the potential of average force is assumed to satisfy

$$w(d)=0, \quad \left.\frac{dw(r)}{dr}\right|_{r=d}=0 . \tag{2.43}$$

The first relation assumes that the electrostatic potential of an ion is completely screened at $r=d$; the second relation implies that $w(r)$ takes on a minimum value there. Use of Eq. (2.39) in Eq. (2.43) leads to

$$c_1=(c_0/2)^2, \quad c_0=2a/d . \tag{2.44}$$

The former is identical to Eq. (2.40). Evaluation of the latter for the bcc lattice yields $c_0=1.137$; for the sc lattice, $c_0=1.241$. These values are reasonably close to the Monte Carlo value, $c_0=1.25$.

The observation that the assumptions introduced in Eq. (2.43) actually correspond to the correlational behavior obtained in the computer experiments reveals a number of salient properties of the strongly coupled plasma. The first relation of Eq. (2.43), in particular, indicates that the screening distance in a strongly coupled plasma is determined solely by the number density of the particles and that the temperature or the thermal effect plays a negligible part in such an act of screening. In the case of a weakly coupled plasma ($\Gamma \ll 1$), on the contrary, the Debye length $\lambda_D=[k_BT/4\pi n(Ze)^2]^{1/2}$ gives the effective screening distance (e.g., Ichimaru, 1973), which is determined through balance between the thermal and electrostatic effects.

3. Enhancement of thermonuclear reaction rate

Enhancement of thermonuclear reaction rate arising from Coulomb correlations in strongly coupled plasmas has important consequences in various aspects of stellar evolution such as carbon ignition in degenerate cores. Salpeter (1954) originally presented an analytic treatment of such an effect in a low-density, high-temperature plasma such that $\Gamma < 1$, and introduced the ion sphere model to describe the effects of interparticle correlations in the strongly coupled regime, $\Gamma > 1$. Later, Salpeter and Van Horn (1969) carried out detailed calculations based on the ion-sphere model.

As we noted earlier, the Monte Carlo simulation has been a powerful tool in the study of Coulomb correlations in strongly coupled plasmas. DeWitt, Graboske, and Cooper (1973) developed a generalized statistical-mechanical theory to describe the effects of plasma screening on nuclear reactions.

Both sets of calculations of the enhancement factor cited above are based on evaluation of the screening potential at zero separation. For justification of this procedure, it may be argued that the classical turning radii for those particles with relative velocities in the vicinity of the Gamow peak are much smaller than the mean ionic distance; hence, the screening potential may be replaced effectively by its value at zero separation.

Basically, however, the nuclear reaction rate depends on the probability of particles tunneling through the repulsive Coulomb barrier; to evaluate the latter probability one must carry out a relevant WKB integration inside the turning radius. It is therefore expected that the spatial dependence of the screening potential will play a crucial part in such an integration.

Mitler (1977) treated the enhancement factor through considering a spatially dependent screening potential obtained in the ion-sphere model; his work thus represents a significant improvement upon the original ion-sphere model of Salpeter (1954). The use of the ion-sphere model, however, is in a way a retreat from the line gained by DeWitt *et al.* (1973), who made use of the results of the Monte Carlo computations on the classical OCP; the screening potential at intermediate distances ($r \simeq a$) can be obtained accurately only by using the results of such numerical experiments. Itoh, Totsuji, and Ichimaru (1977) thus calculated the enhancement factor by taking explicit account of the Monte Carlo results for the screening potential as parametrized in Eq. (2.39). Subsequently, Alastuey and Jancovici (1978) carried out an independent calculation of the enhancement factor by taking into account the spatial dependence of the screening potential, and obtained a result which is in essential agreement with that of Itoh *et al.* (1977).

The penetration probability $p(v)$ of the Coulomb barrier for the reacting nuclei with the relative velocity v and the reduced mass $M/2$ may be given by the WKB integral (Van Horn and Salpeter, 1967) as

$$p(v)=\exp\left[-\frac{2\sqrt{M}}{\hbar}\int_0^r dr'\left[w(r')-\frac{Mv^2}{4}\right]^{1/2}\right], \tag{2.45}$$

where $w(r')$ is the potential of average force [cf. Eq. (2.37)] and r is the classical turning radius determined from

$$w(r)=Mv^2/4 . \tag{2.46}$$

Separating the strongly v-dependent part, we may write the nuclear reaction rate R as

$$R=\int_0^\infty dv\, F(v)\exp(-Q) , \tag{2.47}$$

where $\exp(-Q)$ is the product between $p(v)$ and the Boltzmann factor $\exp(-Mv^2/4k_BT)$. On account of the strong v dependence of $\exp(-Q)$, the integral Eq. (2.47) may be evaluated through expansion of Q around its minimum value $Q(v_0)$ at v_0, where $dQ(v_0)/dv_0=0$ (the Gamow peak); we thus have

$$R\simeq F(v_0)\int_{-\infty}^{\infty} dv \exp\left[-Q(v_0)-\tfrac{1}{2}(v-v_0)^2\frac{d^2}{dv_0^2}Q(v_0)\right] . \tag{2.48}$$

Since the relative velocity v is connected with the classical turning radius r via Eq. (2.46), one finds it convenient to regard Q as a function of r, i.e.,

$$Q(r)=\frac{w(r)}{k_BT}+\frac{2\sqrt{M}}{\hbar}\int_0^r dr'[w(r')-w(r)]^{1/2} , \tag{2.49}$$

and thereby to carry out a statistical average with respect to the distribution of r. The latter distribution can be evaluated by substituting Eqs. (2.38) and (2.39) in Eq. (2.37). Introducing a normalized distance

$$\rho=r\Big/\left[\frac{\hbar^2}{M(Ze)^2}\left[\frac{2\tau}{3\pi}\right]^2\right] , \tag{2.50}$$

and the dimensionless temperature parameter

$$\tau=\left[\left[\frac{27\pi^2}{4}\right]\frac{M(Ze)^4}{\hbar^2k_BT}\right]^{1/3} , \tag{2.51}$$

one expresses the result with good accuracy as (Itoh *et al.*, 1977)

$$Q(\rho)\simeq\frac{\tau}{3}\left[\frac{1}{\rho}+2\rho^{1/2}-\frac{3\Gamma}{\tau}c_0+\left[\frac{3\Gamma}{\tau}\right]^2 c_1\rho-\frac{1}{4}\left[\frac{3\Gamma}{\tau}\right]^2 c_1\rho^{5/2}\right] . \tag{2.52}$$

The enhancement factor is the ratio of Eq. (2.48) calculated with the screening potential to that without it [i.e., $w(r)=(Ze)^2/r$]. The enhancement factor due to strong screening is thus given by $\exp[\tau-Q(\rho_0)]$, where ρ_0 is the value of ρ at which $Q(\rho)$ in Eq. (2.52) is minimized; $(3\Gamma/\tau)\rho_0 a$ then represents the classical turning radius at the Gamow peak. The values of $\tau-Q(\rho_0)$ so computed can be reproduced by the following formula within errors less than 1%:

$$\tau-Q(\rho_0)=1.25\Gamma-0.095\tau(3\Gamma/\tau)^2 . \tag{2.53}$$

The effects of possible deviation of $H(r)$ from Eq. (2.39) in the vicinity of $r=0$ [cf. Eq. (2.41)] have also been investigated (Itoh *et al.*, 1979) and found to induce a negligible correction to Eq. (2.53). For a carbon plasma ($Z=6$) at $T=10^8$ K with mass density 10^9 g/cm^{-3}, the resulting enhancement factor turns out to be $\sim 6\times 10^{16}$; at $T=5\times 10^7$ K with the same mass density it becomes $\sim 3\times 10^{30}$.

An enhancement factor in dense, binary mixture of ions has been calculated by Itoh *et al.* (1979).

D. Analytic treatments of static correlations

1. Density-functional approach

Analytic theories accounting for the static properties of a strongly coupled plasma have been concerned, to a certain degree, with a derivation of a relevant expression for the local-field correction $G(q)$; as explained in Sec. II.A, this function measures the extent to which the particle interactions affect the static correlational properties in such a plasma. In the polarization potential model of condensed matter, proposed by Pines (1966), the local-field correction enters the expression for the scalar polarization potential characterizing that portion of the restoring forces responsible for the collisionless part of the excitation spectrum which couples directly to the density fluctuations in the system.

The local-field correction can be described in terms of the density-functional formalism due originally to Hohenberg, Kohn, and Sham (Hohenberg and Kohn, 1964; Kohn and Sham, 1965; see also Mermin, 1965; Schneider, 1971; Singwi, 1976; Chihara, 1978). In this section I briefly review this formalism as applied to the OCP problems.

The free energy of an interacting inhomogeneous plasma in a static external potential $v_{\rm ext}(\mathbf{r})$ may be expressed as

$$F[n(\mathbf{r})]=\int d\mathbf{r}\, v_{\rm ext}(\mathbf{r})n(\mathbf{r}) +\frac{(Ze)^2}{2}\int d\mathbf{r}\int d\mathbf{r}'\frac{n(\mathbf{r})n(\mathbf{r}')}{|\mathbf{r}-\mathbf{r}'|} +F_0[n(\mathbf{r})]+F_{XC}[n(\mathbf{r})] . \tag{2.54}$$

Here, $F_0[n(\mathbf{r})]$ denotes the free energy of a free-particle system with density $n(\mathbf{r})$; $F_{XC}[n(\mathbf{r})]$ then refers to the remaining exchange and correlation energy of the interacting system.

Assuming that the plasma density has the form

$$n(\mathbf{r})=n+\delta n(\mathbf{r}) ,$$

with $|\delta n(\mathbf{r})|/n \ll 1$ and

$$\int d\mathbf{r}\,\delta n(\mathbf{r})=0 , \tag{2.55}$$

one finds a basic equation of the density-functional formalism through minimization of $F[n(\mathbf{r})]$ with respect to variations of $n(\mathbf{r})$, that is,

$$\frac{\delta F_0[n(\mathbf{r})]}{\delta n(\mathbf{r})}+\frac{\delta F_{XC}[n(\mathbf{r})]}{\delta n(\mathbf{r})}+v_H(\mathbf{r})=0 , \tag{2.56}$$

where

$$v_H(\mathbf{r})=v_{\rm ext}(\mathbf{r})+\int d\mathbf{r}'\frac{(Ze)^2}{|\mathbf{r}-\mathbf{r}'|}\delta n(\mathbf{r}') \tag{2.57}$$

is the Hartree field.

To the lowest order in $\delta n(\mathbf{r})$ the first two terms in Eq. (2.56) should be linear in $\delta n(\mathbf{r})$ on account of Eq. (2.55), so that one writes

$$\int d\mathbf{r}'\left[K_0(\mathbf{r}-\mathbf{r}';n)+K_{XC}(\mathbf{r}-\mathbf{r}';n)+\frac{(Ze)^2}{|\mathbf{r}-\mathbf{r}'|}\right]\times\delta n(\mathbf{r}')+v_{\rm ext}(\mathbf{r})=0\ . \tag{2.58}$$

The kernels, K_0 and K_{XC}, introduced in Eq. (2.58) as the second functional derivatives of $F_0[n(\mathbf{r})]$ and $F_{XC}[n(\mathbf{r})]$ around $n(\mathbf{r})=n$, depend only on $|\mathbf{r}-\mathbf{r}'|$ and n, the average number density. The spatial Fourier transformation of Eq. (2.58) yields

$$[\tilde{K}_0(q;n)+\tilde{K}_{XC}(q;n)+v(q)]\delta\tilde{n}(\mathbf{q})+\tilde{v}_{\rm ext}(\mathbf{q})=0\ . \tag{2.59}$$

Here, for example,

$$\tilde{K}_0(q;n)=\int d\mathbf{r}\,K_0(r;n)\exp(-i\mathbf{q}\cdot\mathbf{r})\ , \tag{2.60}$$

and $v(q)=4\pi(Ze)^2/q^2$.

Equation (2.59) is a relation describing the linear static dielectric response of the plasma. A direct calculation yields

$$\tilde{K}_0(q;n)=-1/\chi_0(q,0) \tag{2.61}$$

(Hohenberg and Kohn, 1964; Mermin, 1965), where $\chi_0(q,0)$ is the static polarizability of a free-particle system; for the classical OCP, $\chi_0(q,0)=-n/k_BT$. The static dielectric function is then obtained from Eq. (2.59) as

$$\varepsilon(q,0)=1-\frac{v(q)\chi_0(q,0)}{1+v(q)G(q)\chi_0(q,0)}\ , \tag{2.62}$$

where we have set

$$\tilde{K}_{XC}(q;n)=-v(q)G(q)\ . \tag{2.63}$$

On comparing Eqs. (2.6) and (2.62), one finds that the function $G(q)$ introduced via Eq. (2.63) corresponds to the local-field correction.

The condition for the onset of a soft-mode CDW instability is obtained from the second functional derivative of $F[n(\mathbf{r})]$, that is,

$$\delta^2F[n(\mathbf{r})]/\delta n(\mathbf{r})^2=0\ . \tag{2.64}$$

One thus finds from Eqs. (2.59) and (2.62) the critical condition for a CDW instability at the wave number q as Eq. (2.36) or equivalently,

$$v(q)+K_0(q)+K_{XC}(q)=0\ . \tag{2.65}$$

A similar criterion for the instability has been obtained also by Chan and Heine (1973).

2. Expressions for the local-field correction

For a classical OCP, the principal effect that goes into determination of the local-field correction is the interparticle correlation brought about by the Coulomb repulsion; no exchange effects need to be taken into consideration. A self-consistent formulation of such a Coulomb-induced local-field effect was proposed by Hubbard (1967) for degenerate electron liquids at metallic densities.

Independently, Singwi, Tosi, Land, and Sjölander (STLS) (1968) advanced a detailed theory of electron correlations at metallic densities, in which a semiclassical calculation of $G(q)$ was given as a functional of $S(q)$. These authors truncated the Bogoliubov-Born-Green-Kirkwood-Yvon (BBGKY) hierarchy of the kinetic equations (e.g., Ichimaru, 1973; Hansen and McDonald, 1976) by assuming that the two-particle distribution function $f_2(\mathbf{r},\mathbf{p};\mathbf{r}',\mathbf{p}'\,|\,t)$ was expressed in terms of the single-particle distribution function $f_1(\mathbf{r},\mathbf{p}\,|\,t)$ as

$$f_2(\mathbf{r},\mathbf{p};\mathbf{r}',\mathbf{p}'\,|\,t)=f_1(\mathbf{r},\mathbf{p}\,|\,t)f_1(\mathbf{r}',\mathbf{p}'\,|\,t)g(\mathbf{r}-\mathbf{r}')\ , \tag{2.66}$$

where $g(\mathbf{r})$ was taken to be the *equilibrium,* radial distribution function. Solving a linear density-response problem in the first equation of the BBGKY hierarchy, they derived the expression

$$G_{\rm STLS}(q)=-\frac{1}{n}\int\frac{d\mathbf{k}}{(2\pi)^3}\frac{\mathbf{q}\cdot\mathbf{k}}{k^2}[S(|\mathbf{q}-\mathbf{k}|)-1] \tag{2.67}$$

for the local-field correction. A combination of Eqs. (2.4) and (2.67) then makes a self-consistent integral equation for determination of $S(q)$ or $G(q)$ in the classical OCP; numerical solution to this equation was carried out by Berggren (1970).

The STLS scheme provided a substantially improved prediction over the RPA scheme on the short-range correlation in the OCP. At the same time a number of shortcomings were noted: When the STLS theory was applied to a weakly coupled OCP ($\Gamma\ll1$), it failed to reproduce the known Γ expansion of the excess internal energy beyond the Debye-Hückel term. According to Abe (1959), the excess internal energy for $\Gamma\ll1$ is expressed as

$$\frac{U_{\rm ex}}{Nk_BT}=-\frac{\sqrt{3}}{2}\Gamma^{3/2}-3\Gamma^3[\tfrac{3}{8}\ln(3\Gamma)+\tfrac{1}{2}\gamma-\tfrac{1}{3}]\ , \tag{2.68}$$

where $\gamma=0.577\,21\ldots$ is Euler's constant; the first term on the right-hand side is the Debye-Hückel term. Some terms of expansion beyond Eq. (2.68) have also been calculated (Cohen and Murphy, 1969).

A second problem noted on the STLS scheme concerns the compressibility sum rule. This sum rule is the requirement that the isothermal compressibility calculated from the evaluation of thermodynamic functions such as Eq. (2.9) be equal to that obtained from the long-wavelength behavior of $S(q)$ as illustrated in Eqs. (2.4) and (2.5). This imposes a structural constraint on $S(q)$, in that the integrated strength of Eq. (2.7) over the entire q domain should be consistent with the limiting values of

$S(q)$ at $q\to 0$ determined from Eqs. (2.4) and (2.5). The STLS theory exhibited a substantial discrepancy between the values of the compressibility calculated in those two different ways.

A couple of proposals were put forward on the expression for $G(q)$ to improve on the points remarked above. Singwi, Sjölander, Tosi, and Land (1970) thus suggested

$$G_{\rm SSTL}(q)=-\frac{1}{n}\int\frac{d\mathbf{k}}{(2\pi)^3}\frac{\mathbf{q}\cdot\mathbf{k}}{k^2\varepsilon(k,0)}\times[S(|\mathbf{q}-\mathbf{k}|)-1]\,, \tag{2.69}$$

which was capable of reproducing Eq. (2.68). Subsequently, through investigation of the compressibility, Schneider (1971) and Vashishta and Singwi (1972) proposed the form

$$G_{\rm VS}(q)=\left[1+a_0 n\frac{\partial}{\partial n}\right]G_{\rm STLS}(q)\,. \tag{2.70}$$

The parameter a_0 is to be chosen in such a way that the resulting formulation satisfies the compressibility sum rule; for the classical OCP, $a_0=\frac{1}{2}$. This formulation, however, fails to reproduce Eq. (2.68) beyond the Debye-Hückel term.

The local-field correction can also be obtained directly from a solution of the second member of the BBGKY hierarchy; the Born-Green equation (e.g., Feynman, 1972) relating between the pair and ternary correlation functions can be transformed in a form (Tago, Utsumi, and Ichimaru, 1981)

$$G(q)=-\frac{1}{nS(q)}\int\frac{d\mathbf{k}}{(2\pi)^3}K(\mathbf{q},\mathbf{k})[S(|\mathbf{q}-\mathbf{k}|)-1+\tfrac{1}{2}\tilde{h}^{(3)}(\mathbf{q}-\mathbf{q},\mathbf{k})]\,, \tag{2.71}$$

where

$$K(\mathbf{q},\mathbf{k})=\frac{\mathbf{q}\cdot\mathbf{k}}{k^2}+\frac{\mathbf{q}\cdot(\mathbf{q}-\mathbf{k})}{|\mathbf{q}-\mathbf{k}|^2}\,, \tag{2.72}$$

$$\tilde{h}^{(3)}(\mathbf{k}_1,\mathbf{k}_2)=n^2\int d\mathbf{r}_{13}\int d\mathbf{r}_{23}h^{(3)}(r_{12},r_{23},r_{31})\exp(-i\mathbf{k}_1\cdot\mathbf{r}_{13}-i\mathbf{k}_2\cdot\mathbf{r}_{23})\,, \tag{2.73}$$

$$\mathbf{r}_{ij}=\mathbf{r}_i-\mathbf{r}_j\,, \tag{2.74}$$

and $h^{(3)}(r_{12},r_{23},r_{31})$ refers to the radial part of the ternary correlation function (e.g., Ichimaru, 1973). The hierarchy can be terminated if the ternary correlation function is expressed in terms of the pair correlation function in Eq. (2.71); a self-consistent integral equation will result through a combination with Eq. (2.4).

Ichimaru (1970, 1978) introduced the convolution approximation in Eq. (2.71), so that the ternary correlation function is expressed as

$$h_C^{(3)}(r_{12},r_{23},r_{31})=h(r_{12})h(r_{23})+h(r_{23})h(r_{31})+h(r_{31})h(r_{12})+n\int d\mathbf{r}_4 h(r_{14})h(r_{24})h(r_{34})\,, \tag{2.75}$$

where

$$h(r)=g(r)-1 \tag{2.76}$$

is the radial part of the pair correlation function. Graphically Eq. (2.75) may be represented as in Fig. 11. It was in fact shown by O'Neil and Rostoker (1965) that the BBGKY long-range solution of the ternary correlation function for an OCP in the weak-coupling limit ($\Gamma\ll 1$) takes the form Eq. (2.75), where the pair correlation function is given by the Debye-Hückel formula,

$$h(r)=-\frac{(Ze)^2}{k_B T r}\exp\left[-\frac{r}{\lambda_D}\right]. \tag{2.77}$$

By adopting the convolution approximation (2.75) in the second BBGKY solution (2.71), one thus automatically guarantees accuracy of the resulting long-range solution of the pair correlation function to the first two terms in the Γ expansion. Abramo and Tosi (1972, 1974) also investigated certain aspects of the convolution approximation.

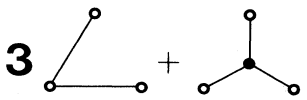

FIG. 11. Convolution approximation for the ternary correlation function.

Substitution of Eq. (2.75) in Eq. (2.71) yields

$$G_C(q)=-\frac{1}{n}\int\frac{d\mathbf{k}}{(2\pi)^3}\frac{\mathbf{q}\cdot\mathbf{k}}{k^2}S(k)\times[S(|\mathbf{q}-\mathbf{k}|)-1]\,. \tag{2.78}$$

Analytic structures of and numerical solution to the resulting integral equation were subsequently studied by Totsuji and Ichimaru (1973, 1974). It was shown explicitly that Eq. (2.78) reproduces the Abe formula, Eq. (2.68); the isothermal compressibility calculated from the long-wavelength expression Eq. (2.5) agrees with the exact result up to the term proportional to $\Gamma^3\ln\Gamma$ in Eq. (2.68). The convolution scheme, Eq. (2.78), thus offers a description of static properties in the classical OCP superior to the STLS scheme, Eq. (2.67). Numerical solutions for the excess internal energy in those various schemes are compared with the Monte Carlo data in the domain $\Gamma\lesssim 3$ in Fig. 12.

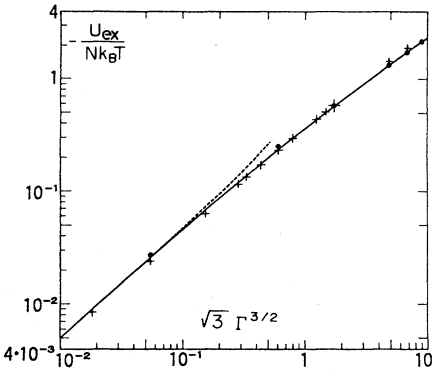

FIG. 12. The excess internal energy versus $\sqrt{3}\,\Gamma^{3/2}$, the coupling constant appropriate to a weakly coupled plasma. The solid curve depicts the theoretical result on the basis of the convolution approximation, Eq. (2.78); the dotted curve, the cluster-expansion result, Eq. (2.68). The filled circles represent the Monte Carlo data of Brush *et al.* (1966); the crosses, solution to the STLS scheme, Eq. (2.67), obtained by Berggren (1970). From Totsuji and Ichimaru (1974).

3. The hypernetted chain equation

For the classical OCP, the hypernetted chain (HNC) equation developed in the theory of liquids (e.g., van Leeuwen, Groeneveld, and De Boer, 1959; Morita, 1960) is known to provide a theoretical description much more accurate than the Percus-Yevick equation (Percus and Yevick, 1958) or the integral equations discussed in the preceding section. We thus begin this section with a brief introduction of the HNC approximation.

In terms of the Mayer cluster expansion (e.g., Rice and Gray, 1965; Hansen and McDonald, 1976), the radial distribution function may be exactly expressed as

$$g(r)=\exp\{-[\phi(r)/k_BT]+N(r)+B(r)\}\ . \tag{2.79}$$

Here $\phi(r)$ represents the interparticle potential [for the OCP, $\phi(r)=(Ze)^2/r$]; $N(r)$ refers to the sum of the nodal diagrams; and $B(r)$, that of all bridge diagrams. The nodal function $N(r)$ can then be written as

$$N(r)=h(r)-c(r)\ , \tag{2.80}$$

where $c(r)$ is the direct correlation function; this function is connected to the pair correlation function $h(r)$ via the Ornstein-Zernike relation,

$$h(r)=c(r)+n\int d\mathbf{r}'c(|\mathbf{r}-\mathbf{r}'|)h(r')\ . \tag{2.81}$$

The HNC approximation corresponds to assuming $B(r)=0$ in Eq. (2.79). One then has a closed set of equations, so that $h(r)$ and $c(r)$ may be calculated from a solution of Eq. (2.81) and the HNC equation,

$$g(r)=1+h(r)$$
$$=\exp\{-[\phi(r)/k_BT]+h(r)-c(r)\}\ . \tag{2.82}$$

In the HNC approximation the local-field correction takes the form

$$G(q)=-\frac{1}{n}\int\frac{d\mathbf{k}}{(2\pi)^3}\frac{\mathbf{q}\cdot\mathbf{k}}{k^2}[S(|\mathbf{q}-\mathbf{k}|)-1]$$
$$\times\{1+[1-G(k)][S(k)-1]\}\ . \tag{2.83}$$

We note here that the STLS scheme Eq. (2.67) may be obtained by setting $G(k)=1$ on the right-hand side of Eq. (2.83); the convolution formula, Eq. (2.78), can be derived by assuming $G(k)=0$ there. Interrelationship and comparison between the HNC, the STLS, the convolution, and other theoretical schemes have been examined and discussed in the literature (e.g., Chihara, 1973; Choquard, 1978; Chihara and Sasaki, 1979).

The numerical solution to the HNC equation for the OCP was carried out by Springer, Pokrant, and Stevens (1973) for the radial distribution function and the excess internal energy in the domain $0.05\le\Gamma\le50$; this solution was subsequently extended more accurately by Ng (1974) in the domain $20\le\Gamma\le7000$.

Those HNC data for the excess internal energy were fitted by DeWitt (1976) with the result

$$U_{ex}/Nk_BT=-0.900\,470\Gamma+0.268\,826\,3\Gamma^{1/2}$$
$$+0.071\,999\,25\ln\Gamma+0.053\,791\,9 \tag{2.84}$$

for $\Gamma>1$. Quantitatively the HNC internal energy agrees with the Monte Carlo data over the entire fluid range $\Gamma<\Gamma_m$ with discrepancies of less than 1%. The main reason for the apparent good agreement of the HNC and Monte Carlo results is that the static Madelung-like term in the HNC energy is very close to that for the Monte Carlo fluid energy, Eq. (2.11). The static term from HNC is nearly identical to the ion-sphere result (-0.9Γ) and is 0.5% below the bcc lattice value ($-0.895\,929\Gamma$), whereas the static term in Eq. (2.11) is 0.18% below the bcc lattice value. The remaining thermal energy from HNC is significantly different from the Monte Carlo form, $\Gamma^{1/2}$ vs $\Gamma^{1/4}$, and the HNC thermal-energy function is numerically larger than the Monte Carlo thermal-energy function; this difference is about 45% at $\Gamma=150$.

This relative inaccuracy of HNC in reproducing the Monte Carlo thermal energy poses a certain problem particularly in the treatment of miscibility in the classical binary mixtures of ions. The study of thermodynamic properties of such a binary ion mixture thus far has been based on the solution of the coupled HNC equations supplemented by a few runs of the Monte Carlo simulation (Hansen and Vieillefosse, 1976; Hansen, Torrie, and Vieillefosse, 1977; Brami, Hansen, and Joly, 1979). It has been found (Hansen *et al.*, 1977) that the Monte Carlo energies are systematically lower than their HNC counterparts, though the relative difference is always less than 1%, a situation quite similar to the OCP. According to these analyses, the excess internal energy of a two-component system with number densities n_1 and n_2 ($n=n_1+n_2$) for charges Z_1 and Z_2 appears to satisfy a linear relation (DeWitt, 1978; Brami *et al.*, 1979),

$$\left[\frac{U_{\rm ex}}{Nk_BT}\right]_{BIM} \simeq x_1 u(Z_1^{5/3}\Gamma_e)+x_2 u(Z_2^{5/3}\Gamma_e) , \tag{2.85}$$

where

$$x_1 = 1-x_2 = n_1/n , \tag{2.86}$$

$$\Gamma_e = e^2/a_e k_B T , \tag{2.87}$$

$$a_e = [4\pi(Z_1 n_1 + Z_2 n_2)/3]^{-1/3} , \tag{2.88}$$

and $u(\Gamma)$ refers to the OCP values of $U_{\rm ex}/Nk_BT$.

A linear relation such as Eq. (2.85) follows directly from the ion-sphere model described in Sec. II.B.2. According to the ion-sphere prescription, the static energy for the binary ion mixture is calculated as

$$(U_{\rm ex}/Nk_BT)_{\rm IS} = -0.9(x_1 Z_1^{5/3} + x_2 Z_2^{5/3}) \times e^2/a_e k_B T . \tag{2.89}$$

When the negative-charge density or a_e is kept constant, this expression depends linearly on the composition x_1 or x_2, as Eq. (2.85) does. Since both the Monte Carlo and HNC internal energies in the strong coupling domain [cf. Eqs. (2.11) and (2.84)] are dominated by the Madelung-like contributions proportional to Γ, it is naturally expected that a linear relation such as Eq. (2.85) will hold to a good degree of accuracy and that the Monte Carlo and HNC values will closely agree with each other for the binary ion mixtures, as well.

To the extent that Eq. (2.85) or (2.89) is applicable, one can thus define and calculate an "effective" electric charge $Z_{\rm eff}$ by setting the right-hand side of Eq. (2.89) equal to $-0.9Z_{\rm eff}^2 e^2/ak_BT$ [cf. Eq. (1.5)]. This is thus an average charge in the ion-sphere scaling (Salpeter, 1954), and is given by

$$Z_{\rm eff} = (\overline{Z^{5/3}}\,\overline{Z}^{1/3})^{1/2} . \tag{2.90}$$

Here the averages of charges are defined as

$$\overline{Z^\nu} = x_1 Z_1^\nu + x_2 Z_2^\nu . \tag{2.91}$$

Validity of such an ion-sphere scaling has also been demonstrated in the behavior of screening functions for the binary ion mixtures (Itoh *et al.*, 1979).

If a linear relation such as Eq. (2.85) holds *exactly*, there will be no difference in the excess free energy between the mixed phase and the separated phase of the binary ion mixture so long as the density of the negative-charge background is kept constant. Since there additionally exists the ideal entropy of mixing, which acts to lower the free energy in the mixed phase, this would imply that the different ions could mix at any ratio. In order to treat the problem of miscibility, one must therefore have a reliable knowledge on the extent of deviation from Eq. (2.85), which should stem from the thermal energy contributions. Here the HNC approach is not sufficiently accurate, as we have seen; indications from the Monte Carlo simulations are not conclusive yet, since the deviations are close to the Monte Carlo noise level (DeWitt, 1978).

4. Modifications of the HNC scheme

The HNC approximation, though superior to all the analytic schemes proposed thus far for the treatment of the OCP, still exhibits a systematic departure from the Monte Carlo results in the strong-coupling domain $\Gamma > 1$. We have noted its relative inaccuracy in predicting the thermal energy part of the excess internal energy. As we observe in Figs. 13(a) and 14, the behaviors of the HNC radial distribution function and screening potential differ somewhat from those indicated in the Monte Carlo simulation; the amplitudes of the oscillations in $g(r)$ are usually underestimated in HNC. The compressibility sum rule is violated significantly in the HNC equation (Baus and Hansen, 1980). It is therefore meaningful to attempt a further improvement of the HNC scheme for the analytic treatment of the OCP.

Obviously from the derivation of the HNC equation (2.82), a possible area of improvement lies in the treatment of the bridge functions $B(r)$. Through investigation of the Monte Carlo simulation data on fluids with a wide class of different interparticle potentials, Rosenfeld and Ashcroft (1979) advanced the following ansatz of universality: To within the accuracy of present-day computer-simulation studies [usually about 2% for $g(r)$] the bridge functions constitute the same family of

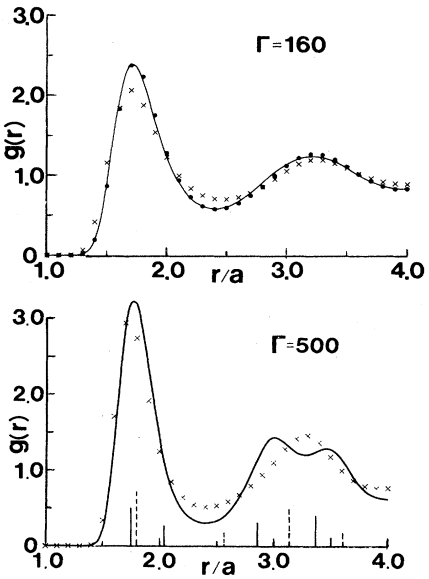

FIG. 13. (a) The radial distribution function at $\Gamma = 160$. The filled circles represent the Monte Carlo results due to Slattery *et al.* (1980); the crosses, the HNC results. The solid curve depicts an improved HNC calculation, on the basis of Eq. (2.102). From Iyetomi and Ichimaru (1982a). (b) The radial distribution function computed in the improved HNC scheme (solid curve) and that in the simple HNC scheme (crosses) for the OCP with $\Gamma = 500$. The vertical solid and dashed lines are proportional to the numbers of the particles located in the neighboring bcc and fcc lattice sites divided by the square of the interparticle separation. From Iyetomi and Ichimaru (1982b).

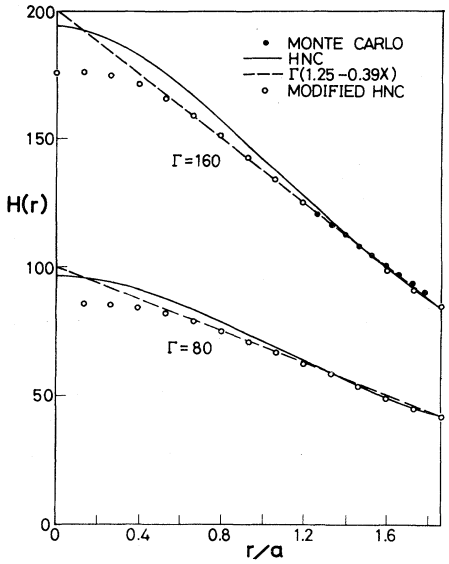

FIG. 14. Screening potential at $\Gamma=80$ and 160. The solid curves refer to the HNC results; the dashed curves, Eq. (2.39). The filled circles represent Monte Carlo data; the open circles, the results of the modified HNC calculation due to Rosenfeld and Ashcroft (1979). From Rosenfeld and Ashcroft (1979).

curves, irrespective of the assumed pair potential. In view of the known parametrized results for hard spheres (cf. Sec. II.B.3), this ansatz then leads to an improved HNC theory applicable to any potential: One chooses the hard-sphere bridge functions $B_{\rm HS}(r;\eta)$ and replaces $\phi(r)$ in Eq. (2.82) by $\phi(r)-k_BTB_{\rm HS}(r;\eta)$; the only free parameter η—the packing fraction for the hard-sphere system—may be determined by requiring thermodynamic consistency, such as the compressibility sum rule. As the comparison in Fig. 14 illustrates, the thermodynamics and radial distribution resulting from this modified HNC scheme are nearly indistinguishable from the exact Monte Carlo results.

Another possibility of improvement on the HNC equation stems from application of the density-functional approach described in Sec. II.D.1 (Iyetomi and Ichimaru, 1982a). One here begins by placing a test particle of the same kind as the plasma particles at $\mathbf{r}=0$, and regards its Coulomb potential as $v_{\rm ext}(r)$ in Eq. (2.54). The resulting density variation, $n(r)=n+\delta n(r)$, then gives the radial distribution function as (e.g., Percus, 1964)

$$g(r)=n(r)/n\ ,\quad \text{or}\quad h(r)=\delta n(r)/n\ . \tag{2.92}$$

The function $F_0[n(r)]$ will be treated exactly according to

$$F_0[n(r)]=U_0+k_BT\int d\mathbf{r}'n(r')\{\ln[n(r')]-1\}\ , \tag{2.93}$$

where the internal energy U_0 is independent of $\delta n(r)$. The exchange and correlation part is expanded with respect to $\delta n(r)$, so that

$$\begin{aligned}F_{XC}[n(r)]=F_{XC}[n]&+\frac{1}{2!}\int d\mathbf{r}\int d\mathbf{r}'K_{XC}(\mathbf{r}-\mathbf{r}')\delta n(r)\delta n(r')\\&+\frac{1}{3!}\int d\mathbf{r}\int d\mathbf{r}'\int d\mathbf{r}''K_{XC}^{(3)}(\mathbf{r}-\mathbf{r}',\mathbf{r}-\mathbf{r}'')\delta n(r)\delta n(r')\delta n(r'')\\&+\frac{1}{4!}\int d\mathbf{r}\int d\mathbf{r}'\int d\mathbf{r}''\int d\mathbf{r}'''K_{XC}^{(4)}(\mathbf{r}-\mathbf{r}',\mathbf{r}-\mathbf{r}'',\mathbf{r}-\mathbf{r}''')\delta n(r)\delta n(r')\delta n(r'')\delta n(r''')+\cdots\ .\end{aligned} \tag{2.94}$$

The function $K_{XC}(\mathbf{r}-\mathbf{r}')$ has been introduced in Eq. (2.58); relations such as Eq. (2.63) are to be noted on this function. The kernels, $K_{XC}^{(3)},K_{XC}^{(4)},\ldots$, basically correspond to nonlinear density-response functions of the system. In a different context, some formal aspect of such nonlinear response has been studied by Kalman and his collaborators (e.g., Kalman, 1978; Golden, 1978).

A solution of Eq. (2.56) with the aid of Eqs. (2.4), (2.57), and (2.81) then yields Eq. (2.37), with

$$w(r)=\frac{(Ze)^2}{r}-k_BT[h(r)-c(r)]+\left[\frac{\delta}{\delta n(r)}F_{XC}[n(r)]\right]^{(\geq 3)}\ . \tag{2.95}$$

Here the last term represents the sum of the contributions from those terms containing $K_{XC}^{(3)}$ and higher in the expansion (2.94) (Iyetomi and Ichimaru, 1982a). In view of Eqs. (2.79) and (2.80), one thus finds

$$B(r)=-\frac{1}{k_BT}\left[\frac{\delta}{\delta n(r)}F_{XC}[n(r)]\right]^{(\geq 3)}\ . \tag{2.96}$$

The bridge functions therefore correspond to that part of the screening potential involving the nonlinear density-response kernels in the expansion of Eq. (2.94).

Salient features of the HNC equation may be illustrated through examination of those terms neglected in it. The double Fourier transformation of $K_{XC}^{(3)}$ is explicitly calculated as

$$\tilde{K}_{XC}^{(3)}(\mathbf{q}_1,\mathbf{q}_2)=\frac{k_BT}{n^2}\left[1-\frac{S^{(3)}(\mathbf{q}_1,\mathbf{q}_2)}{S(q_1)S(q_2)S(q_3)}\right]\ , \tag{2.97}$$

where $\mathbf{q}_3=\mathbf{q}_1+\mathbf{q}_2$, and

$$S^{(3)}(\mathbf{q}_1,\mathbf{q}_2)=-2+S(q_1)+S(q_2)+S(q_3)+\tilde{h}^{(3)}(\mathbf{q}_1,\mathbf{q}_2)\ . \tag{2.98}$$

This function represents the double Fourier transformation of the radial part of the ternary distribution function.

Let us note that Eq. (2.97) contains a product of three static structure factors in its denominator. As a combination of Eqs. (2.4) and (2.5) indicates, the static structure factor vanishes in the long-wavelength limit for the system with long-range Coulomb interaction. Unless due care is taken in the evaluation of $S^{(3)}(\mathbf{q}_1,\mathbf{q}_2)$, therefore, Eq. (2.97) will retain a divergent behavior as q_1, q_2, or q_3 approaches zero. Higher-order kernels such as $\tilde{K}_{XC}^{(4)}(\mathbf{q}_1,\mathbf{q}_2,\mathbf{q}_3)$ involve terms containing correspondingly higher-order products of the structure factors in their denominators.

When the convolution approximation Eq. (2.75) is adopted in the calculation of Eq. (2.98), one finds that $\tilde{K}_{XC}^{(3)}(\mathbf{q}_1,\mathbf{q}_2)$ of Eq. (2.97) identically vanishes. Similarly, one can show that $\tilde{K}_{XC}^{(4)}(\mathbf{q}_1,\mathbf{q}_2,\mathbf{q}_3)$ likewise vanishes when the quaternary correlation function is expressed in the convolution approximation. One may thus conclude that the HNC equation is obtained in the density-functional formalism if the convolution approximation is adopted in the calculation of the functional derivatives of $F_{XC}[n(r)]$ in Eq. (2.94). Here one sees the reason why the HNC scheme has been so successful in describing the static properties of the classical OCP: The convolution approximation on which the HNC equation is based guarantees convergence of the functional derivatives of $F_{XC}[n(r)]$ in the long-wavelength domain for the Coulomb interacting system. Relation between the HNC equation and the convolution approximation has been elucidated also through the technique of the nodal expansion of the potential of average force (del Rio and DeWitt, 1969; Deutsch, Furutani, and Gombert, 1976).

Since the convolution approximation accurately takes account of long-range correlation in the Coulomb system, the area where one seeks to improve the HNC approximation is the short-range correlation. We thus write the ternary correlation function as a sum of the convolution expression Eq. (2.75) and a correction thereto,

$$h_{CK}^{(3)}(r_{12},r_{23},r_{31})=h_{C}^{(3)}(r_{12},r_{23},r_{31}) +\delta h^{(3)}(r_{12},r_{23},r_{31}) . \tag{2.99}$$

A simple and typical correlation term describing the short-range effect is the Kirkwood superposition-approximation term as depicted in the first, triangular diagram on the right-hand side of Fig. 15. Substitution of this Kirkwood term alone in Eq. (2.97) would, however, lead to a divergent expression in the long-wavelength domain, as it cannot cancel the structure factors in the denominator. To avoid such a divergence one must convolute each interacting vertex and collect all the diagrams as depicted in Fig. 15. We then find

$$[K_{XC}^{(3)}(\mathbf{r}-\mathbf{r}',\mathbf{r}-\mathbf{r}'')]_{CK}=-k_BTh(|\mathbf{r}-\mathbf{r}'|) \times h(|\mathbf{r}'-\mathbf{r}''|)h(|\mathbf{r}''-\mathbf{r}|) , \tag{2.100}$$

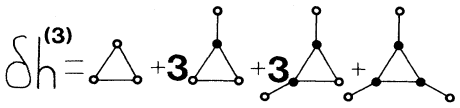

FIG. 15. Kirkwood superposition approximation and its convoluted terms.

whence the Bridge functions, Eq. (2.96), are obtained as

$$B_{CK}(r)=\frac{n^2}{2}\int d\mathbf{r}'\int d\mathbf{r}''h(|\mathbf{r}-\mathbf{r}'|)h(|\mathbf{r}'-\mathbf{r}''|) \times h(|\mathbf{r}''-\mathbf{r}|)h(r')h(r'') . \tag{2.101}$$

It turns out that the bridge function (2.101) corresponds to the simplest elementary bridge diagram shown in Fig. 16.

On the basis of those calculations one now has a systematic scheme of improving the HNC equation in the framework of the OCP theory (Iyetomi and Ichimaru, 1982a): One first solves the HNC equation Eq. (2.82) and writes the resulting correlation functions as $h_{\mathrm{HNC}}(r)$ and $c_{\mathrm{HNC}}(r)$. The bridge function is then evaluated by stretching the short-range part to approximate ion-sphere values as

$$B(r)=\left\{(C-1)\exp\left[-\left[\frac{r}{\xi a}\right]^2\right]+1\right\}B_{CK}(r) , \tag{2.102}$$

where $B_{CK}(r)$ is calculated by substituting $h_{\mathrm{HNC}}(r)$ on the right-hand side of Eq. (2.101). The stretching coefficient C is determined with the aid of Eqs. (2.38), (2.41), and (2.95) as

$$C=[1.057\Gamma+c_{\mathrm{HNC}}(0)+1]/B_{CK}(0) ;$$

the other parameter takes on the value $\xi=1.6$, reflecting the condition $B_{CK}(\xi a)\simeq 0$. Finally, one replaces $\phi(r)$ in Eq. (2.82) by $\phi(r)-k_BTB(r)$, and thereby solves the resulting HNC equation together with Eq. (2.81). A result computed according to this scheme is also shown in Fig. 13(a); a significant improvement over the original HNC result is clearly observed. The excess internal energy obtained in the improved scheme now agrees with the Monte Carlo data with digression less than 0.15%.

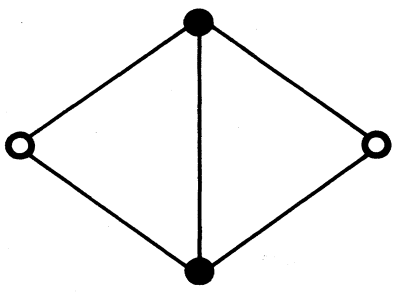

FIG. 16. Bridge diagram for Eq. (2.101).

5. Possibility of an amorphous glassy state

Iyetomi and Ichimaru (1982b) extended the solution of the improved HNC equation into the supercooled domain, $\Gamma > \Gamma_m$. In this domain it has been observed that the modification over the simple HNC scheme is substantial and that the difference widens as Γ increases. At the moment we have no published Monte Carlo data with which to compare the results to assure accuracy. [Unpublished Monte Carlo data for $g(r)$ obtained at $\Gamma=180$ and 200 by Slattery *et al.* (1980) agree excellently with the improved HNC results.] The improved HNC results are presented here as a microscopic solution to the OCP correlation function in the supercooled domain, in the expectation that their accuracy, established in the subcritical domain ($\Gamma \leq 160$), may be carried over in this domain, as well.

The most striking features in the improved HNC solution are the broadening (at $\Gamma=200$), and the subsequent splitting into two parts (for $\Gamma \geq 300$), of the second peak in $g(r)$; the case with $\Gamma=500$ is shown in Fig. 13(b). We may interpret this splitting as an indication of the short-range crystalline order extended to the third and fourth nearest-neighbor particles. In the simple HNC scheme, analogous splitting of the second peak has been observed for $\Gamma \geq 5000$ (Ng, 1974). To guide the eye we show by vertical solid or dashed lines in Fig. 13(b) the numbers of the particles located in the neighborhood bcc or fcc lattice sites divided by the square of the interparticle separation. Since the numbers of the second nearest-neighbor particles are relatively small in the bcc and fcc lattices, they would not contribute to creation of substantial peak structures.

It has been argued in Sec. II.C.2 that the characteristic feature in the short-range correlation up to the first peak of $g(r)$ may be accounted for in terms of a harmonic lattice model even in the subcritical domain ($4 \leq \Gamma \leq 160$). We now find that such a crystalline order extends itself to the third and fourth nearest-neighbor particles for $\Gamma \geq 300$. This observation may suggest an amorphous glassy state of the OCP in which minicrystals with internal crystalline order developed over several lattice constants are randomly distributed. A way to confirm formation of such a glassy state would be to monitor an abrupt decrease in the coefficient of self-diffusion; a preliminary indication from the Monte Carlo runs at $\Gamma=500$ appears to sustain such a picture (DeWitt, private communication).

For the classical OCP, the knowledge on $g(r)$ can be transformed into the static dielectric function $\varepsilon(q,0)$ via Eqs. (2.1) and (2.6); the condition for the onset of a soft-mode CDW instability is given by Eq. (2.36). Such a criterion has been examined in Fig. 6; as we see here, we may expect that the metastability of the fluid phase will persist well beyond $\Gamma=500$.

It has been stated in Sec. I.A that the Γ parameters of the white dwarfs may range 10—200; some of them have thus passed through the crystallization point Γ_m in their processes of cooling. If a supercooled OCP is difficult to freeze, as has been indicated, the interior of such a white dwarf may remain in an amorphous glassy state, whose thermodynamic functions are continuations of those in the subcritical fluid phase.

E. Dynamic properties

1. Velocity autocorrelation function

The velocity autocorrelation function (VAF) offers one of the simplest physical quantities revealing the dynamic properties of a many-particle system. The VAF is the correlation function for the velocity $\mathbf{v}_1(t)$ of a tagged particle "1" at time t with its initial velocity $\mathbf{v}_1(0)$, that is,

$$Z(t)=\tfrac{1}{3}\langle \mathbf{v}_1(t)\cdot\mathbf{v}_1(0)\rangle = \langle v_{1x}(t)v_{1x}(0)\rangle \ . \tag{2.103}$$

In Eq. (2.103), $\langle \cdots \rangle$ denotes a statistical average over an equilibrium ensemble; isotropy of the system is assumed, so that a Cartesian component $v_{1x}(t)$ of the velocity suffices for a description of $Z(t)$.

The long-time behavior of the VAF is related to the coefficients of self-diffusion and friction, D_s and $1/\tau_s$; these are calculated through the Kubo formula and the Einstein relation as

$$\int_0^\infty dt\, Z(t)=D_s=\tau_s\frac{k_BT}{M} \ , \tag{2.104}$$

where M is the particle mass.

The short-time behavior of the VAF reveals the extent of local-field effects via the frequency-moment sum rules (e.g., Ichimaru, Totsuji, Tange, and Pines, 1975). Expanding the VAF as

$$\frac{Z(t)}{Z(0)}=1+\frac{A_2}{2!}+\frac{A_4}{4!}t^4+\cdots \ , \tag{2.105}$$

one finds that the coefficients, $A_2, A_4, \ldots$, can be calculated with the knowledge of static correlation functions. In particular, A_2 is expressed as (de Gennes, 1959)

$$A_2=\frac{n}{M}\int d\mathbf{r}\left[\frac{\partial\phi(r)}{\partial x}\right]\left[\frac{\partial g(r)}{\partial x}\right] \ , \tag{2.106}$$

where $\phi(r)$ is the interparticle potential. For a three-dimensional OCP one simply has $A_2=-\omega_p^2/3$ on account of $h(0)=g(0)-1=-1$, where

$$\omega_p^2=4\pi(Ze)^2n/M \tag{2.107}$$

is the square of the plasma frequency. For a two-dimensional layer of electrons, A_2 has been computed directly from Eq. (2.106) (Itoh *et al.*, 1978). The expression for A_4 involves the ternary correlation function (Ichimaru *et al.*, 1975; Hansen, 1978; Nagano and Ichimaru, 1980).

The VAF for a three-dimensional, strongly coupled OCP has been extensively measured by Hansen and his collaborators (Hansen, Pollock, and McDonald, 1974; Hansen, McDonald, and Pollock, 1975) through the tech-

nique of molecular dynamics simulation over a wide range of the Γ values. One may classify the VAF so computed into three types as illustrated in Fig. 17: At $\Gamma=0.993$, the VAF exhibits a behavior of the *simple decay* type; at $\Gamma=9.7$ and 19.7, the VAF turns into the *oscillatory decay* type; and finally at $\Gamma=59.1$, 110.4, and 152.4, the VAF shows the *damped oscillatory* behavior. The distinction between the oscillatory decay type and the damped oscillatory type may be made in relation to the possibility of the VAF's moving into negative domain, indicating a reversal of the tagged-particle velocity. Those qualitative changes in the VAF may point to essential differences in the internal structure of the strongly coupled OCP.

A theoretical investigation of the VAF was carried out by Gould and Mazenko (1975, 1977) on the basis of the fully renormalized kinetic theory formalism (e.g., Mazenko, 1974). They introduced an effective interaction approximation for a reduced two-body problem and calculated the memory function of the VAF, incorporating the hydrodynamic modes for the long-time behavior. The diffusion coefficient and the memory function computed in this scheme showed a semiquantitative agreement with the results of the molecular dynamics simulation.

Sjödin and Mitra (1977; see also, Mitra and Sjödin, 1978; Sjölander, 1978) investigated the self- and collective motion of the OCP with the aid of a kinetic theory of classical fluids developed by Sjögren and Sjölander (1978). The memory function of the VAF was expressed in terms of the propagator for the density fluctuations and its self part, in a way analogous to the Gould and Mazenko theory. They adopted a Gaussian approximation for the self part, and thereby computed the VAF at $\Gamma=1$ and 10.

Nagano and Ichimaru (1980) analyzed the memory function of the VAF separately in the short-time and long-time domains, with the aid of the frequency moment sum rules and a hydrodynamic consideration. For the hydrodynamic analysis they evoked the idea of an equivalent hard-sphere system (cf. Sec. II.B.3), and employed the calculation of a frequency-dependent friction coefficient for the vibrational motion of a spherical body in a Navier-Stokes fluid (e.g., Zwanzig and Bixon, 1970; Landau and Lifshitz, 1959). Through interpolation of those two calculations of the memory function, they attempted to explain the physical origin of the three different types of the observed VAF in the following way:

When $\Gamma\simeq 1$, the interparticle correlation is relatively weak, so that the tagged particle readily loses the memory of its initial state after collisions with mutually independent, surrounding particles; the simple decay type is expected for the VAF.

As Γ increases, the short-range order evidenced by the oscillatory behavior in the radial distribution function begins to appear (cf. Fig. 1); it is known from the Monte Carlo simulation that the onset of such a short-range order takes place at $\Gamma\simeq 3$. The mean potential field around the tagged particle now acts to induce an oscillatory motion superposed on the predominantly decay behavior. The correlation effect is not so strong yet as to produce the reversal of the initial velocity; the oscillatory decay type may result.

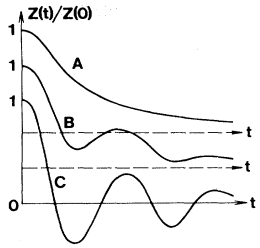

FIG. 17. Schematic drawing of three types of the velocity autocorrelation function observed in the molecular dynamics simulation of Hansen *et al.* (1974, 1975): (A) depicts the simple decay type; (B), the oscillatory decay type; (C), the damped oscillatory type.

As Γ approaches the crystallization point, the short-range order becomes so pronounced that the harmonic lattice model (see Sec. II.B.2) starts to apply; it was shown in Eq. (2.17) that the harmonic lattice model provides an accurate account of the excess internal energy for $70\leq\Gamma\leq 160$. In the harmonic lattice model the short-range order is described by that of an equivalent crystalline lattice; the particles perform vibrational motion around their equilibrium positions. The reversal of the tagged particle velocity from its initial value is naturally expected in these circumstances; the damped oscillatory behavior of the VAF may result. The same effect can also be accounted for in relation to the penetration depth term in the generalized hydrodynamic friction.

Molecular dynamics simulation of the VAF for the two-dimensional classical layer of electrons on a spherical surface was carried out by Hansen, Lebesque, and Weis (1979). A theoretical account of this experiment was offered by Baus (1980).

2. Dynamic structure factor

The dynamic structure factor $S(q,\omega)$ represents the wave number and frequency spectrum of density fluctuation excitations in a many-particle system. It is defined and calculated as the space-time Fourier transform of the density-density correlation function (e.g., Ichimaru, 1973),

$$S(q,\omega)=\frac{1}{2\pi}\int_{-\infty}^{\infty}d(t_1-t_2)\int d(\mathbf{r}_1-\mathbf{r}_2)\langle n(\mathbf{r}_1,t_1)n(\mathbf{r}_2,t_2)\rangle \exp[-i\mathbf{q}\cdot(\mathbf{r}_1-\mathbf{r}_2)+i\omega(t_1-t_2)]\,, \tag{2.108}$$

where $n(\mathbf{r},t)$ refers to the number density at space-time, $\mathbf{r}$ and t. The static structure factor introduced in Eq. (2.1) then derives from Eq. (2.108) as

$$S(q)=\frac{1}{N}\int_{-\infty}^{\infty}d\omega\, S(q,\omega)\ . \tag{2.109}$$

Spectral functions for current fluctuations can be defined and calculated analogously to Eq. (2.108).

Molecular dynamics computations of the dynamic structure factor were carried out by Hansen *et al.* (1974, 1975) for three-dimensional OCP systems, and by Totsuji and Kakeya (1980) for two-dimensional systems of surface electrons. In the long-wavelength domain the frequency spectra of density fluctuations exhibited sharp peak structures, indicating existence of a well-defined plasma-wave mode; the characteristic dispersion of the plasma wave was determined from such an observation. The frequency spectra of transverse current fluctuations were also measured; existence of a well-defined shear mode was thereby suggested in those strongly coupled states near the crystallization points.

A number of investigators (e.g., Hansen *et al.*, 1975; Abramo and Parrinello, 1975; Sjödin and Mitra, 1977; Bosse and Kubo, 1978a, 1978b; Takeno and Yoshida, 1979; Cauble and Duderstadt, 1981) have attempted to reproduce those experimental values of the dynamic structure factor for three-dimensional OCP by theoretical means. All of those theories rely on the memory-function formalism or the projection-operator method (Mori, 1965a, 1965b; Zwanzig, 1961). Some quantities characterizing those memory functions are determined with the aid of the frequency-moment sum rules applicable to the longitudinal and transverse fluctuation spectra. The relaxation processes are treated phenomenologically (e.g., Cauble and Duderstadt, 1981) by choosing appropriate values for the transport coefficients. Bosse and Kubo (1978a, 1978b), on the other hand, have used a mode-coupling approximation for the longitudinal and transverse memory functions; this theory thus takes account of those decay processes of current fluctuations into pairs of current and density fluctuations due to interparticle interactions. Theoretical spectra quite analogous to the experimental ones have been obtained by these methods.

Kinetic theory for density and current fluctuations in a strongly coupled OCP has been developed and applied for the calculation of the shear viscosity by Wallenborn and Baus (1978; see also, Baus, 1978). It has been speculated that the discovery of well-defined shear modes in the molecular dynamics simulations may offer another demonstration for the latticelike short-range order in the three- and two-dimensional OCP near the crystallization points (Itoh and Ichimaru, 1980a, 1980b).

3. Dielectric response function

The dynamic structure factor of the plasma can be calculated with the knowledge of the dielectric response function $\varepsilon(q,\omega)$ via the fluctuation-dissipation theorem (Callen and Welton, 1951; Kubo, 1957); for the classical OCP, this theorem relates (e.g., Ichimaru, 1973)

$$S(q,\omega)=-\frac{Vk_BTq^2}{4\pi^2(Ze)^2\omega}\,\mathrm{Im}\frac{1}{\varepsilon(q,\omega)}\ . \tag{2.110}$$

A combination of Eqs. (2.109) and (2.110) yields the first equality of Eq. (2.6).

The dielectric response function may be defined as the ratio between the externally applied potential field $\phi_{\rm ext}(\mathbf{q},\omega)$ with wave vector $\mathbf{q}$ and frequency ω and the resulting total field $\phi_{\rm tot}(\mathbf{q},\omega)$ in the plasma, that is,

$$\phi_{\rm tot}(\mathbf{q},\omega)=\phi_{\rm ext}(\mathbf{q},\omega)/\varepsilon(q,\omega)\ . \tag{2.111}$$

It is therefore a kind of linear-response function. A dielectric formulation or a description of the plasma properties in terms of the dielectric response function will be treated in more detail later in Sec. III.A.

For a weakly coupled OCP ($\Gamma\ll 1$), the dielectric response function may be calculated from a solution of the linearized Vlasov equation (Vlasov, 1938; Ichimaru, 1973); it is expressed in the RPA formula as

$$\varepsilon(q,\omega)=1+\frac{q_D^2}{q^2}W\left[\frac{\omega}{q(k_BT/M)^{1/2}}\right]\ . \tag{2.112}$$

Here q_D refers to the Debye wave number given by Eq. (2.3), and the W function is defined by

$$W(z)=1-z\exp\left[-\frac{z^2}{2}\right]\int_0^z dy\exp\left[\frac{y^2}{2}\right]+i\left[\frac{\pi}{2}\right]^{1/2}z\exp\left[-\frac{z^2}{2}\right]\ . \tag{2.113}$$

This function, sometimes called the plasma dispersion function (Fried and Conte, 1961), is closely related to the error function of a complex argument z. Substitution of Eq. (2.112) in Eq. (2.6) reproduces Eq. (2.2).

For a theoretical treatment of a strongly coupled plasma, one must take account of the essential correlation effects, which are neglected in Eq. (2.112). The local-field corrections in Sec. II.D.2, such as Eqs. (2.67), (2.69), (2.70), and (2.78), were originally formulated in connection with the dielectric response function expressed as

$$\varepsilon(q,\omega)=1+\frac{(q_D/q)^2W[\omega/q(k_BT/M)^{1/2}]}{1-(q_D/q)^2G(q)W[\omega/q(k_BT/M)^{1/2}]}\ . \tag{2.114}$$

Since those expressions for the local-field correction account only for static effects independent of ω, a theory based on Eq. (2.114) is applicable to a description of the static properties such as Eq. (2.6). It has been used, however, for an approximate calculation of the plasma-wave dispersion relation.

To go beyond the RPA description, one may attempt to include the nonlinear polarizabilities in perturbation expansions with respect to the external disturbance. Some formal structures of such a nonlinear polarizability have been investigated (e.g., Golden, Kalman, and Silev-

itch, 1974; Golden and Kalman, 1979).

Ichimaru (1977) carried out a systematic renormalization of the single-particle propagators and took account of the strong correlations through diagrammatic resummation of polarization processes and vertex corrections. The dielectric response function is written in a form of Eq. (2.114) where $G(q)$ is replaced by the dynamic local-field correction $G(q,\omega)$; this function is formulated as a functional of $\varepsilon(q,\omega)$, $S(q,\omega)$, and the single-particle distribution function. The system of equations is then closed by another relation stemming from the fluctuation-dissipation theorem. The resulting theory has been examined to conform with a number of rigorous boundary conditions, such as dynamic modification of effective particle interactions brought about by strong correlations, frequency-moment sum rules, and reproduction of exact results known in the static properties of the OCP. Numerical solution to the set of nonlinear integral equations has not been obtained, however.

4. Long-wavelength excitations

In the limit of long wavelengths, the plasma consists essentially of sets of elementary excitations, weakly interacting with each other. The properties of those elementary excitations can then be analyzed in terms of the moment sum rules in the frequency domain of the dynamic structure factor to various orders of approximation (Ichimaru, Totsuji, Tange, and Pines, 1975). The sum rules are evaluated exactly with the knowledge of the static correlation functions of the system (e.g., de Gennes, 1959; Puff, 1965; Forster, Martin, and Yip, 1968). We may thus employ the results of investigations such as those described in Sec. II.D, for the examination of the elementary excitations in the long-wavelength limit.

To investigate the properties of the long-wavelength excitations in the OCP, we express the dynamic structure factor in that domain as a superposition of the contributions from the plasma oscillations, the single-particle excitations, and the collisional excitations (Ichimaru *et al.*, 1975):

$$S(q,\omega)=\frac{N}{2}S_p(q)[\delta(\omega-\omega_q)+\delta(\omega+\omega_q)] +S_s(q,\omega)+S_c(q,\omega)\ . \tag{2.115}$$

Here ω_q represents the characteristic frequency of the plasma oscillation with the wave number q; the frequencies of the single-particle and collisional excitations, $S_s(q,\omega)$ and $S_c(q,\omega)$, are measured in units of their characteristic frequencies, $q(k_BT/M)^{1/2}$ and $\bar{\omega}$. The collisional excitations are the classical counterpart to the multipair excitations in the degenerate electron liquid (Pines and Nozières, 1966). It is important to recognize that the characteristic frequency $\bar{\omega}$ remains finite in the long-wavelength limit, $q\to 0$.

The frequency moments of the dynamic structure factor are defined and calculated according to

$$\langle\omega^l\rangle=\frac{1}{N}\int_{-\infty}^{\infty}d\omega\,\omega^l S(q,\omega)\ . \tag{2.116}$$

The moment at $l=0$ is the same as Eq. (2.109), giving rise to the static structure factor. The $l=2$ term yields the f-sum rule; the evaluation of the $l=4$ moment involves the pair correlation function; the $l=6$ moment involves the ternary correlation function.

Various functions in Eq. (2.115) may be expanded in power series of $(q/q_D)^2$ in the long-wavelength domain. The frequency of the plasma oscillation is thus written as

$$\omega_q=\omega_p[1+\delta(q/q_D)^2+\cdots]\ , \tag{2.117}$$

where the coefficient δ characterizes the plasma-wave dispersion. One can define the static structure factors, $S_s(q)$ and $S_c(q)$, associated with $S_s(q,\omega)$ and $S_c(q,\omega)$ in accord with Eq. (2.109); those structure factors, as well as $S_p(q)$, are likewise expanded in powers of $(q/q_D)^2$.

Comparing the terms proportional to $(q/q_D)^2$ in the sum rules (2.116), we find that $S_p(q)$ begins with $(q/q_D)^2$, while the first nonvanishing terms in $S_s(q)$ and $S_c(q)$ are proportional to $(q/q_D)^4$. The contributions of the plasma oscillations thus exhaust the entire strength of the dynamic structure factor in the long-wavelength limit.

The dispersion δ in the plasma-wave frequency may be analyzed directly from a sum-rule analysis of the dielectric response function. If the existence of the collisional excitations is totally neglected, one can complete the sum-rule analysis up to the $l=4$ term in Eq. (2.116); the result is (Ichimaru and Tange, 1974; Abramo and Tosi, 1974)

$$\delta=\frac{3}{2}+\frac{2}{15}\frac{U_{\rm ex}}{Nk_BT}\ . \tag{2.118}$$

The first term on the right-hand side is the RPA contribution stemming from Eq. (2.112). The second term representing a correlational contribution takes on negative values as Eqs. (2.11) and (2.12) illustrate; the dispersion coefficient as evaluated in Eq. (2.118) becomes negative for a strongly coupled OCP with $\Gamma\gg 1$.

The presence of collisional excitations becomes significant as we proceed to take into account the next $l=6$ term, as well, in Eq. (2.116); we then obtain

$$\delta=\tfrac{3}{2}+\tfrac{1}{2}\tau(\Gamma)-\frac{2}{15}\frac{U_{\rm ex}}{Nk_BT}\ , \tag{2.119}$$

where

$$\tau(\Gamma)=-\frac{3n(Ze)^2}{10\pi k_BT}\int d\mathbf{r}\int d\mathbf{r}'h^{(3)}(\mathbf{r},\mathbf{r}') \times\left[\frac{(\mathbf{r}\cdot\mathbf{r}')^3}{(rr')^5}-\frac{\mathbf{r}\cdot\mathbf{r}'}{(rr')^3}\right] \tag{2.120}$$

and $h^{(3)}(\mathbf{r},\mathbf{r}')$ is the same ternary correlation function as introduced in connection with Eq. (2.73); here we use $\mathbf{r}=\mathbf{r}_{13}$ and $\mathbf{r}'=\mathbf{r}_{23}$. Numerical values of $\tau(\Gamma)$ have been

computed with the aid of the convolution approximation, Eq. (2.75) (Ichimaru *et al.*, 1975).

Contrary to Eq. (2.118), the dispersion coefficient computed according to Eq. (2.119) takes on values slightly above the RPA value $\frac{3}{2}$ in the weak coupling regime $\Gamma<1$. As Γ exceeds a critical value around unity, Eq. (2.119) moves into the domain below $\frac{3}{2}$ and then goes over to negative domain with further increase of Γ, following the trend of Eq. (2.118) in the strong-coupling regime. Qualitatively analogous prediction on the dispersion coefficient has been obtained by Baus (1977) through a different approach.

The negative dispersion of the plasma wave in the strongly coupled OCP has been clearly observed in the molecular dynamics simulation experiments (Hansen *et al.*, 1974, 1975). The experimental results, however, are not sufficiently accurate that one can distinguish between the predictions of Eqs. (2.118) and (2.119) in the weak-coupling regime.

III. DEGENERATE ELECTRON LIQUIDS

A. Dielectric formulation

1. Basic relations

The wave number and frequency dependent, longitudinal dielectric function $\varepsilon(q,\omega)$, defined through Eq. (2.111) in Sec. II.E.3, is an essential quantity for description of the properties of the degenerate electron liquids; these may be found in metals and related substances, such as the laser-compressed plasmas and the interiors of heavy planets. Here again, the dynamic structure factor $S(q,\omega)$ defined by Eq. (2.108), portraying the spectrum of density-fluctuation excitations, is related directly to $\varepsilon(q,\omega)$ via the fluctuation-dissipation theorem. In the description of the long-wavelength and low-frequency excitations, the Landau-Silin theory of the charged Fermi liquid has been useful (e.g., Pines and Nozières, 1966).

Experimentally, the dynamic structure factor of electrons in metal has been measured through the technique of x-ray scattering spectroscopy or electron energy-loss spectroscopy (e.g., Raether, 1980). The static properties, such as the static structure factor, the radial distribution function, and the ground-state energy, may then be investigated with the knowledge of the integrated values of $S(q,\omega)$ over the frequencies. This section contains descriptions of some of those fundamental relations (see e.g., Pines and Nozières, 1966, for details), which will be of use in later sections.

The fluctuation-dissipation theorem as applied to the degenerate electron plasma at $T=0$ yields the relation

$$S(q,\omega)=-\frac{\hbar V q^2}{4\pi^2 e^2}\,\mathrm{Im}\frac{1}{\varepsilon(q,\omega)}\quad(\omega\geq 0)\,. \tag{3.1a}$$

The static structure factor $S(q)$ is calculated in accord with Eq. (2.109), which now reads

$$S(q)=-\frac{\hbar q^2}{4\pi^2 n e^2}\int_0^\infty d\omega\,\mathrm{Im}\frac{1}{\varepsilon(q,\omega)}\,. \tag{3.1b}$$

The radial distribution function is then obtained from the inverse Fourier transform of Eq. (2.1).

For calculation of the ground-state energy it is convenient to define an integral,

$$\gamma_\infty(r_s)=\frac{1}{5q_F}\int_0^\infty dq\,[1-S(q)]\,, \tag{3.2}$$

where

$$q_F=(3\pi^2 n)^{1/3} \tag{3.3}$$

is the Fermi wave number of a paramagnetic electron system with the number density n. The integral (3.2) is proportional to the excess internal energy treated in Eq. (2.7); it is a function of r_s alone for the degenerate electron system under consideration. The ground-state energy $E(r_s)$ per electron in Rydbergs ($\mathrm{Ry}=me^2/2\hbar^2=13.6$ eV) is then calculated as

$$E(r_s)=E_0(r_s)-\frac{10}{\pi\lambda r_s^2}\int_0^{r_s} dx\,\gamma_\infty(x)\,, \tag{3.4}$$

where $\lambda\equiv(4/9\pi)^{1/3}=0.521\ldots$ and

$$E_0(r_s)=\frac{3}{5\lambda^2 r_s^2}=\frac{2.21}{r_s^2}\quad(\mathrm{Ry}) \tag{3.5}$$

is the kinetic-energy contribution of the electrons occupying the Fermi sphere.

In the high-density limit $r_s\to 0$, the major source of interparticle correlation is the exchange effect brought about by the Pauli principle between those particles with parallel spin. The Hartree-Fock approximation applies, and the resulting structure factor is

$$S_{\mathrm{HF}}(q)=\begin{cases}\dfrac{3}{4}\dfrac{q}{q_F}-\dfrac{1}{16}\left[\dfrac{q}{q_F}\right]^3\,, & q\leq 2q_F\\ 1\,, & q>2q_F\,.\end{cases} \tag{3.6}$$

Substitution of this expression in Eq. (3.2) yields

$$\gamma_\infty^{\mathrm{HF}}=\tfrac{3}{20}\,, \tag{3.7}$$

so that the ground-state energy, Eq. (3.4), in the Hartree-Fock approximation is

$$\begin{aligned}E_{\mathrm{HF}}(r_s)&=\frac{3}{5\lambda^2 r_s^2}-\frac{3}{2\pi\lambda r_s}\\&=\frac{2.21}{r_s^2}-\frac{0.916}{r_s}\quad(\mathrm{Ry})\,.\end{aligned} \tag{3.8}$$

The correlation energy $E_c(r_s)$ is defined as the difference between the ground-state energy (3.4) and that in the Hartree-Fock approximation, Eq. (3.8), that is,

$$\begin{aligned}E_c(r_s)&=E(r_s)-E_{\mathrm{HF}}(r_s)\\&=\frac{10}{\pi\lambda r_s^2}\int_0^{r_s} dx\,[\tfrac{3}{20}-\gamma_\infty(x)]\,.\end{aligned} \tag{3.9}$$

For a degenerate electron gas in the weak-coupling regime ($r_s\ll 1$), it is known that the RPA gives an ade-

quate description; the dielectric function takes the Lindhard expression (Lindhard, 1954),

$$\varepsilon_0(q,\omega)=1-v(q)\chi_0(q,\omega)\ , \tag{3.10}$$

with

$$v(q)=4\pi e^2/q^2\ , \tag{3.11}$$

$$\chi_0(q,\omega)=\frac{2}{\hbar V}\sum_{\mathbf{p}}\frac{f_0(p)-f_0(|\mathbf{p}+\mathbf{q}|)}{\omega-\omega_{\mathbf{pq}}+i0}\ . \tag{3.12}$$

Here $f_0(q)$ is the unit step function,

$$f_0(q)=\begin{cases}1\ , & q\le q_F\\ 0\ , & q>q_F\end{cases} \tag{3.13}$$

representing the Fermi distribution at zero temperature,

$$\omega_{\mathbf{pq}}=(\hbar/2m)(2\mathbf{p}\cdot\mathbf{q}+q^2)\ , \tag{3.14}$$

and the positive infinitesimal 0 in the denominator of Eq. (3.12) serves to indicate that the response function is evaluated with the retarded boundary conditions. The static values of the polarizability, Eq. (3.12), are given by

$$\chi_0(q,0)=-\frac{3n}{2E_F}\left[\frac{1}{2}+\frac{q_F}{2q}\left[1-\frac{q^2}{4q_F^2}\right]\ln\left|\frac{q+2q_F}{q-2q_F}\right|\right]\ . \tag{3.15}$$

The static screening function $\varepsilon_0(q,0)$ in the RPA is then obtained from Eqs. (3.10) and (3.15).

The ground-state energy in the RPA can be evaluated by substituting Eq. (3.10) in Eq. (3.1a) and then by following the steps of Eqs. (3.1b), (3.2), and (3.4). Gell-Mann and Brueckner (1957) carried out a resummation of the ring diagrams, the result of which is equivalent to the RPA treatment. Adding to this an explicit Monte Carlo evaluation of the second-order exchange diagram contributions, they rigorously determined the first few terms of the ground-state energy in the high-density r_s expansion as

$$E_{\mathrm{GB}}(r_s)=\frac{2.21}{r_s^2}-\frac{0.916}{r_s}+0.062\ln r_s-0.096\ \ (\mathrm{Ry})\ . \tag{3.16}$$

Theoretical predictions on the basis of the RPA, while adequate for a description of an electron gas in weak-coupling regime, have failed to account for salient features observed experimentally in the electron liquids at metallic densities. For a treatment of the degenerate electron liquid in the strong-coupling regime ($r_s\gtrsim 1$), one must find a way to go beyond such an RPA description. In the following sections we shall review some of those methods hitherto proposed.

2. Polarization potential approach

As we have briefly noted in Sec. II.E.3, it is always possible to write the dielectric response function in a form

$$\varepsilon(q,\omega)=1-\frac{v(q)\chi_0(q,\omega)}{1+v(q)G(q,\omega)\chi_0(q,\omega)}\ . \tag{3.17}$$

Since the RPA expression (3.10) is recovered simply by setting $G(q,\omega)=0$ in Eq. (3.17), the dynamic local-field correction $G(q,\omega)$ measures the extent to which non-RPA effects are involved in the description of the system properties. Earlier theories on such local-field functions were reviewed by Kugler (1975).

The polarization potential approach to condensed matter, proposed originally by Pines (1966), is closely related to the formulation of dielectric function as in Eq. (3.17). This approach has been applied successfully to the description of elementary excitations and transport properties in HeII and in liquid helium-3 (Aldrich, Pethick, and Pines, 1976a , 1976b; Aldrich and Pines, 1976; Bedell and Pines, 1980a, 1980b). We now examine the polarization potential approach applied to the degenerate electron liquid.

Let $\phi_{\mathrm{pol}}(q,\omega)$ be the effective potential of interaction produced by the presence of density fluctuations $\delta\rho(q,\omega)$ in the plasma, which may be expressed as

$$\phi_{\mathrm{pol}}(q,\omega)=\psi(q,\omega)\delta\rho(q,\omega)\ . \tag{3.18}$$

The function $\psi(q,\omega)$ introduced here generally differs from the bare Coulomb potential, Eq. (3.11), due to the exchange and correlation effects between electrons. We next introduce the screened density response function $\chi_{\mathrm{sc}}(q,\omega)$ against the electrostatic potential $\phi_{\mathrm{ext}}(q,\omega)+\phi_{\mathrm{pol}}(q,\omega)$ via

$$\delta\rho(q,\omega)=\chi_{\mathrm{sc}}(q,\omega)[\phi_{\mathrm{ext}}(q,\omega)+\phi_{\mathrm{pol}}(q,\omega)]\ . \tag{3.19}$$

The dielectric response function is then calculated in accord with Eq. (2.111), which in the present case reads

$$\frac{1}{\varepsilon(q,\omega)}=1+v(q)\frac{\delta\rho(q,\omega)}{\phi_{\mathrm{ext}}(q,\omega)}\ . \tag{3.20}$$

The result takes the form

$$\varepsilon(q,\omega)=1-\frac{v(q)\chi_{\mathrm{sc}}(q,\omega)}{1-[\psi(q,\omega)-v(q)]\chi_{\mathrm{sc}}(q,\omega)}\ . \tag{3.21}$$

The essence of this approach thus lies in the introduction of an effective interaction potential $\psi(q,\omega)$ between microscopic density fluctuations and the consideration of a screened density response against a renormalized potential field in the plasma.

In the original treatment of Pines (1966), the restoring forces (3.18) responsible for the collisionless part of the excitation spectrum are described by two kinds of self-consistent fields: a scalar polarization potential which couples directly to the density fluctuations, and a vector polarization potential which couples to the particle-current density. In terms of the present notation, this model then yields

$$\psi(q,\omega)=v(q)\left[1-G(q)-\left[\frac{\omega}{q}\right]^2 G_1(q)\right]\ , \tag{3.22}$$

where $G(q)$ is the (static) local-field correction [cf. Eq. (2.63)] and $G_1(q)$ characterizes the vector-potential response related to the backflow effect.

Since the exchange and correlation effects have already been renormalized in the polarization potential Eq. (3.18), one may argue that the screened response function $\chi_{sc}(q,\omega)$ is given approximately by a free-electron polarizability, such as Eq. (3.12). Comparing Eq. (3.21) with Eq. (3.17), one then finds a correspondence,

$$\psi(q,\omega)=v(q)[1-G(q,\omega)] . \tag{3.23}$$

In the formulation of the static theory, one may further argue that the most important effect of the local-field correction stems from its static evaluation at $\omega=0$, i.e., $G(q,\omega=0)=G(q)$. Equation (3.17) can then be approximated as

$$\varepsilon(q,\omega)=1-\frac{v(q)\chi_0(q,\omega)}{1+v(q)G(q)\chi_0(q,\omega)} . \tag{3.24}$$

The dielectric response function of this form has been frequently derived in the literature (see, e.g., Kugler, 1975); it is valid for only an approximate treatment of the static properties.

3. Self-consistency conditions

A number of exact boundary conditions have been derived for the dielectric response function of the electron liquid. Those may be used as criteria by which internal consistency of a given dielectric formulation may be judged. This section lists some of those conditions.

a. Compressibility sum rule

In the long wavelength limit, the local-field correction $G(q)$ is expressed in a form proportional to q^2, so that

$$\lim_{q\to 0} G(q)=\gamma_0(r_s)(q/q_F)^2 . \tag{3.25}$$

The coefficient $\gamma_0(r_s)$ is connected with the compressibility

$$\kappa=-\left[V\frac{\partial P}{\partial V}\right]^{-1} \tag{3.26}$$

via the compressibility sum rule (e.g., Pines and Nozières, 1966) as

$$\frac{\kappa_0}{\kappa}=1-\left[\frac{4\lambda r_s}{\pi}\right]\gamma_0(r_s) , \tag{3.27}$$

where $\kappa_0=3/2E_F n$ is the compressibility of the noninteracting Fermi system.

The compressibility, on the other hand, can be evaluated directly from the ground-state energy (3.4) or the correlation energy (3.9), according to the definition (3.26), as

$$\frac{\kappa_0}{\kappa}=1-\frac{\lambda r_s}{\pi}+\frac{\lambda^2}{6}r_s^6\frac{d}{dr_s}\left[r_s^{-2}\frac{d}{dr_s}E_c(r_s)\right] . \tag{3.28}$$

The compressibility sum rule thus imposes a self-consistency condition that Eqs. (3.27) and (3.28) be equal. In the present notation this condition reads (Utsumi and Ichimaru, 1980b)

$$\gamma_0(r_s)=-\tfrac{5}{2}\gamma_\infty(r_s)+\tfrac{5}{12}r_s\frac{d\gamma_\infty(r_s)}{dr_s}+\frac{25}{6r_s}\int_0^{r_s}dx\,\gamma_\infty(x) . \tag{3.29}$$

The left-hand side of this equation involves the long-wavelength behavior of the dielectric function via Eq. (3.25), while the right-hand side depends on integrated values of $1-S(q)$ over the entire wave number space.

Combination of Eqs. (3.9) and (3.29) yields

$$\gamma_0(r_s)=\frac{1}{4}-\frac{\pi\lambda}{24}\left[r_s^3\frac{d^2E_c(r_s)}{dr_s^2}-2r_s^2\frac{dE_c(r_s)}{dr_s}\right] , \tag{3.30a}$$

$$\gamma_\infty(r_s)=\frac{3}{20}-\frac{\pi\lambda}{10}\left[r_s^2\frac{dE_c(r_s)}{dr_s}+2r_sE_c(r_s)\right] . \tag{3.30b}$$

The first terms on the right-hand side of Eqs. (3.30) are the Hartree-Fock values, correct in the weak-coupling limit, $r_s\to 0$.

b. Frequency-moment sum rules

The high-frequency expansion of $1/\varepsilon(q,\omega)$ takes the form

$$\frac{1}{\varepsilon(q,\omega)}=1+v(q)\left[\frac{M_1(q)}{\omega^2}+\frac{M_3(q)}{\omega^4}+\cdots\right] . \tag{3.31}$$

The coefficients, $M_1(q),M_3(q),\ldots,$ are evaluated in terms of the statistical averages of the equal-time commutators:

$$M_l(q)=\frac{1}{\hbar V}\left[i\frac{\partial}{\partial t}\right]^l\langle[\rho_{\mathbf{q}}(t),\rho_{\mathbf{q}}^\dagger(0)]\rangle\,|_{t=0} , \tag{3.32}$$

where

$$\rho_{\mathbf{q}}(t)=\sum_{j=1}^{N}\exp[-i\mathbf{q}\cdot\mathbf{r}_j(t)] \tag{3.33}$$

is the Heisenberg operator representing the Fourier component of the density fluctuations. Explicitly, one finds (Puff, 1965; Pathak and Vashishta, 1973)

$$M_1(q)=nq^2/m , \tag{3.34}$$

$$M_3(q)=(nq^2/m)\{4\langle K\rangle\omega_0(q)/\hbar+\omega_0^2(q)+\omega_p^2[1-I(q)]\} . \tag{3.35}$$

Here $\langle K\rangle$ represents the average kinetic energy per electron,

$$\omega_0(q)=\hbar q^2/2m , \tag{3.36}$$

$$I(q)=-\frac{1}{n}\int\frac{d\mathbf{k}}{(2\pi)^3}K(\mathbf{q},\mathbf{k})\frac{\mathbf{k}\cdot\mathbf{q}}{q^2}\times[S(|\mathbf{q}-\mathbf{k}|)-1] , \tag{3.37}$$

and $K(\mathbf{q},\mathbf{k})$ has been defined in Eq. (2.72).

Equation (3.34) represents the f-sum rule; Eq. (3.35) will be referred to as the third frequency-moment sum rule. The fifth frequency-moment sum rule $M_5(q)$ is the quantum-mechanical counterpart to the classical calculation, such as the one leading to Eq. (2.119); it involves the ternary correlation function. The function $I(q)$ in Eq. (3.37) corresponds to the high-frequency limit of the dynamic local-field correction in Eq. (3.17), that is,

$$I(q)=\lim_{\omega\to\infty} G(q,\omega) . \tag{3.38}$$

In the long-wavelength limit, it is proportional to q^2 and takes the form

$$\lim_{q\to 0} I(q)=\gamma_\infty(r_s)(q/q_F)^2 , \tag{3.39}$$

where $\gamma_\infty(r_s)$ is given by Eq. (3.2) or (3.30b).

c. Positivity of the radial distribution function

The positivity of the radial distribution function is expressed as

$$g(r)\geq 0 . \tag{3.40}$$

This condition follows because $g(r)$ is a probability.

d. Short-range correlation

Kimball (1973, 1976) has obtained a self-consistency relation between the large q limit of $S(q)$ and $g(0)$ as

$$g(0)=\frac{3\pi a_B}{8q_F^3}\lim_{q\to\infty}\{q^4[1-S(q)]\} , \tag{3.41}$$

where $a_B=\hbar^2/me^2$ is the Bohr radius. In the derivation of Eq. (3.41), he observes that the radial distribution function at short distances may be determined by the solution to the two-particle Schrödinger equation, which yields the expansion

$$g(r)=g(0)+[g(0)/a_B]r+\cdots . \tag{3.42}$$

On the other hand, a direct analysis of the inverse Fourier transform of Eq. (2.1) indicates

$$\left.\frac{d}{dr}g(r)\right|_{r=0}=\frac{3\pi}{8q_F^3}\lim_{q\to\infty}\{q^4[1-S(q)]\} , \tag{3.43}$$

whence Eq. (3.41) follows.

When the dielectric function is written in the form (3.24), the frequency integration of Eq. (3.1b) pertaining to the evaluation of the right-hand side of Eq. (3.41) can be explicitly carried out (Kimball, 1973). Equation (3.41) then relates the large q limit of $G(q)$ with $g(0)$ as

$$\lim_{q\to\infty} G(q)=1-g(0) . \tag{3.44}$$

This is therefore the self-consistency condition for the dielectric function (3.24) in the short-range correlation. Condition (3.44) was obtained earlier by Shaw (1970).

If one stays with the frequency-dependent local-field correction as in Eq. (3.17), however, Niklasson (1974) has shown that

$$\lim_{q\to\infty} G(q,\omega)=\tfrac{2}{3}[1-g(0)] .$$

B. Theoretical approaches

Various theoretical approaches have been used for the calculation of the dielectric function and correlation functions in the degenerate electron liquids; some of them are summarized in this section. Predictions of the theories will be described in the following sections.

1. Equation-of-motion approach

Let the Hamiltonian of the electron system be

$$H=\sum_{\mathbf{p}\sigma}\left[\frac{\hbar^2p^2}{2m}\right]c^\dagger_{\mathbf{p}\sigma}c_{\mathbf{p}\sigma}+\frac{1}{2V}\sum_{\substack{\mathbf{pp'q}\\ \sigma\sigma'}} v(q)c^\dagger_{\mathbf{p}+\mathbf{q}\sigma}c^\dagger_{\mathbf{p'}-\mathbf{q}\sigma'}c_{\mathbf{p'}\sigma'}c_{\mathbf{p}\sigma} , \tag{3.45}$$

where $c^\dagger_{\mathbf{p}\sigma}$ and $c_{\mathbf{p}\sigma}$ are the creation and annihilation operators for an electron with momentum $\hbar\mathbf{p}$ and spin σ. The Heisenberg equation of motion for the Wigner distribution,

$$\rho_{\mathbf{pq}\sigma}=c^\dagger_{\mathbf{p}\sigma}c_{\mathbf{p}+\mathbf{q}\sigma} , \tag{3.46}$$

of an electron-hole pair is then calculated as

$$i\hbar\frac{\partial}{\partial t}\rho_{\mathbf{pq}\sigma}(t)=[\rho_{\mathbf{pq}\sigma},H]$$

$$=\hbar\omega_{\mathbf{pq}}\rho_{\mathbf{pq}\sigma}(t) \tag{3.47a}$$

$$+\frac{1}{V}v(q)(n_{\mathbf{p}\sigma}-n_{\mathbf{p}+\mathbf{q}\sigma})\rho_{\mathbf{q}}(t) \tag{3.47b}$$

$$+\frac{1}{V}\sum_{\mathbf{k}(\neq\mathbf{p})} v(|\mathbf{k}-\mathbf{p}|)[(n_{\mathbf{k}\sigma}-n_{\mathbf{k}+\mathbf{q}\sigma})\rho_{\mathbf{pq}\sigma}(t)-(n_{\mathbf{p}\sigma}-n_{\mathbf{p}+\mathbf{q}\sigma})\rho_{\mathbf{kq}\sigma}(t)] \tag{3.47c}$$

$$+\frac{1}{V}\sum_{\substack{\mathbf{k}\\ (\neq 0,\mathbf{q})}} v(k)\sum_{\substack{\mathbf{p'}\sigma'\\ [\neq(\mathbf{p},\sigma)(\mathbf{p}+\mathbf{q},\sigma)]}}[\rho_{\mathbf{p},\mathbf{q}-\mathbf{k},\sigma}(t)\rho_{\mathbf{p'}-\mathbf{k},\mathbf{k},\sigma'}(t)-\rho_{\mathbf{p'k}\sigma'}(t)\rho_{\mathbf{p}+\mathbf{k},\mathbf{q}-\mathbf{k},\sigma}(t)] . \tag{3.47d}$$

Here ω_{pq} has been defined by Eq. (3.14),

$$n_{p\sigma}=c^{\dagger}_{p\sigma}c_{p\sigma}\ , \tag{3.48a}$$

$$\rho_q=\sum_{p\sigma}\rho_{pq\sigma}\ . \tag{3.48b}$$

In the RPA, only the terms (3.47a) and (3.47b) are retained in the equation of motion. The term (3.47c) stems from the exchange effect alone, as may be clear from its involvement of $v(|\mathbf{k}-\mathbf{p}|)$. The remaining term (3.47d) represents those nonlinear contributions arising from Coulomb coupling. The last two terms, therefore, describe those non-RPA effects which need to be taken into consideration in the treatment of a degenerate electron liquid in the strong-coupling regime.

There have been advanced various theoretical proposals to take account of such a non-RPA effect. For example, Toigo and Woodruff (1970, 1971) calculated the dynamic local-field correction $G(q,\omega)$ arising from the exchange term (3.47c), in an approximation which would conserve a frequency moment of the nonlinear density response. Dynamical exchange effects were also considered by Devreese, Brosens, and Lemmens [(1980); see also, Brosens, Devresse, and Lemmens (1980) and earlier publications cited in these papers)] through a perturbation-theoretical method; detailed numerical computations were carried out.

Niklasson (1974) formulated the dielectric response of the electron system with inclusion of the non-RPA terms such as (3.47c) and (3.47d), through a study of the equation of motion for the two-particle distribution in the presence of the external field. Limiting behavior of the resulting $G(q,\omega)$ at large q or ω was investigated explicitly in connection with relations such as Eqs. (3.41)–(3.44). The equation-of-motion approach to the dielectric function was pursued further by Dharmawardana (1976). The mass operator and the dynamic local-field correction were formulated with successive approximations in the interaction potential; contacts with the compressibility sum rule and the frequency moment sum rules were thereby made. Subsequently, Tripathy and Mandal (1977) and Mandal, Rao, and Tripathy (1978) treated a similar problem with a perturbation-theoretical approximation.

Utsumi and Ichimaru (1980a) started with the exact equation of motion (3.47) and projected it onto a model equation as follows:

$$i\hbar\frac{\partial}{\partial t}\rho_{pq}(t)=\hbar\omega_{pq}\rho_{pq}(t)+\frac{1}{V}v(q)[1-G(q)]\langle n_p-n_{p+q}\rangle\rho_q(t)$$
$$-i\hbar\left[\frac{2}{\pi}\right]^{1/2}\frac{\Omega(q)}{\tau(q)}\int_0^t ds\exp(-\tfrac{1}{2}\Omega^2(q)s^2)\left[\rho_{pq}(t-s)+\frac{2\langle n_p-n_{p+q}\rangle}{\hbar V\omega_{pq}Q(q,0)}\rho_q(t-s)\right]\ , \tag{3.49}$$

where

$$\rho_{pq}=\sum_{\sigma}\rho_{pq\sigma}\ ,\quad n_p=\sum_{\sigma}n_{p\sigma}\ , \tag{3.50}$$

$$Q(q,\omega)=\frac{2}{\hbar V}\sum_{p}\frac{\langle n_p-n_{p+q}\rangle}{\omega-\omega_{pq}+i0}\ . \tag{3.51}$$

This function reduces to the Lindhard polarizability (3.12) when the expectation value $\langle n_p\rangle$ is approximated by $f_0(p)$ defined by Eq. (3.13). Single-particle spectrum in the degenerate electron system has been treated by Hedin (1965), Lundqvist (1968), and others.

The RPA contributions in Eq. (3.47) correspond to the first term on the right-hand side of Eq. (3.49) and that part of the second term independent of $G(q)$. The rest of the terms are an approximate representation of the non-RPA terms, (3.47c) and (3.47d). Those terms describing the exchange and Coulomb coupling effects are characterized by three functions: the static local-field correction, $G(q)$; the relaxation rate in the long-time response, $1/\tau(q)$; and the relaxation frequency in the short-time response, $\Omega(q)$. The functions $G(q)$ and $1/\tau(q)$ are calculated from the first two terms in the small ω expansion of the nonlinear density response stemming from (3.47c) and (3.47d). The characteristic frequency $\Omega(q)$ is then determined from the frequency-moment sum rules (cf. Sec. III.A.3.b).

By its construction, Eq. (3.49) conserves the local number of particles, as it readily reduces to

$$i\hbar\frac{\partial}{\partial t}\rho_q(t)=\sum_{p}\hbar\omega_{pq}\rho_{pq}(t)\ , \tag{3.52}$$

which is a continuity equation. Mermin (1970) showed a way to secure such a conservation law within a relaxation time approximation; his treatment corresponds to taking the limit, $G(q)\to 0$ and $\Omega(q)\to 0$, in Fig. (3.49). Similarly, the static local-field correction theories [e.g., Singwi *et al.* (1968, 1970); Vashishta and Singwi (1972); Utsumi and Ichimaru (1980b); see Kugler (1975) and Sec. III.C below for many others] may be recovered by letting $1/\tau(q)\to 0$ in Eq. (3.49).

Once Eq. (3.49) is established, the dielectric response function can be calculated as (Utsumi and Ichimaru, 1980a)

$$\varepsilon(q,\omega)=1-\frac{v(q)(\tilde{\omega}/\omega)Q(q,\tilde{\omega})}{1+\{v(q)(\tilde{\omega}/\omega)G(q)+[(\tilde{\omega}-\omega)/\omega Q(q,0)]\}Q(q,\tilde{\omega})}\ , \tag{3.53}$$

where

$$\tilde{\omega}=\omega+\left[\frac{2}{\pi}\right]^{1/2}\frac{\Omega(q)}{\omega\tau(q)}\left[W\left[\frac{\omega}{\Omega(q)}\right]-1\right] \tag{3.54}$$

and the W function has been defined by Eq. (2.113). Involvement of this function in Eq. (3.53) is a consequence of a Gaussian approximation adopted in Eq. (3.49) for the description of the short-time relaxation behavior. Clearly, Eq. (3.53) can be rewritten in the form (3.17), so that the static and dynamic local-field corrections are taken into account. It has been shown that Eq. (3.53) provides a description of the long-wavelength excitations with inclusion of multipair excitations.

In the equation-of-motion approach summarized above, the exchange and correlation effects beyond the RPA have been singled out by the terms (3.47c) and (3.47d). Such effects have been investigated also with the aid of other theoretical techniques such as resummation of various diagrams and memory-function formalism. In the following sections we take up some of those theories.

2. Diagrammatic approach

Exchange and correlation effects in the degenerate electron system beyond the RPA have been studied intensively through investigation and partial summation of contributions stemming from various diagrams. In this section, we briefly look at theoretical work in these areas, although such a classification is by no means unique.

Hubbard (1958) and Geldart and Vosko (1966) analyzed the exchange effects and thereby advanced explicit expressions for the local-field correction (see Sec. III.C below). Kleinman (1967, 1968) and Langreth (1969) considered derivation of approximate screening functions using many-body techniques.

Yasuhara (1972, 1974) treated the short-range correlation through a summation of the electron-electron ladder diagrams. Lowy and Brown (1975) also considered the ladder sum of unscreened Coulomb interactions to describe the short-range part of the effective interaction, which was then smoothly interpolated to the long-range RPA effective interaction. Bedell and Brown (1978) rephrased the same physical concept in the polarization-potential language (cf. Sec. III.A.2), and constructed a density-density response function in which the bare Coulomb interaction is replaced by a local average of the ladder diagrams, including both direct and exchange terms.

Geldart and Taylor (1970a) calculated the lowest-order Hartree-Fock corrections to the wave number dependence of the static screening function; higher-order exchange and correlation effects were investigated subsequently (Geldart and Taylor, 1970b). Holas, Aravind, and Singwi (1979) explicitly evaluated those polarization diagrams, first order in the electron-electron interaction, beyond the RPA at arbitrary wave number and frequency; the plasmon dispersion and the shape of $S(q,\omega)$ predicted in this calculation were compared with experimental data for Al. Dharma-wardana and Taylor (1980) considered an approximation scheme to the Hartree-Fock ladder series in the treatment of the dielectric function.

The effects of the electron-electron interaction on the dynamic properties of the plasmons and other elementary excitations were investigated through diagrammatic techniques by DuBois and Kivelson (1969) and Hasegawa and Watabe (1969). Damping rate of high-frequency excitations was evaluated by Glick and Long (1971).

3. Memory function approach

The dynamic properties of the electron system have been investigated also in the general framework of the memory function formalism (Mori, 1965a, 1965b). Theories in this category include Jindal, Singh, and Pathak (1977); Mukhopadhyay and Sjölander (1978); De Raedt and De Raedt (1978); and Yoshida, Takeno, and Yasuhara (1980). In these theories one readily takes account of high-frequency requirements, such as the frequency-moment sum rules. Low-frequency properties, such as those described by the static local-field correction and the long-time relaxation rate, on the other hand, are usually taken from other sources or are not adequately taken into consideration.

4. Variational calculations

On the side of numerical evaluations of the basic quantities for the degenerate electron liquids, we note the development in variational calculations performed with various trial functions. Earlier work in these directions includes Monnier (1972), Lee and Ree (1972), Keiser and Wu (1972), Stevens and Pokrant (1973), and Chakravarty and Woo (1976).

Ceperley (1978) performed fermion Monte Carlo variational calculations assuming the trial function of the Bijl-Dingle-Jastrow type, and thereby determined the equation of state of the uniform electron one-component plasma in two and three dimensions. Phase properties of the Wigner crystal and of the spin-polarized and unpolarized fluids were investigated.

Lantto (1980) and Zabolitzky (1980) carried out variational calculations of the electron-gas correlations, where the Jastrow trial function is chosen to minimize the ground-state energy in the Fermi hypernetted-chain (FHNC) approximation by solving the corresponding Euler-Lagrange equation for the pair correlation function. Ceperley and Alder (1980) performed an exact stochastic simulation of the Schrödinger equation for charged bosons and fermions by the Green's function Monte Carlo (GFMC) method (e.g., Ceperley and Kalos, 1979). Numerical data obtained through those computer-simulation studies provide not only accurate information but also useful boundary conditions for the development of an analytic theory. In the subsequent sections we shall compare predictions in various theoretical schemes with those computer-simulation data.

C. Static local-field correction

The dielectric function of the form Eq. (3.24) has been studied frequently because of its relative simplicity as

compared with Eq. (3.17). It involves only the static local-field correction $G(q)$ to characterize the strong-coupling effect. Once $G(q)$ is known, various thermodynamic quantities and correlational properties can be calculated through the procedures outlined in Sec. III.A.1. In this section we shall examine some of the explicit expressions proposed for $G(q)$.

1. Exchange and correlation contributions

Taking account of the exchange contributions, Hubbard (1958) first proposed

$$G_H(q)=\frac{q^2}{2(q^2+q_F^2)} . \tag{3.55}$$

This expression satisfies the short-range boundary condition (3.44) at $r_s=0$ [i.e., $g(0)=\frac{1}{2}$]; it does not, however, agree with the long-wavelength boundary condition (3.25) as $\gamma_0=\frac{1}{4}$ at $r_s=0$ [cf. Eq. (3.30a)]. Geldart and Vosko (1966) modified Eq. (3.55) so that the condition (3.25) at $r_s=0$ is also satisfied:

$$G_{\rm GV}(q)=\frac{q^2}{2(q^2+2q_F^2)} . \tag{3.56}$$

At a nonzero value of r_s, however, neither Eq. (3.55) nor (3.56) satisfies the conditions (3.25) and (3.44).

Toigo and Woodruff (1970, 1971) carried out a microscopic calculation of the exchange effect to obtain a dynamic local-field correction, $G(q,\omega)$; the resulting values of $G(q,0)$ are consistent with Eq. (3.25) at $r_s=0$. Condition (3.44) does not follow in this case, however, since the dielectric function now takes the form Eq. (3.17) (Niklasson, 1974). The function $G(q,0)$ obtained by Toigo and Woodruff involves a logarithmic singularity at $q=2q_F$ accompanied by a mild peak at $q\simeq 1.95q_F$; these features are consequences of discontinuity in the Fermi distribution (3.13) at $q=q_F$.

Singwi *et al.* (1968) advanced a theoretical scheme in which the effects of Coulomb repulsion between electrons may be self-consistently taken account of in the calculation of $G(q)$. This scheme was later modified by Vashishta and Singwi (1972), to improve on the situation with the compressibility sum rule. We have already taken up those schemes in Sec. II.D.2, with the expressions for $G(q)$ given by Eqs. (2.67) and (2.70). For the degenerate electron liquids at metallic densities, Vashishta and Singwi chose $a_0=\frac{2}{3}$ in Eq. (2.70), by which the compressibility sum rule was almost identically satisfied. The local-field correction $G(q)$ and the screening function $[\varepsilon(q,0]^{-1}$ calculated in the Vashishta-Singwi scheme are plotted in Figs. 18 and 19 at $r_s=1$ and 4. In subsequent sections, we will look at implications of those theoretical schemes, through numerical comparison of ground-state energy and correlation function calculations with those of other theories.

Utsumi and Ichimaru (1980b) split the calculation of the static local-field correction into two separate contributions, namely, the exchange and nonlinear Coulomb coupling terms, stemming, respectively, from (3.47c) and (3.47d):

$$G(q)=G_{\rm ex}(q)+G_c(q) . \tag{3.57}$$

Since the exchange term $G_{\rm ex}(q)$ represents the local-field correction in the Hartree-Fock limit, $r_s\to 0$, they were led to adopt the expression

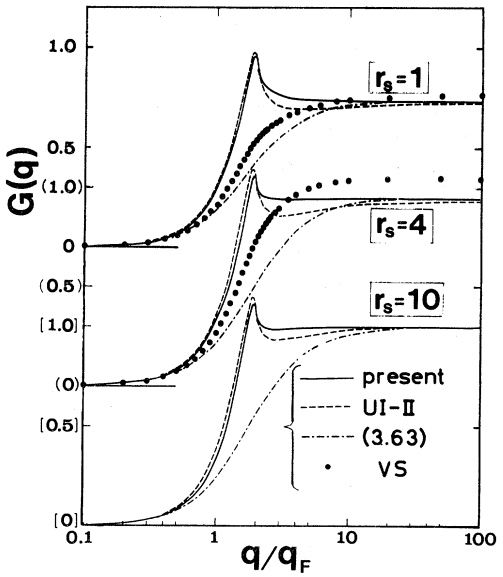

FIG. 18. Static local-field correction $G(q)$ at $r_s=1$, 4, and 10 evaluated in various theoretical schemes. VS refers to Eq. (2.70) with $a_0=\frac{2}{3}$; UI-II is the result of Utsumi and Ichimaru (1980b); "present" depicts the parametrization of Eq. (3.65). The chain curves represent parametrization of the Hubbard type based on Eq. (3.63).

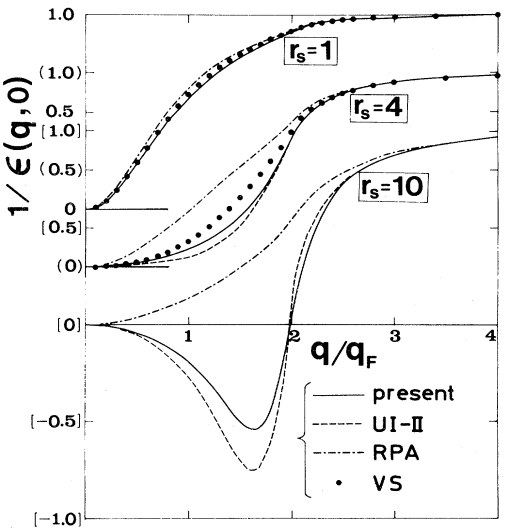

FIG. 19. Screening function $[\epsilon(q,0)]^{-1}$ at $r_s=1$, 4, and 10 evaluated in various theoretical schemes. VS refers to Eqs. (3.24) and (2.70), with $a_0=\frac{2}{3}$; UI-II is the result of Utsumi and Ichimaru (1980b); "present" depicts Eq. (3.24) with Eq. (3.65); and RPA corresponds to Eq. (3.10).

$$G_{\rm ex}(q)=\frac{q^2}{128q_F^2}\left[11+\frac{15q^2}{4q_F^2}+\frac{3(4q_F^2-q^2)(28q_F^2+5q^2)}{16q_Fq}\ln\left|\frac{2q_F+q}{2q_F-q}\right|\right] \tag{3.58}$$

through considerations of the limiting behaviors, Eqs. (3.25) and (3.44), together with the logarithmic singularity at $q=2q_F$.

The local-field correction $G_c(q)$ arising from the Coulomb correlations can likewise be calculated from the low-frequency response in (3.47d), as (Utsumi and Ichimaru, 1980b)

$$G_c(q)=-\frac{1}{n}\int\frac{d\mathbf{k}}{(2\pi)^3}K(\mathbf{q},\mathbf{k})S_{\rm WS}(k)[S(|\mathbf{q}-\mathbf{k}|)-S_{\rm HF}(|\mathbf{q}-\mathbf{k}|)]\ . \tag{3.59}$$

Here $K(\mathbf{q},\mathbf{k})$ and $S_{\rm HF}(q)$ have been defined by Eqs. (2.72) and (3.6);

$$S_{\rm WS}(q)=q^2/(q^2+q_{\rm WS}^2) \tag{3.60}$$

is a screening factor in accord with the Wigner-Seitz sphere model, with the characteristic wave number $q_{\rm WS}$ defined as

$$\frac{q_{\rm WS}}{q_F}=\frac{3}{2\pi}-\lambda\frac{d}{dr_s}[r_s^2E_c(r_s)]\ , \tag{3.61}$$

a relation derived from Eqs. (3.2) and (3.9).

To the lowest order in the structure factor, a direct calculation from (3.47d) would have given an expression for $G_c(q)$ which involves the RPA screening factor, $[\varepsilon_0(k,0)]^{-1}$, in place of $S_{\rm WS}(k)$ in Eq. (3.59). The screening length associated with $[\varepsilon_0(k,0)]^{-1}$ is the inverse of the Fermi-Thomas wave number,

$$q_{\rm FT}=\sqrt{3}m\omega_p/\hbar q_F\ .$$

As we enter the strongly coupled regime $r_s\gtrsim 1$, however, this length loses its meaning as a screening length; the average number of particles involved in the sphere of radius $q_{\rm FT}^{-1}$ soon becomes less than unity. The screening factor $[\varepsilon_0(k,0)]^{-1}$ thus fails to take account of the important correlational effects in the strongly coupled electron liquid with $r_s\gtrsim 1$. An improved calculation scheme may be obtained through an appropriate renormalization of the screening factor in such a way as to incorporate the actual screening properties of the system, as in Eqs. (3.60) and (3.61).

For degenerate electron liquids at metallic and lower densities, Eq. (3.61) turns out to be almost independent of r_s, so that the effective screening radius of Eq. (3.60) obeys the Wigner-Seitz sphere scaling, that is, $q_{\rm WS}\sim q_F$. The use of Eq. (3.60) in place of the RPA screening function $[\varepsilon_0(q,0]^{-1}$ represents an essential renormalization of screening in Eq. (3.59). [Significance of such a renormalization in a strongly coupled classical plasma has been elucidated numerically by Tago *et al.* (1981)]. As we observe in Eq. (3.59), the extent of the Coulombic local-field correction is measured by the departure of $S(q)$ from its Hartree-Fock value, $S_{\rm HF}(q)$; in the Hartree-Fock limit ($r_s\to 0$), $G_c(q)$ naturally vanishes.

The values of $G(q)$ and $[\varepsilon(q,0)]^{-1}$ computed with Eqs. (3.57)–(3.59) are plotted in Figs. 18 and 19 at $r_s=1$, 4, and 10. Consequences of this theoretical scheme will also be examined numerically in later sections.

2. Parametrized expression

In the self-consistent formulation (e.g., Singwi *et al.*, 1968; Vashishta and Singwi, 1972; Utsumi and Ichimaru, 1980b) of the dielectric function, essential quantities such as the local-field correction are obtained through a numerical solution to a complex set of nonlinear integral equations; the result is usually presented in the form of a numerical table at discrete r_s values. The situation is quite similar in the cases of the computer simulation study based on variational principles; the result is available only for a few discrete r_s values where the simulation was carried out. For the numerical studies of strong-coupling effects in degenerate electron liquids it will be useful to derive a parametrized expression for the local-field correction which accurately fits the results of the self-consistent formulation as well as those of the variational calculations.

To achieve this end, Taylor (1978) proposed a simple formula,

$$G(q)=\gamma_0(r_s)(q/q_F)^2\ , \tag{3.62}$$

emphasizing the long-wavelength behavior, Eq. (3.25). He argues that apparent inaccuracy of Eq. (3.62) in the short-wavelength domain may be inconsequential, since the polarizability $\chi_0(q,0)$ quickly vanishes there. A close examination reveals, however, that its divergent behavior at large q leads to fatal predictions. One can in fact show (Ichimaru and Utsumi, 1981) that even with a modification of Eq. (3.62) into a form of Hubbard type,

$$G(q)=a_0q^2/(q^2+a_1q_F^2)\ , \tag{3.63}$$

so that both Eqs. (3.25) and (3.44) are accommodated by the choice of

$$\begin{aligned} a_0&=1-g(0)\ ,\\ a_1&=[1-g(0)]/\gamma_0(r_s)\ , \end{aligned} \tag{3.64}$$

the self-consistency conditions in the compressibility sum rule and the short-range correlation cannot be adequately satisfied.

On the suggestion of the results of their microscopic calculations, Ichimaru and Utsumi (1981) adopted the formula

$$G(q)=A\left[\frac{q}{q_F}\right]^4+B\left[\frac{q}{q_F}\right]^2+C + \left[A\left[\frac{q}{q_F}\right]^4+(B+\tfrac{8}{3}A)\left[\frac{q}{q_F}\right]^2-C\right] \times\frac{4q_F^2-q^2}{4q_Fq}\ln\left|\frac{2q_F+q}{2q_F-q}\right| . \quad (3.65)$$

Essential ingredients that go into determination of the parameters A, B, and C, are the Monte Carlo data of Ceperley and Alder (1980) for $E_c(r_s)$, the ladder diagram calculation of $g(0)$ by Yasuhara (1972), and the dielectric formulation of Utsumi and Ichimaru (1980b).

As noted in Sec. III.B.4, Ceperley and Alder carried out GFMC computations for $E_c(r_s)$ at $r_s=1$, 2, 5, 10, 20, 50, and 100. Vosko, Wilk, and Nusair (1980) then derived an interpolation formula of those data through a Padé approximant technique. The formula so fitted for the paramagnetic fluid phase reads

$$r_s\frac{dE_c(r_s)}{dr_s}=b_0\frac{1+b_1x}{1+b_1x+b_2x^2+b_3x^3} , \quad (3.66)$$

where $x=\sqrt{r_s}$, $b_0=0.062\,181\,4$, $b_1=9.813\,79$, $b_2=2.822\,24$, and $b_3=0.736\,411$. We use Eq. (3.66) via Eqs. (3.30a) and (3.25) to determine the long-wavelength behavior of Eq. (3.65). Earlier, Isihara and Montroll (1971; Isihara, 1972) interpolated the Gell-Mann and Brueckner high-density formula (3.16) and the low-density formula of Carr, Coldwell-Horsfall, and Fein (1961) through an analogous method of Padé approximants.

Through a resummation of the electron-electron ladder diagrams, Yasuhara (1972) obtained the expression

$$g(0)=\frac{1}{8}\left[\frac{z}{I_1(z)}\right]^2 , \quad (3.67)$$

where $z=4(\lambda r_s/\pi)^{1/2}$, $\lambda=(4/q\pi)^{1/3}$, and $I_1(z)$ is the modified Bessel function of the first kind and of the first order. We use Eq. (3.67) via Eq. (3.44) to determine the short-range behavior of Eq. (3.65).

The parameters in Eq. (3.65) are consequently determined as

$$A=0.029 \quad (0\le r_s\le 15) \quad (3.68)$$

$$B=\tfrac{9}{16}\gamma_0(r_s)-\tfrac{3}{64}[1-g(0)]-\tfrac{16}{15}A , \quad (3.69)$$

$$C=-\tfrac{3}{4}\gamma_0(r_s)+\tfrac{9}{16}[1-g(0)]-\tfrac{16}{5}A . \quad (3.70)$$

The particular value of A in Eq. (3.68) is adopted so that Eq. (3.65) closely simulates the results of the microscopic calculation (Utsumi and Ichimaru, 1980b) and so that the positivity condition (3.40) is secured. Figures 18 and 19 show the resulting values of Eqs. (3.65) and (3.24) at $r_s=1$, 4, and 10. As we shall see in the subsequent sections, the detailed features of the theory represented by the fitting formula (3.65) agree well with those of the variational calculations; the parametrized dielectric function satisfies the self-consistency conditions in the compressibility sum rule and the short-range correlation to a good degree of accuracy.

D. Static properties

1. Radial distribution function

With the dielectric function (3.24), one calculates the radial distribution function via Eqs. (3.1a), (3.1b), and (2.1). Figure 20 shows the values of $g(r)$ at $r_s=1$, 4, and 10, computed in the Vashishta-Singwi scheme, Eq. (2.70) (at $r_s=1$ and 4 only); in the Utsumi-Ichimaru scheme, Eq. (3.57); with the parametrized expression (3.65); and by the FHNC method (Lantto, 1980 and private communication). Figure 21 also exhibits the $g(r)$ values computed in other schemes at different r_s values.

To examine accuracy in the description of the short-range correlation, I have prepared Table I, which lists the values of $g(0)$ computed in various theoretical schemes as well as in the FHNC variational method. We find that the recent results in the dielectric formulation converge well with those of the variational calculation; the positivity condition (3.40) is maintained.

2. Correlation energy

The correlation energy $E_c(r_s)$ per electron in Rydbergs is calculated from Eq. (3.9) with the aid of Eq. (3.2). Table II lists the values of $-E_c(r_s)$ obtained in various dielectric formulations, variational calculations, and interpolation procedures. Here again we observe that the results of recent dielectric formulations converge well with those of the latest variational calculations. Agreement between the interpolated values of Vosko *et al.*

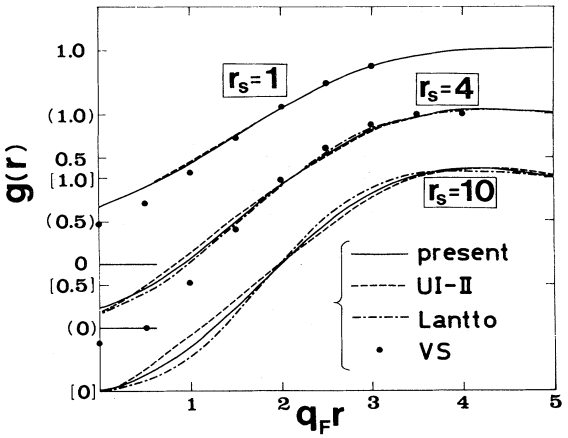

FIG. 20. Radial distribution function $g(r)$ at $r_s=1$, 4, and 10 evaluated in various methods. VS is based on Eqs. (3.24) and (2.70), with $a_0=2/3$; UI-II is the result of Utsumi and Ichimaru (1980b); "present" is derived from Eqs. (3.24) and (3.65); and "Lantto" refers to the FHNC calculation by Lantto (to be published). At $r_s=1$, Lantto's data coincide with the solid curve.

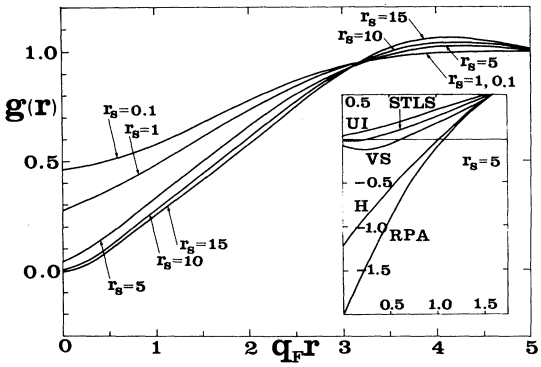

FIG. 21. Radial distribution function $g(r)$ calculated by Utsumi and Ichimaru (1980b) at various values of r_s. In the insert, the predictions of various theories on the short-range behavior of $g(r)$ are compared at $r_s=5$: RPA refers to the theory based on Eq. (3.10); H is based on Eqs. (3.24) and (3.55); STLS, Eqs. (3.24) and (2.67); VS, Eqs. (3.24) and (2.70); and UI, Eqs. (3.24) and (3.57)–(3.59). From Utsumi and Ichimaru (1980b).

(1980) and the results with the parametrized local-field correction (3.65) indicates that the latter scheme satisfies the compressibility sum rule to a good degree of accuracy.

We next take up the correlation energy contributions $E_c(q;r_s)$ from different regions of momentum transfer (e.g., Pines and Nozières, 1966). This quantity is directly related to the static structure factor,

$$E_c(q;r_s)=\frac{1}{r_s}\int_0^{r_s} dr_s[S(q)-S_{\rm HF}(q)] , \tag{3.71}$$

so that the correlation energy is calculated as

$$E_c(r_s)=\frac{2}{\pi\lambda r_s q_F}\int_0^{\infty} dq\, E_c(q;r_s) . \tag{3.72}$$

In the long-wavelength limit, Eq (3.71) is expanded as

$$E_c(q;r_s)=-\frac{3}{4}\left[\frac{q}{q_F}\right]+\left[\frac{3\pi}{4\lambda r_s}\right]^{1/2}\left[\frac{q}{q_F}\right]^2+\cdots . \tag{3.73}$$

The first term on the right-hand side of Eq. (3.73) is the contribution of $S_{\rm HF}(q)$ in Eq. (3.71); the second term stems from the long-wavelength plasmon contribution (e.g., Pines and Nozières, 1966)

$$S(q)\to\frac{E_F}{\hbar\omega_p}\left[\frac{q}{q_F}\right]^2 , \tag{3.74}$$

where

$$\omega_p=(4\pi ne^2/m)^{1/2} . \tag{3.75}$$

The numerical results for $E_c(q;r_s)$ predicted in the dielectric formulations with Eqs. (3.57) and (3.65) are compared in Fig. 22 with those of the FHNC calculation by Zabolitzky (1980, and private communication) at $r_s=1$, 4, and 10. The interpolation scheme of Nozières and Pines (1958) at $r_s=4$ is also included in the figure, together with the RPA values at $r_s=1$. We find a reasonably good agreement between those recent results, with a notable exception in the appearance of mild bumps around $q=2q_F$ in the dielectric formulations. As Eq. (3.71) indicates, a bump in $E_c(q;r_s)$ reflects the existence of an analogous bump in $S(q)$.

3. Wigner crystallization

Since Wigner's pioneering work (Wigner, 1934, 1938) on the possibility of crystallization of the electron gas at sufficiently low densities, much effort has been devoted toward theoretical understanding of the phase properties of such an electron system in its ground state. The critical r_s value at which the electron gas turns into the Wigner solid has been estimated by many investigators in various methods.

On the basis of Lindemann's melting criterion, which states that the Wigner solid will melt when the mean vibrational amplitude of a particle about its lattice position reaches a certain fraction δ of the interparticle spacing, Nozières and Pines (1958) proposed the critical value $r_s\simeq 20$; in this estimation $\delta=\frac{1}{4}$ was assumed. Later, Coldwell-Horsfall and Maradudin (1960) calculated the mean vibrational amplitude and thereby pointed out that the numerical estimate of the critical r_s value is very sensitive to the choice of δ; their result, $r_s=0.4054\delta^{-4}$, would predict $r_s=104$ for $\delta=\frac{1}{4}$ but $r_s=6.5$ for $\delta=\frac{1}{2}$.

TABLE I. Values of $g(0)$ in various calculations. RPA refers to the calculation based on Eq. (3.10); H, Eqs. (3.24) and (3.55); STLS, Singwi *et al.* (1968); VS, Vashishta and Singwi (1972); Y, Yasuhara (1972); L, Lantto (1980 and private communication); Z. Zabolitzky (1980); UI, Utsumi and Ichimaru (1980b); IU, Ichimaru and Utsumi (1981).

	$r_s=1$	$r_s=2$	$r_s=3$	$r_s=4$	$r_s=5$	$r_s=6$	$r_s=10$
RPA	−0.12	−0.65	−1.13	−1.57	−2.00	−2.60	
H	0.08	−0.28	−0.61	−0.91	−1.21	−1.49	
STLS	0.24	0.11	0.04	0.006	−0.02	−0.03	
VS	0.19	0.034	−0.04	−0.07	−0.075	−0.08	
Y	0.266	0.150	0.088	0.053	0.033	0.021	
L	0.269	0.163	0.102	0.065	0.042	0.028	0.006
Z	0.302	0.202	0.143	0.105	0.081		0.032
UI	0.276	0.168	0.107	0.070	0.046	0.031	0.005
IU	0.279	0.181	0.128	0.094	0.070	0.052	0.011

TABLE II. Values of $-E_c(r_s)$ mRy in various calculations. RPA refers to the calculation based on Eq. (3.10); H, Eqs. (3.24) and (3.55); STLS, Singwi *et al.* (1968); TW, Toigo and Woodruff (1970, 1971); VS, Vashishta and Singwi (1972); L. Lantto (1980 and private communication); Z, Zabolitzky (1980); CA, Ceperley and Alder (1980); VWN, Vosko *et al.* (1980); UI, Utsumi and Ichimaru (1980b); IU, Ichimaru and Utsumi (1981).

	$r_s=1$	$r_s=2$	$r_s=3$	$r_s=4$	$r_s=5$	$r_s=6$	$r_s=10$	$r_s=15$	$r_s=20$
RPA	157	124	105	94	85	78			
H	131	102	86	76	69	64			
STLS	124	92	75	64	56	50	36		22
TW	134	95	79	68	61				
VS	112	89	75	65	58	52			
L	118	86.5	70.9	61.0	54.0		35.5		22.1
Z	114.1	85.9	71.0	61.2	54.1		35.5		21.8
CA	119	90.2			56.3		37.22		23.00
VWN	120.0	89.6	73.8	63.6	56.3	50.7	37.09	28.30	23.10
UI	115.7	85.0	69.2	59.2	52.0	46.6	33.5	25.1	20.3
IU	117.4	86.9	71.1	61.0	53.8	48.3	35.0	26.5	21.3

To avoid such an uncertainty, de Wette (1964) formulated a stability criterion for the Wigner lattice, stating that in order for a solid structure to exist the single-particle potential should exhibit a localized well with at least one bound state. An upper and a lower limit for the melting density thereby estimated corresponded to $r_s \simeq 47$ and $r_s \simeq 100$. Van Horn (1967) then attempted to improve on the criterion of de Wette by taking into account the possibility of electrons occupying interstitial positions. Assuming that a half of the electrons were at interstitial positions, he found the melting condition, $r_s \simeq 27$.

The critical density for the melting transition may be evaluated directly through comparison of energies between the liquid and crystalline states. Glyde, Keech, Mazighi and Hansen (1976) computed the fluid ground-state energy by using a variational Jastrow wave function, and the energy in the solid phase by using a self-consistent harmonic lattice theory; they thereby found the critical value $r_s \simeq 70$. Ceperley (1978) performed fermion Monte Carlo variational calculations of the ground-state energies for three phases, namely, the Wigner crystal, the normal or unpolarized fluid, and the polarized or ferromagnetic fluid. The results of such calculations indicated that the Wigner crystal had the lowest energy for $r_s > 67$; the totally polarized fluid was the ground state for $26 < r_s < 67$; and the unpolarized fluid was stable at high densities, $r_s < 26$. Recently Ceperley and Adler (1980) calculated those energies by a stochastic simulation of the Schrödinger equation and obtained somewhat different numerical results for the critical conditions.

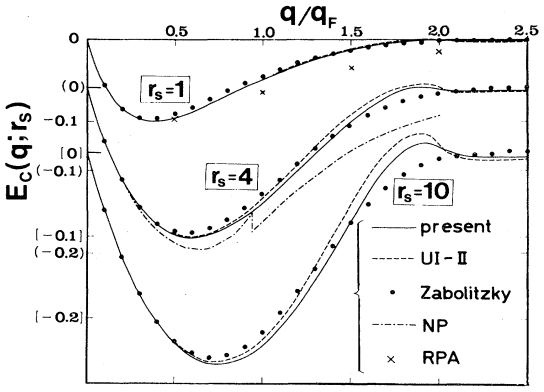

FIG. 22. Correlation energy contributions $E_c(q;r_s)$ from different regions of momentum transfer at $r_s=1$, 4, and 10: RPA refers to the calculation based on Eq. (3.10); NP, the interpolation of Nozières and Pines (1958); "Zabolitzky", the FHNC calculation by Zabolitzky (private communication); UI-II, the result of Utsumi and Ichimaru (1980b); "present" is derived from Eqs. (3.24) and (3.65).

On the basis of the dielectric formulation with Eq. (3.57), Utsumi and Ichimaru (1981b) computed the ground-state energy of low-density electron fluids; comparing this result with the energies in the bcc crystalline state evaluated by Carr *et al.* (1961), Glyde *et al.* (1976), and Ceperley (1978), they estimated the transition density to be $r_s = 12-27$. It was also noted that those estimates are quite sensitive to small variations in the fluid and crystalline energies; those energy curves are almost parallel to each other near the point of intersection. Determination of the transition density is a delicate affair requiring extremely accurate evaluations of the energies of both the crystalline solid and the strongly coupled liquid.

4. Instabilities in low-density electron liquids

Static properties of degenerate electron liquids at metallic and lower densities have been extensively investigated in the dielectric formulation by Utsumi and Ichimaru (1981b) and Iyetomi, Utsumi, and Ichimaru (1981a). In this section I briefly summarize their findings.

(a) The electronic pressure,

$$P = -\frac{nr_s}{3}\frac{dE(r_s)}{dr_s}\ , \quad (\mathrm{Ry\,cm^{-3}}) \tag{3.76}$$

becomes negative for $r_s > 4.2$. Analogous negative pressure is found in a strongly coupled classical OCP when

Eq. (2.11) is substituted in Eq. (2.9). This does not immediately imply a thermodynamic instability of the system, however, since the rigid background of neutralizing charge usually assumed can make an infinite reservoir of positive pressure.

(b) The compressibility (3.26) and the static dielectric function $\varepsilon(q,0)$ become negative for $r_s > 5.3$. An example for the latter function has been shown in Fig. 19, and its classical counterpart in Fig. 4. Again, this negative compressibility does not imply an instability of the system, when a rigid background of compensating charge is assumed.

(c) Ferrell's condition (Ferrell, 1958)

$$\frac{d^2}{dr_s^2}[r_s^2 E(r_s)] \leq 0 \tag{3.77}$$

for stability of the electron-liquid ground state (cf. Sec. II.B.5 for discussion) breaks down when r_s exceeds ~ 65. Violation of condition (3.77) means existence of a state other than the homogeneous liquid state that would lower the system energy. It thus follows that the critical r_s value for the Wigner transition should be smaller than 65.

When the dielectric function is expressed in the form (3.24), the left-hand side of (3.77) may be calculated as (Ichimaru *et al.*, 1982)

$$\frac{d^2}{dr_s^2}[r_s^2 E(r_s)] = -\frac{8\hbar\lambda E_F}{3\pi^3 n^2}\int_0^\infty \frac{dx}{x^2}\int_{-\infty}^{\infty} dy \left[\frac{\chi_0(xq_F,iy)}{1-\frac{8\lambda r_s E_F}{3\pi n x^2}[1-G(xq_F)]\chi_0(xq_F,iy)}\right]^2 \times \left[1-G(xq_F)-r_s\frac{d}{dr_s}G(xq_F)\right], \tag{3.78}$$

In the RPA, $G(q)=0$, so that Misawa (1968) showed

$$d^2[r_s^2 E_{\rm RPA}(r_s)]/dr_s^2 \leq 0 .$$

As we observe—for example in Fig. 18—the local-field correction arising from the exchange and correlation effects has the property

$$\frac{\partial}{\partial r_s}[r_s G(q)] \geq 0 , \tag{3.79}$$

giving rise to a positive contribution on the right-hand side of Eq. (3.78); inclusion of the local-field correction thus has a destabilizing effect in the Ferrell criterion (3.77).

(d) The onset condition for a CDW instability has been given by Eq. (2.36). Extrapolating the plots of $\varepsilon(q,0)_{\rm max}$ for the degenerate electron liquids into low-density regime, analogously to Fig. 6, Iyetomi *et al.* (1981a) infer that condition (2.36) may be reached at $r_s \simeq 85$ with the critical wave number $q_{\rm cr} = 1.875 q_F$. Here again it has been shown that the local-field correction arising from the exchange and correlation effects has a tendency to induce an inhomogeneous state. The use of local approximation for exchange and correlation, which depends only on the information contained in the limit (3.25), can thus lead to manifestly inaccurate predictions on the onset of the CDW instability.

If the spin dependence of the polarizabilities is taken into account, one can analogously analyze the onset condition for a spin-density-wave (SDW) instability (e.g., Overhauser, 1968).

Various instabilities noted in this section may lead to interesting physical consequences if they are coupled with finiteness of the pressure or the compressibility of the ionic background. These problems, however, have not been investigated in sufficient detail.

E. Application of the static screening function

1. High-density plasmas

The properties of high-density plasmas, consisting of ions obeying the classical statistics and electrons forming degenerate quantum liquids, have been the subjects of intensive study lately, because they make practical models for laser-compressed plasmas, the interiors of heavy planets and of degenerate stars, and the outer crusts of the neutron stars. A most simplified treatment of such a high-density plasma consists in consideration of a classical OCP, as in Sec. II, where the electrons are assumed to form a rigid, uniform background neutralizing the average space-charge field of the ions. Such a model provides a rigorous description of the system in the high-density limit of the electrons.

For the description of actual high-density plasma systems, however, the OCP model amounts to something of an oversimplification, since the electrons do form a *polarizable* medium. The Coulomb potential between the ions is screened by the electrons, turning thereby into an effective short-range potential. In the framework of the linear-response theory, the screening action may generally be described in terms of the dielectric function $\varepsilon(q,\omega)$ of the degenerate electron liquid, in which the ions are now assumed to form a uniform positive-charge background. Since the Fermi energy of the electrons is much greater than the thermal energy of the ions in many of the practical cases, one may evoke the adiabatic approximation for the motion of the electrons, so that only the static part $\varepsilon(q,0)$ of the dielectric function enters the screening of the interionic potentials.

In the following two sections we shall look at some of the theoretical treatments on the thermodynamic and

transport properties of high density plasmas, based on a composite model where the ions are treated as a classical OCP and the electrons as a degenerate quantum liquid. In the numerical computations, $Z=1$ is assumed so that the results are valid to hydrogen plasmas; the methods are equally applicable to other kinds of plasmas, however, as far as the effects of the Coulomb correlations are concerned.

2. Thermodynamic properties

A number of investigators have treated the thermodynamic properties of high-density plasmas: Hubbard and Slattery (1971) carried out a Monte Carlo simulation of such a system with the Lindhard screening function. Ross and Seale (1974) employed a hard-sphere variational calculation also with the Lindhard screening function; Stevenson (1975) likewise carried out a hard-sphere variational calculation for hydrogen-helium fluid mixtures. DeWitt and Hubbard (1976) performed an improved Monte Carlo study for such a mixed system with the Lindhard screening function. Galam and Hansen (1976) carried out an extensive study of the thermodynamic properties on the basis of an OCP variational principle coupled with the screening functions of Lindhard (1954), of Geldart and Vosko (1966), and of Toigo and Woodruff (1970, 1971). Very recently, Iyetomi *et al.* (1981b) investigated the screening effects of the degenerate electron liquid on the thermodynamic properties of dense plasmas, using the improved screening function proposed by Utsumi and Ichimaru (1980b).

For a treatment of dense plasmas, the following conditions are assumed: The thermal de Broglie wavelength of the ions is much smaller than the average interionic spacing; the ions may be regarded as classical particles. The electrons are degenerate, so that $k_BT/E_F \ll 1$; more precisely, it suffices to assume $k_BT/E_F < 0.1$. The electrons are nonrelativistic, so that $E_F \ll mc^2$ or $r_s \gg 10^{-2}$. Those conditions are satisfied in many cases of practical interest.

Eliminating the electronic coordinates by the adiabatic approximation, one writes the Hamiltonian of the system as

$$H = E_e + K + \frac{1}{2V}\sum_{\mathbf{q}(\neq 0)} v(q)\{[\rho_{\mathbf{q}}\rho_{-\mathbf{q}}/\varepsilon(q,0)] - N\} \ . \tag{3.80}$$

Here E_e represents the ground-state energy of the electron liquid; K refers to the kinetic energy of the ions, and $\rho_{\mathbf{q}}$ are the Fourier components of the ion-density fluctuations. In Eq. (3.80), the electron-ion interaction is assumed to be weak; only the linear response term is retained (Galam and Hansen, 1976). The terms E_e and K, being simply additive in Eq. (3.80), will be omitted hereafter. Thus the problem effectively turns into one of a single-component ionic fluid.

The thermodynamic properties may be analyzed by the variational method with the aid of the Gibbs-Bogoliubov inequality (2.20). It has been shown numerically by Galam and Hansen (1976) that the OCP reference system gives lower estimates of the free energy than the hard-sphere system; OCP makes a reference system superior to the hard-sphere system. In the OCP reference system, one regards its "effective charge" e' as the variational parameter. The effective charge physically describes the extent to which the ionic charge e is reduced due to the electron screening.

The Gibbs-Bogoliubov inequality (2.20) now reads

$$\frac{F}{Nk_BT}(\Gamma,r_s) \le \frac{\tilde{F}}{Nk_BT}(\Gamma',\Gamma,r_s) \ , \tag{3.81}$$

where

$$\frac{\tilde{F}}{Nk_BT}(\Gamma',\Gamma,r_s) = \frac{F^{\mathrm{OCP}}}{Nk_BT}(\Gamma') + \frac{a\Gamma}{\pi}\int_0^\infty dq\, S^{\mathrm{OCP}}(q;\Gamma')\left[\frac{1}{\varepsilon(q,0)} - 1\right] + \frac{\Gamma-\Gamma'}{\Gamma'}\frac{U^{\mathrm{OCP}}}{Nk_BT}(\Gamma') \ , \tag{3.82}$$

$$\Gamma' = (e')^2/ak_BT \tag{3.83}$$

is the effective coupling constant; $F^{\mathrm{OCP}}(\Gamma')$, $U^{\mathrm{OCP}}(\Gamma')$, and $S^{\mathrm{OCP}}(q;\Gamma')$ refer to the excess free energy, the excess internal energy, and the static structure factor of the OCP with Γ' (cf. Secs. II.A and II.B.1). The variational parameter Γ' is then determined from the minimization condition:

$$\frac{\partial}{\partial\Gamma'}\frac{\tilde{F}}{Nk_BT}(\Gamma',\Gamma,r_s)\bigg|_{\Gamma,r_s} = 0 \ . \tag{3.84}$$

The use of Γ' both as the variational parameter in general and as the specific solution to Eq. (3.84) should not cause any confusion.

Table III lists the values of Γ' so computed with the Lindhard screening function and with the UI screening function derived by Utsumi and Ichimaru (1980b). We here observe that the variational Γ' with the UI screening function lies systematically smaller than that with the Lindhard screening function. This implies that the exchange and Coulomb local-field corrections between electrons act further to reduce the ionic correlations. This reduction can be accounted for in the following way: When electrons are attracted to the vicinity of an ion, both the kinetic energy of, and Coulomb energy between, those electrons generally increase. The screening action and thereby the effective reduction of the ionic charge will be completed when those energy increments are balanced by the energy decrement due to the electron-ion attraction. In the Lindhard screening function, where no effects of microscopic exchange and

TABLE III. The Γ' values in the OCP variational method with the Lindhard [Eq. (3.10)] and UI [Utsumi and Ichimaru (1980b)] screening functions. From Iyetomi *et al.* (1981c).

	$r_s=0.5$		$r_s=1.0$		$r_s=1.5$	
Γ	Lindhard	UI	Lindhard	UI	Lindhard	UI
6	3.97	3.84	2.89	2.47		
10	6.67	6.45	4.94	4.36	3.83	2.69
20	13.26	12.78	9.59	8.34	7.33	5.46
40	26.34	25.30	18.36	15.50	13.34	9.24
70	45.73	43.82	31.12	25.64	21.65	13.66
100	64.71	61.86	43.34	35.26	29.50	17.43
120	77.23	73.70	51.12	41.32	34.46	19.72
140	89.84	85.57	58.66	47.12	39.18	21.87
160	102.73	97.65	66.00	52.66	43.67	23.89

Coulomb holes around an electron are taken into account, the magnitude of the Coulomb energy between electrons tends to be overestimated. The screening action and the effective reduction in the ionic charge are thus underestimated in the case of the Lindhard screening function.

The variational estimates of the free energy may then be obtained by substituting the solution Γ' to Eq. (3.84) in Eq. (3.82). Other thermodynamic quantities, such as the pressure P, may likewise be calculated, as (Galam and Hansen, 1976)

$$\frac{P}{nk_BT}(\Gamma,r_s)=\frac{1}{3}\frac{U}{Nk_BT}(\Gamma,_s) - \frac{a\Gamma}{3\pi}\int_0^\infty dq\, S^{\mathrm{OCP}}(q;\Gamma')\frac{\partial}{\partial r_s}\left[\frac{1}{\varepsilon(q,0)}\right] . \tag{3.85}$$

Figures 23 and 24 exhibit the calculated deviations of the thermodynamic quantities from the OCP values due to the screening effect of the electrons with $r_s=1.5$. The deviations are defined as the differences between the thermodynamic quantities with the electron screening and the corresponding OCP values; thus for the free energy

$$\Delta\left[\frac{F}{Nk_BT}\right]=\frac{\tilde{F}}{Nk_BT}(\Gamma',\Gamma,r_s)-\frac{F^{\mathrm{OCP}}}{Nk_BT}(\Gamma) , \tag{3.86}$$

where the variational Γ' determined from Eq. (3.84) is to be used in the first term. The entries with the UI screening function are the results of Iyetomi *et al.* (1981b); the others are taken from Galam and Hansen (1976). We observe in those figures that the screening corrections to the thermodynamic quantities are rather insensitive to the choice of the screening function, except perhaps for the case of $\Delta(P/nk_BT)$.

3. Electric resistivity

In a high-density plasma where the Fermi energy of the electrons is large, coupling between the electrons and the ions is correspondingly weak; the Ziman formula (Ziman, 1961) is thus applicable to the calculation of the scattering rate between them. Several investigators in the past computed the electric resistivity on the basis of the Ziman formula; they include Hubbard and Lampe (1969), Stevenson and Ashcroft (1974), Flowers and Itoh (1976), Minoo, Deutsch, and Hansen (1976), and Iyetomi, Utsumi, and Ichimaru (1981c). All of those calculations took account of the electron screening effect on the effective electron-ion interaction via an appropriate dielectric screening function of the electrons. Iyetomi *et al.* (1981c) took additional account of the reduction in the ionic correlations brought about by the screening action of the electrons, which had been expressed in terms of the Γ' values of Table III.

According to the Ziman formula, the electric resistivity may be calculated as

$$\rho_e=\frac{m^2}{12\pi^3\hbar^3e^2n}\int_0^{2q_F}dq\, q^3\,|\,\Phi(q)\,|^2S_i(q) , \tag{3.87}$$

where $\Phi(q)$ is the Fourier transform of the effective interaction potential between the electrons and the ions, and $S_i(q)$ refers to the ionic structure factor. Other

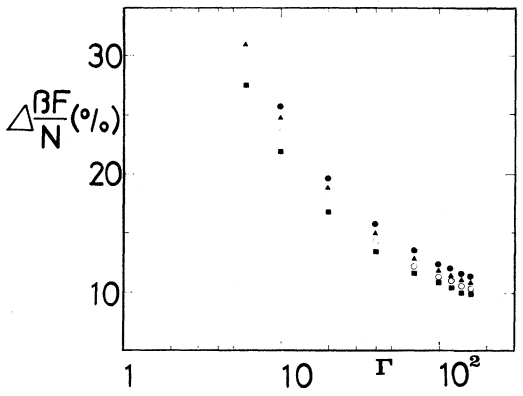

FIG. 23. Deviation of the Helmholtz free energy from its OCP value due to the electron screening at $r_s=1.5$. The points with closed squares refer to those obtained with the Lindhard screening function (3.10); open circles, with the Geldart-Vosko screening function Eqs. (3.24) and (3.56); closed triangles, with the screening function due to Toigo and Woodruff (1970); and closed circles, with the Utsumi-Ichimaru screening function Eqs. (3.24) and (3.57)–(3.59). $\beta=1/k_BT$. From Iyetomi *et al.* (1981b).

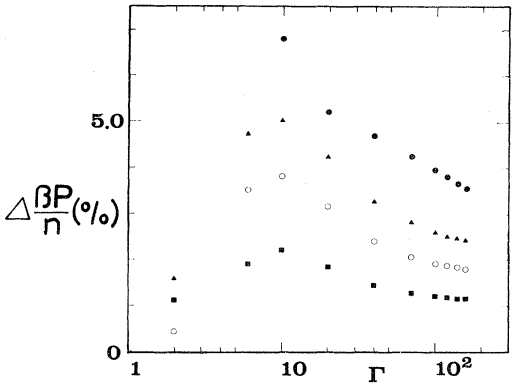

FIG. 24. Deviation of the pressure from its OCP value due to the electron screening at $r_s=1.5$. Designation of points is the same as Fig. 23. $\beta=1/k_BT$. From Iyetomi *et al.* (1981b).

transport coefficients, such as the electronic thermal conductivity, may be treated analogously (e.g., Minoo *et al.*, 1976).

The screening function $\varepsilon(q,0)$ of the electrons has influences on the two terms $\Phi(q)$ and $S_i(q)$ in the integrand of Eq. (3.87). First, the Coulomb interaction between the electrons and the ions turns into a short-range one:

$$\Phi(q)=-4\pi e^2/q^2\varepsilon(q,0)\ . \tag{3.88}$$

Since this effect acts to decrease the scattering cross section, it has a tendency also to decrease the magnitude of the electric resistivity.

The other effect refers to the effective reduction in the ionic correlations, described by $S_i(q)$, which stems from the electron screening of the ionic charges. This effect acts to enhance the density fluctuations of the ions in the intermediate wave number domain just below $2q_F$, and thereby to increase the electric resistivity.

In Fig. 25, the numerical values of the normalized resistivity,

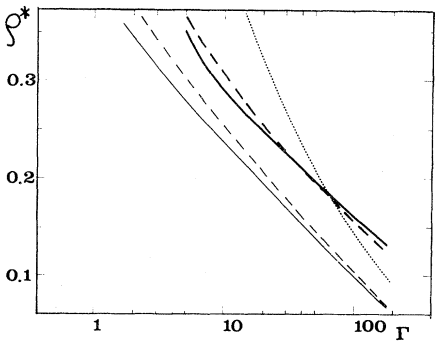

FIG. 25. Normalized electric resistivity, Eq. (3.89), versus Γ at $r_s=1.0$. The dotted curve refers to the values obtained in the approximation scheme (a) of Sec. III.E.3; the thin dashed curve, (b) with the Lindhard screening function (3.10); the thin solid curve, (b) with the UI screening function, Eqs. (3.24) and (3.57)–(3.59); the thick dashed curve, (c) with the Lindhard screening function; the thick solid curve, (c) with the UI screening function. From Iyetomi *et al.* (1981c).

$$\rho^*=\rho_e/\rho_{e0}\ , \tag{3.89}$$

are plotted for $r_s=1.0$, computed in various approximation schemes, where

$$\rho_{e0}=\frac{16}{9}\frac{a_B\hbar}{e^2}r_s^3$$
$$=38.6r_s^3\ \ (\mu\Omega\ \text{cm})\ . \tag{3.90}$$

In scheme (a), $\Phi(q)=-4\pi e^2/q^2$ and $S_i(q)=S^{\rm OCP}(q;\Gamma)$ are taken, so that the screening effects of the electrons are ignored in the evaluations of both the effective potential $\Phi(q)$ and the ionic structure factor $S_i(q)$. In scheme (b), Eq. (3.88) and $S_i(q)=S^{\rm OCP}(q;\Gamma)$ are assumed, so that the effective interaction is now screened. Finally, in scheme (c), the structure factor is also renormalized according to the OCP variational principle,

$$S_i(q)=S^{\rm OCP}(q;\Gamma')\ , \tag{3.91}$$

where Γ' is the variational value listed in Table III. The features exhibited in Fig. 25 may be understood in terms of competition between the screening effect on $\Phi(q)$ and the renormalization effect on $S_i(q)$, as remarked earlier.

F. Dynamic properties

1. General survey

During the past decades, a substantial amount of effort has been expended on the experimental study of the dynamic structure factor $S(q,\omega)$ associated with the valence electrons in metals, through the techniques of x-ray scattering spectroscopy and electron energy-loss spectroscopy [see, e.g., Raether (1980) for a review and further references]. The dynamic structure factor refers to the spectral function of the density fluctuation excitations in such an electron system (Pines and Nozières, 1966). The experiments have revealed the frequency dispersion, the linewidth, and the spectral shape of the plasmon excitations, as well as the detailed features of the contributions coming from other elementary excitations.

In various instances, the theory on the basis of the RPA has failed to account for salient features observed in experiments. Such a discord has been anticipated, however, since the RPA is basically a weak-coupling theory. The electrons in metal are, on the contrary, a strongly Coulomb-coupled system, for which the coupling constant $r_s=2-6$. As noted in Secs. III.A and III.B, many investigators have attempted to go beyond the RPA description, by taking account of certain non-RPA effects arising from the exchange and Coulomb correlations. Those theories have achieved only limited success in comparing their numerical predictions with the experimental data.

In the following sections, we shall take up certain aspects of those comparisons in some detail. In so doing we particularly refer to the theoretical model (3.53) proposed by Utsumi and Ichimaru (1980a, 1981a), since it encompasses many of the existing theories as its limiting

cases; their calculations were compared rather extensively with various scattering data.

In the dielectric response function (3.53), the strong-coupling effects were described by three characteristic functions: $G(q)$, $1/\tau(q)$, and $\Omega(q)$. The forms of the static local-field correction $G(q)$ proposed by various theories were reviewed in Sec. III.C; in the formulation of Utsumi and Ichimaru (1980b) $G(q)$ was determined according to Eqs. (3.57)–(3.59).

The long-time relaxation rate $1/\tau(q)$ has been calculated, in a way analogous to Eq. (3.59), as (Utsumi and Ichimaru, 1981a)

$$\frac{1}{\omega_p\tau(q)}=-\frac{1}{n}\int\frac{d\mathbf{k}}{(2\pi)^3}K(\mathbf{q},\mathbf{k})\frac{\pi m\omega_p\theta(2q_F-k)}{2\hbar q_F k}[S_{\rm WS}(k)]^2[S(|\mathbf{k}-\mathbf{q}|)-S_{\rm HF}(|\mathbf{k}-\mathbf{q}|)]\ . \tag{3.92}$$

Here $\theta(x)$ is the unit step function, and Eqs. (2.72), (3.6), and (3.60) have been used. Clearly, $1/\tau(q)$ is proportional to q^2 in the long-wavelength domain, reflecting the conservation of the total momentum in the electron system. Quantities related to $1/\tau(q)$ have also been formulated by DuBois and Kivelson (1969) and by Hasegawa and Watabe (1969).

The characteristic frequency $\Omega(q)$ for short-time relaxation has been determined in accord with the third frequency-moment sum rule (3.35) as

$$\Omega(q)/\omega_p=(\pi/2)^{1/2}\omega_p\tau(q)[G(q)-I(q)]\ , \tag{3.93}$$

where $I(q)$ has been defined by Eq. (3.37); hence, $\Omega(q)$ is proportional to the difference between the low- and high-frequency limits of the frequency-dependent local-field correction $G(q,\omega)$. It has been argued (Utsumi and Ichimaru, 1980a) that the frequency $\Omega(q)$ should correspond to a characteristic frequency of the multipair excitations: Clearly, $\Omega(q)$ remains finite in the long-wavelength limit; no Pauli principle restrictions are apparently involved in the calculation of Eq. (3.93).

2. Coefficient of plasmon dispersion

The plasmon pole $\omega=\omega(q)$ of the dynamic structure factor may be determined from

$$\varepsilon(q,\omega(q))=0\ . \tag{3.94}$$

We set its long-wavelength solution as

$$\omega(q)=\omega_p+2\alpha\omega_F(q/q_F)^2\ , \tag{3.95}$$

with $\omega_F=E_F/\hbar$; this equation defines the coefficient α of the plasmon dispersion.

Assuming that the electron-liquid model may provide a good description of the electrons in metal, one computes the dispersion coefficient from Eq. (3.53) as

$$\alpha=\alpha_{RPA}-\frac{\omega_p}{4\omega_F}\left[\gamma_\infty(r_s)+[\gamma_0(r_s)-\gamma_\infty(r_s)]\times{\rm Re}W\left[\frac{\omega_p}{\Omega(0)}\right]\right]\ , \tag{3.96}$$

where

$$\alpha_{\rm RPA}=3\omega_F/5\omega_p \tag{3.97}$$

is the dispersion coefficient evaluated in the RPA. Equation (3.96) thus takes account of both static and dynamic strong-coupling effects in the dispersion coefficient, arising from the exchange and Coulomb correlations. As Eqs. (3.25) and (3.39) indicate, the quantities $\gamma_0(r_s)$ and $\gamma_\infty(r_s)$ stem from the static and high-frequency limits of the local-field correction; Eq. (3.96) then mixes those two contributions in the way determined by the frequency ratio $\omega_p/\Omega(0)$.

The expressions for α obtained in various theories may be regarded as certain limiting cases of Eq. (3.96). For instance, if one disregards the relaxation effect in the short-time domain and thereby lets $\Omega(0)\to\infty$, then Eq. (3.96) reduces to

$$\alpha_0=\alpha_{\rm RPA}-(\omega_p/4\omega_F)\gamma_0(r_s)\ . \tag{3.98}$$

This expression corresponds to those obtained by Singwi *et al.* (1968, 1970), by Vashishta and Singwi (1972), and by Lowy and Brown (1975), although the schemes of evaluation for $\gamma_0(r_s)$ differ from one theory to the other. Basically, these are static theories and thus involve the static local-field correction represented by $\gamma_0(r_s)$.

In the weak-coupling limit of $r_s\to 0$, one retains the lowest-order contributions of the exchange effects only, and finds $\gamma_0(0)=\frac{1}{4}$ [cf. Eq. (3.30a)]. In this limit, Eq. (3.98) becomes

$$\alpha_{\rm TW}=\alpha_{\rm RPA}-\omega_p/16\omega_F\ , \tag{3.99}$$

the expression derived by Toigo and Woodruff (1970, 1971).

If, on the other hand, one assumes that the plasmon has a sufficiently high energy that an approximation $\omega_p/\Omega(0)\to\infty$ is applicable, then Eq. (3.69) reduces to

$$\alpha_\infty=\alpha_{\rm RPA}-(\omega_p/4\omega_F)\gamma_\infty(r_s)\ . \tag{3.100}$$

This is the expression obtained by Pathak and Vashishta (1973) and by Jindal, Singh, and Pathak (1977). These authors took account of the third frequency-moment sum rule, which is reflected in the involvement of $\gamma_\infty(r_s)$.

Finally, one notes that the lowest-order exchange contributions to $\gamma_\infty(r_s)$ may be evaluated by going over to the weak-coupling limit, $r_s\to 0$, so that $\gamma_\infty(0)=\frac{3}{20}$ [cf. Eq. (3.30b)]. In this limit, one finds from Eq. (3.100)

$$\alpha_{\rm NP}=\alpha_{\rm RPA}-3\omega_p/80\omega_F\ . \tag{3.101}$$

This expression was obtained by Nozières and Pines (1958) and by DuBois (1959).

For comparison the values of $\alpha/\alpha_{\rm RPA}$ as computed according to Eqs. (3.96) and (3.98)–(3.101) are shown in

Fig. 26. In the computations of Eqs. (3.98) and (3.100), the values of $\gamma_0(r_s)$ and $\gamma_\infty(r_s)$ obtained by Utsumi and Ichimaru (1980b) have been used. In Fig. 26 the experimental data on various metals as compiled by Raether (1980) are also plotted. We may interpret those data as indicating collectively that the experimental values for α are significantly different from the RPA prediction (3.97) and that the discrepancies widen as r_s increases. Since the measured values are rather widely scattered and are attached with large error bars, it does not appear feasible to draw a quantitative conclusion from the comparison in Fig. 26.

3. Plasmon linewidth

The critical wave number q_c is defined as that wave number at which the plasmon dispersion merges into the continuum of the single-pair excitations (e.g., Pines and Nozières, 1966). In the long-wavelength domain such that $q<q_c$, the plasmon suffers no Landau damping; it decays only through collisional processes. In the electron-liquid calculations as exemplified in Sec. III.F.1, the decay rate of plasmon would vanish in the long-wavelength limit since $1/\tau(q)$ is proportional to q^2. In actual metals, however, the linewidths of the plasmon spectra observed by scattering experiments (e.g., Kloos, 1973; Zacharias, 1975; Gibbons, Schnatterly, Ritsko, and Fields, 1976; Krane, 1978) take on nonvanishing, finite values in the limit of $q\to 0$. This observation clearly indicates the necessity of considering those additional scattering processes of electrons which would not conserve the total momentum of the electrons; examples of such metallic effects are the interband transitions, and scattering with phonons, impurities, and so on (Nozières and Pines, 1959).

General expressions for the dielectric tensor associated with the Bloch electrons in real crystals were derived long ago (Nozières and Pines, 1959; Ehrenreich and Cohen, 1959; Adler, 1962). Subsequently, Hasegawa (1971) and Sturm (1976) developed a pseudopotential theory of the linewidth of the long-wavelength plasmon in simple metals, and thereby explained its wave number dependence (Sturm, 1977, 1978a) on the nearly free electron approximation. Bross (1978) carried out analogous investigations by taking account of certain band-structure effects.

The extra scattering processes arising from the metallic effects may be included phenomenologically in the dielectric formulation (3.53) by modifying the definition (3.54) of $\tilde{\omega}$ into the form

$$\tilde{\omega}=\omega+\left[\frac{2}{\pi}\right]^{1/2}\frac{\Omega(q)}{\omega\tau(q)}\left[W\left[\frac{\omega}{\Omega(q)}\right]-1\right]+\frac{i}{\tau_0(q)}\,, \tag{3.102}$$

where $1/\tau_0(q)$ describes the decay rate of the density fluctuation excitations due to those nonconserving scattering processes. The full width at half maximum $w(q)$ of the plasmon peak in $S(q,\omega)$ measures the decay rate of the plasmon, which is calculated from the imaginary part of $\omega(q)$ in the solution to Eq. (3.94). Figure 27 shows the numerical results so computed for $r_s=2$ in various approximations and the experimental values (Zacharias, 1975; Gibbons *et al.*, 1976) for Al. The approximations adopted are

(a) *Constant relaxation time approximation.* This corresponds to the use of the dielectric function (3.53) with $\tilde{\omega}$ defined as Eq. (3.102). For $r_s=2$, $1/\omega_p\tau_0(q)=1/\omega_p\tau_0(0)=0.03$ is assumed, appropriate to Al (e.g., Kloos, 1973; Gibbons *et al.*, 1976; Krane, 1978).

(b) *Electron liquid model.* This amounts to assuming $1/\omega_p\tau_0(q)=0$ in (a) or using Eq. (3.54) in Eq. (3.53).

(c) *Static approximation to the local-field correction.* This further takes $1/\tau(q)=0$ in (b) or assumes Eq. (3.24) for the dielectric function.

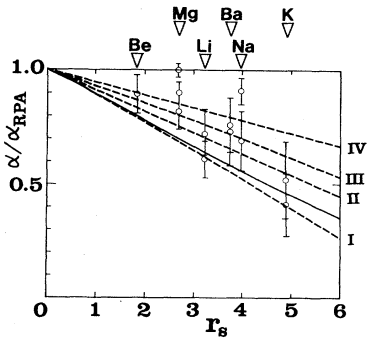

FIG. 26. Plasmon dispersion coefficient α divided by the RPA value $\alpha_{\rm RPA}$ vs r_s in various approximations. Solid curve corresponds to Eq. (3.96). Dashed curves I-IV correspond to α_0, $\alpha_{\rm TW}$, α_∞, and $\alpha_{\rm NP}$ in Eqs. (3.98)–(3.101), respectively. The experimental results for Be, Mg, Li, Ba, Na, and K are taken from Raether (1980). From Utsumi and Ichimaru (1981a).

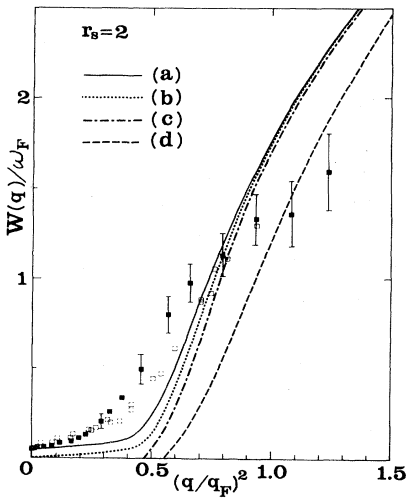

FIG. 27. Full width at half maximum, $w(q)$ vs $(q/q_F)^2$ for $r_s=2$ in schemes (a)–(d) of Sec. III.F.3. Experimental results for Al are taken from Zacharias (1975)—solid squares; and Gibbons *et al.* (1976)—open squares. From Utsumi and Ichimaru (1981a).

(d) *RPA*. This is approached by letting $G(q)=0$ in (c) or by adopting Eq. (3.10).

The major cause of the discrepancy between calculation (a) and the experimental data in Fig. 27 may be attributed to the adopted assumption $1/\tau_0(q)=1/\tau_0(0)$, which fails to account for the q dependence inherent in those scattering processes contributing to $1/\tau_0(q)$. We may conclude from such a comparison that the electron-electron interaction in the electron liquid provides only a minor contribution to the plasmon decay processes in actual crystalline metals.

4. Plasmon dispersion curve

It has been observed experimentally that the plasmon dispersion curve flattens as the wave number increases into the short-wavelength domain $q>q_c$. This is a strong-coupling effect in the electron liquid, since a calculation based on the RPA theory does not account for such a flattening. Computed results of the dispersion curve in the short-wavelength domain are shown in Fig. 28 for $r_s=2$ (Utsumi and Ichimaru, 1981a); the four curves correspond to the four approximation schemes, (a)—(d), introduced in the preceding section. Experimental values for Al obtained by various investigators (Höhberger, Otto, and Petri, 1975; Zacharias, 1975; Gibbons *et al.*, 1976; Batson, Chen, and Silcox, 1976) are also plotted in Fig. 28. An analogous experiment has been carried out recently by Priftis and Boviatsis (1981).

The local-field correction arising from the short-range static correlations, which is included in scheme (c), already shows a substantial effect in lowering the plasmon energy and flattening its dispersion over the RPA values in Fig. 28. This tendency becomes more pronounced as we proceed to include the dynamic local-field effects in (a) and (b). Improved agreement with the experimental indications appears to be obtained when those dynamic effects are taken into account.

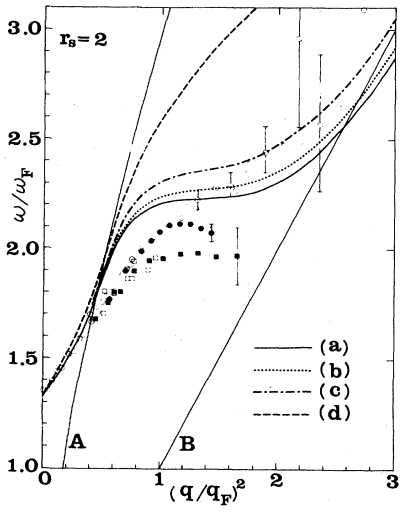

FIG. 28. Plasmon dispersion curves versus $(q/q_F)^2$ in approximations (a)—(d) of Sec. III.F.3 for $r_s=2$. Experimental results for Al are taken from Höhberger *et al.* (1975)—solid circles; Zacharias (1975)—solid squares; Gibbons *et al.* (1976)—open squares; Batson *et al.* (1976)—open circles. The line A represents the boundary of the single-pair-excitation continuum, $\omega/\omega_F=2(q/q_F)+(q/q_F)^2$, and the line B refers to the peak frequency of the dynamic structure factor in the noninteracting case, $\omega/\omega_F=(q/q_F)^2$. From Utsumi and Ichimaru (1981a).

Gupta, Aravind, and Singwi (1978) calculated the density fluctuation spectrum of an electron liquid including the local-field correction and the back flow of the quasiparticles, along the scheme of Eq. (3.22). They thereby obtained an excitation spectrum, showing a certain degree of flattening over the RPA spectrum for Al.

Dynamic correlations in an electron liquid were investigated by taking account of the first few exchange terms in the perturbation series expansion (Holas *et al.*, 1979; Brosens *et al.*, 1980). Dispersion curves at $r_s=2$ were calculated and compared with the experimental data for Al.

Band-structure effects on the plasmon dispersion in simple metals were studied by Sturm (1978b) and Bross (1978).

5. Asymmetry in the peak structure of $S(q,\omega)$

In the short-wavelength domain such that $q>q_c$, the plasmon peak merges into the continuum of the single-pair excitations; the peak structure of $S(q,\omega)$ exhibits an asymmetric character. Such an asymmetric behavior has been specifically monitored for Al in the experiment carried out by Gibbons *et al.* (1976). They measured the average frequency between the two half-maximum frequencies of $S(q,\omega)$ and compared it with the peak frequency.

Figure 29 shows those two—average and peak—frequencies obtained for Al, together with the theoretical values for $r_s=2$ computed in scheme (a) of Sec. III.F.3 (Utsumi and Ichimaru, 1981a). Although the absolute values of those frequencies show definite discrepancies between the experiment and the theory as in the comparison of Fig. 28, the ratio between the two frequencies appears to be well described by the theory.

6. Fine structures in $S(q,\omega)$

Platzman and Eisenberger (1974) reported an experimental observation of double-peak or peak-and-shoulder structures in the excitation spectra of the electron liquids in Be, Al, and C over the wave number domain of $1.13<q/q_F<2.10$. Theoretical efforts are directed toward accounting for such fine structures in the excitation spectra (e.g., Mukhopadhyay, Kalia, and Singwi, 1975; De Raedt and De Raedt, 1978; Barnea, 1979; Awa, Yasuhara, and Asahi, 1981). The basic idea evoked in some of those theories is to consider the lifetime effects arising from higher-order coupling between plasmons and single-pair excitations.

As may be clear from comparisons between experiments and theories described in the foregoing sections,

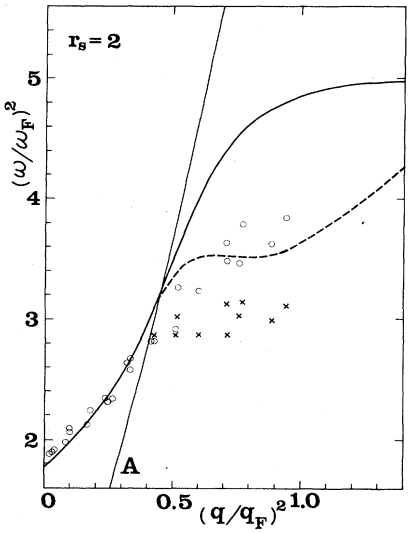

FIG. 29. Peak frequency and the average frequency between two half-maximum frequencies of $S(q,\omega)$ vs $(q/q_F)^2$ for $r_s=2$ in scheme (a) of Sec. III.F.3. The solid curve represents the peak frequency; the dashed curve, the average frequency. Experimental results for Al are taken from Gibbons *et al.* (1976): open circles represent the peak frequency; crosses, the average frequency. Line A refers to the boundary of the single-pair-excitation continuum. From Utsumi and Ichimaru (1981a).

certain features of the excitation spectra are rather strongly influenced by the metallic effects, as well as by the electron-liquid effects. In addition, even for a dynamic theory attempting to account for fine structures in the frequency spectra, one must make sure that the spectral function so obtained be consistent with various sum-rule requirements, such as reproduction of known results in the correlation function (cf. Sec. III.D.1) and in the correlation energy (cf. Sec. III.D.2), and fulfillment of the self-consistency conditions mentioned in Sec. III.A.3. Some of the theories cited above have ignored those requirements. It is still an open problem to develop a dynamic theory of $S(q,\omega)$ in metals accounting for those observed fine structures in a way consistent with the fundamental sum-rule requirements.

ACKNOWLEDGMENTS

The author wishes to thank D. Pines for encouragement and pertinent suggestions on the preparation of this review. He acknowledges many useful discussions with H. E. DeWitt, N. Itoh, K. S. Singwi, A. Sjölander, and H. Totsuji on various topics covered in this article. He is also grateful to L. J. Lantto and J. G. Zabolitzky for communicating numerical data of their FHNC calculations prior to publication. The author's colleagues at the University of Tokyo, namely, H. Iyetomi, K. Tago, and K. Utsumi, participated in various phases of research described here and in particular provided assistance in preparing figures and tables included; Ms. K. Morishima and Ms. M. Ohashi carefully typed the entire manuscript. This work was supported in part by the Japanese Ministry of Education, Science, and Culture through Research Grant No. 56380001.

REFERENCES

Abe, R., 1959, Prog. Theor. Phys. **22**, 213.
Abramo, M. C., and M. Parrinello, 1975, Lett. Nuovo Cimento **12**, 667.
Abramo, M. C., and M. P. Tosi, 1972, Nuovo Cimento B **10**, 21.
Abramo, M. C., and M. P. Tosi, 1974, Nuovo Cimento B **21**, 363.
Adler, S. L., 1962, Phys. Rev. **126**, 413.
Alastuey, A., and B. Jancovici, 1978, Astrophys. J. **226**, 1034.
Alder, B. J., and T. E. Wainwright, 1959, J. Chem. Phys. **31**, 459.
Aldrich, C. H., C. J. Pethick, and D. Pines, 1976a, Phys. Rev. Lett. **37**, 845.
Aldrich, C. H., C. J. Pethick, and D. Pines, 1976b, J. Low Temp. Phys. **25**, 691.
Aldrich, C. H., and D. Pines, 1976, J. Low Temp. Phys. **25**, 677.
Awa, K., H. Yasuhara, and T. Asahi, 1981, Solid State Commun. **38**, 1285.
Barnea, G., 1979, J. Phys. C **12**, L263.
Batson, P. E., C. H. Chen, and J. Silcox, 1976, Phys. Rev. Lett. **37**, 937.
Baus, M., 1977, Phys. Rev. A **15**, 790.
Baus, M., 1978, in *Strongly Coupled Plasmas,* edited by G. Kalman (Plenum, New York), p. 279.
Baus, M., 1980, J. Phys. C. **13**, L41.
Baus, M., and J.-P. Hansen, 1980, Phys. Rep. **59**, 1.
Bedell, K., and G. E. Brown, 1978, Phys. Rev. B **17**, 4512.
Bedell, K., and D. Pines, 1980a, Phys. Rev. Lett. **45**, 39.
Bedell, K., and D. Pine, 1980b, Phys. Lett. A **78**, 281.
Berggren, K. F., 1970, Phys. Rev. A **1**, 1783.
Bernu, B., and P. Vieillefosse, 1978, Phys. Rev. A **18**, 2345.
Bernu, B., P. Vieillefosse, and J. P. Hansen, 1977, Phys. Lett. **63A**, 301.
Bosse, J., and K. Kubo, 1978a, Phys. Rev. Lett. **40**, 1660.
Bosse, J., and K. Kubo, 1978b, Phys. Rev. A **18**, 2337.
Brami, B., J. P. Hansen, and F. Joly, 1979, Physica A **95**, 505.
Brosens, F., J. T. Devreese, and L. F. Lemmens, 1980, Phys. Rev. B **21**, 1363.
Bross, H., 1978, J. Phys. F **8**, 2631.
Brueckner, K. A., and S. Jorna, 1974, Rev. Mod. Phys. **46**, 325.
Brush, S. G., H. L. Sahlin, and E. Teller, 1966, J. Chem. Phys. **45**, 2102.
Callen, H. B., and T. A. Welton, 1951, Phys. Rev. **83**, 34.
Carnahan, N. F., and K. E. Sterling, 1969, J. Chem. Phys. **51**, 635.
Carr, W. J., R. A. Coldwell-Horsfall, and A. E. Fein, 1961, Phys. Rev. **124**, 747.
Cauble, R., and J. J. Duderstadt, 1981, Phys. Rev. A **23**, 3182.
Ceperley, D. M., 1978, Phys. Rev. B **18**, 3126.
Ceperley, D. M., and B. J. Alder, 1980, Phys. Rev. Lett. **45**, 566.
Ceperley, D. M., and M. H. Kalos, 1979, in *Monte Carlo Methods in Statistical Physics,* edited by K. Binder (Springer-Verlag, New York), p. 145.
Chakravarty, S., and C.-W. Woo, 1976, Phys. Rev. B **13**, 4815.
Chan, S.-K., and V. Heine, 1973, J. Phys. F **3**, 795.
Chihara, J., 1973, Prog. Theor. Phys. **50**, 409.
Chihara, J., 1978, Prog. Theor. Phys. **59**, 76.
Chihara, J., and K. Sasaki, 1979, Prog. Theor. Phys. **62**, 1533.

Choquard, Ph., 1978, in *Strongly Coupled Plasmas,* edited by G. Kalman (Plenum, New York), p. 347.
Cohen, E. G. D., and T. J. Murphy, 1969, Phys. Fluids **12**, 1404.
Coldwell-Horsfall, R. A., and A. A. Maradudin, 1960, J. Math. Phys. **1**, 395.
Cole, M. W., 1974, Rev. Mod. Phys. **46**, 451.
Cole, M. W., and M. H. Cohen, 1969, Phys. Rev. Lett. **23**, 1238.
Debye, P., and E. Hückel, 1923, Phys. Z. **24**, 185.
de Gennes, P. G., 1959, Physcia **25**, 825.
del Rio, F., and H. E. DeWitt, 1969, Phys. Fluids **12**, 791.
De Raedt, H., and B. De Raedt, 1978, Phys. Rev. B **18**, 2039.
Deutsch, C., Y. Furutani, and M. M. Gombert, 1976, Phys. Rev. A **13**, 2244.
Deutsch, C., Y. Furutani, and M. M. Gombert, 1981, Phys. Rep. **69**, 85.
Devreese, J. T., F. Brosens, and L. F. Lemmens, 1980, Phys. Rev. B **21**, 1349.
de Wette, F. W., 1964, Phys. Rev. **135**, A287.
DeWitt, H. E., 1976, Phys. Rev. A **14**, 1290.
DeWitt, H. E., 1978, in *Strongly Coupled Plasmas,* edited by G. Kalman (Plenum, New York), p. 81.
DeWitt, H. E., H. C. Graboske, and M. S. Cooper, 1973, Astrophys. J. **181**, 439.
DeWitt, H. E., and W. B. Hubbard, 1976, Astrophys. J. **205**, 295.
DeWitt, H. E., and Y. Rosenfeld, 1979, Phys. Lett. A **75**, 79.
Dharma-wardana, M. W. C., 1976, J. Phys. C **9**, 1919.
Dharma-wardana, M. W. C., and R. Taylor, 1980, J. Phys. F **10**, 2217.
Dolgov, O. V., D. A. Kirzhnits, and E. G. Maksimov, 1981, Rev. Mod. Phys. **53**, 81.
DuBois, D. F., 1959, Ann. Phys. (N.Y.) **8**, 24.
DuBois, D. F., and M. G. Kivelson, 1969, Phys. Rev. **186**, 409.
Ebeling, W., W. D. Kraeft, and D. Kremp, 1977, *Theory of Bound States and Ionization Equilibrium in Plasmas and Solids* (Akademie-Verlag, Berlin).
Ehrenreich, H., and M. H. Cohen, 1959, Phys. Rev. **115**, 786.
Fantoni, S., and S. Rosati, 1975, Nuovo Cimento **25**, 593.
Fasolino, A., M. Parrinello, and M. P. Tosi, 1978, Phys. Lett. A **66**, 119.
Ferrell, R. A., 1958, Phys. Rev. Lett. **1**, 443.
Feynman, R. P., 1972, *Statistical Mechanics* (Benjamin, New York).
Fisher, D. S., B. I. Halperin, and P. M. Platzman, 1979, Phys. Rev. Lett. **42**, 798.
Flowers, E., and N. Itoh, 1976, Astrophys. J. **206**, 218.
Forster, D., P. C. Martin, and S. Yip, 1968, Phys. Rev. **170**, 155.
Fried, B. D., and S. D. Conte, 1961, *The Plasma Dispersion Function* (Academic, New York).
Galam, S., and J.-P. Hansen, 1976, Phys. Rev. A **14**, 816.
Gann, R. C., S. Chakravarty, and G. V. Chester, 1979, Phys. Rev. B **20**, 326.
Geldart, D. J. W., and R. Taylor, 1970a, Can. J. Phys. **48**, 155.
Geldart, D. J. W., and R. Taylor, 1970b, Can. J. Phys. **48**, 167.
Geldart, D. J. W., and S. H. Vosko, 1966, Can. J. Phys. **44**, 2137.
Gell-Mann, and K. A. Brueckner, 1957, Phys. Rev. **106**, 364.
Gibbons, P. C., S. E. Schnatterly, J. J. Ritsko, and J. R. Fields, 1976, Phys. Rev. B **13**, 2451.
Glick, A. J., and W. F. Long, 1971, Phys. Rev. B **4**, 3455.
Glyde, H. R., G. H. Keech, R. Mazighi, and J. P. Hansen, 1976, Phys. Lett. A **58**, 226.
Golden, K. I., 1978, in *Strongly Coupled Plasmas,* edited by G. Kalman (Plenum, New York), p. 223.
Golden, K. I., and G. Kalman, 1979, Phys. Rev. A **19**, 2112.
Golden, K. I., G. Kalman, and M. B. Silevitch, 1974, Phys. Rev. Lett. **33**, 1544.
Gould, H., and G. F. Mazenko, 1975, Phys. Rev. Lett. **35**, 1455.
Gould, H., and G. F. Mazenko, 1977, Phys. Rev. A **15**, 1274.
Graboske, H. C., J. B. Pollack, A. S. Grossman, and R. J. Olness, 1975, Astrophys. J. **199**, 265.
Grandey, R. A., 1978, in *Strongly Coupled Plasmas,* edited by G. Kalman (Plenum, New York), p. 427.
Grimes, C. C., 1978, Surf. Sci. **73**, 397.
Grimes, C. C., and G. Adams, 1979, Phys. Rev. Lett. **42**, 795.
Gupta, A. K., P. K. Aravind, and K. S. Singwi, 1978, Solid State Commun. **26**, 49.
Hansen, J. P., 1973, Phys. Rev. A **8**, 3096.
Hansen, J. P., 1978, in *Strongly Coupled Plasmas,* edited by G. Kalman (Plenum, New York), p. 117.
Hansen, J. P., D. Levesque, and J. J. Weis, 1979, Phys. Rev. Lett. **43**, 979.
Hansen, J. P., and I. R. McDonald, 1976, *Theory of Simple Liquids* (Academic, New York).
Hansen, J. P., I. R. McDonald, and E. L. Pollock, 1975, Phys. Rev. A **11**, 1025.
Hansen, J. P., E. L. Pollock, and I. R. McDonald, 1974, Phys. Rev. Lett. **32**, 277.
Hansen, J. P., G. M. Torrie, and P. Vieillefosse, 1977, Phys. Rev. A **16**, 2153.
Hansen, J. P., and P. Vieillefosse, 1976, Phys. Rev. Lett. **37**, 391.
Hasegawa, M., 1971, J. Phys. Soc. Jpn. **31**, 649.
Hasegawa, M., and M. Watabe, 1969, J. Phys. Soc. Jpn. **27**, 1393.
Hedin, L., 1965, Phys. Rev. **139**, 796 A.
Hockney, R. W., and T. R. Brown, 1975, J. Phys. C. **8**, 1813.
Höhberger, H. J., A. Otto, and E. Petri, 1975, Solid State Commun. **16**, 175.
Hohenberg, P., and W. Kohn, 1964, Phys. Rev. **136**, 864 B.
Holas, A., P. K. Aravind, and K. S. Singwi, 1979, Phys. Rev. B **20**, 4912.
Hubbard, J., 1958, Proc. R. Soc. London, Ser. A **243**, 336.
Hubbard, J., 1967, Phys. Lett. A **25**, 709.
Hubbard, W. B., and M. Lampe, 1969, Astrophys. J. Suppl. **18**, 297.
Hubbard, W. B., and W. L. Slattery, 1971, Astrophys. J. **168**, 131.
Ichimaru, S., 1970, Phys. Rev. A **2**, 494.
Ichimaru, S., 1973, *Basic Principles of Plasma Physics* (Benjamin, Reading, Mass.).
Ichimaru, S., 1977, Phys. Rev. A **15**, 744.
Ichimaru, S., 1978, in *Strongly Coupled Plasmas,* edited by G. Kalman (Plenum, New York), p. 187.
Ichimaru, S., H. Iyetomi, and K. Utusmi, 1982, Phys. Rev. B **25**, 1374.
Ichimaru, S., and K. Tago, 1981, J. Phys. Soc. Jpn. **50**, 409.
Ichimaru, S., and T. Tange, 1974, Phys. Rev. Lett. **32**, 102, 569 E.
Ichimaru, S., H. Totsuji, T. Tange, and D. Pines, 1975, Prog. Theor, Phys. **54**, 1077.
Ichimaru, S., and K. Utsumi, 1981, Phys. Rev. B **24**, 7385.
Isihara, A., 1972, Phys. Konden. Mater. **15**, 225.
Isihara, A., and E. W. Montroll, 1971, Proc. Nat. Acad. Sci. USA **68**, 3111.
Itoh, N., and S. Ichimaru, 1977, Phys. Rev. A **16**, 2178.
Itoh, N., and S. Ichimaru, 1979, Phys. Rev. A **19**, 2476.
Itoh, N., and S. Ichimaru, 1980a, Phys. Rev. A **22**, 1318.

Itoh, N., and S. Ichimaru, 1980b, Phys. Rev. B **22**, 1459.
Itoh, N., S. Ichimaru, and S. Nagano, 1978, Phys. Rev. B **17**, 2862.
Itoh, N., H. Totsuji, and S. Ichimaru, 1977, Astrophys. J. **218**, 477 [Erratum: Astrophys. J. **220**, 742 (1978)].
Itoh, N., H. Totsuji, S. Ichimaru, and H. E. DeWitt, 1979, Astrophys. J. **234**, 1079 [Erratum: Astrophys. J. **239**, 414 (1980)].
Ivanov, Yu. V., V. B. Mintsev, V. E. Fortov, and A. N. Dremin, 1976, Zh. Eksp. Teor. Fiz **71**, 216 [Sov. Phys.—JETP **44**, 112 (1976)].
Iyetomi, H., and S. Ichimaru, 1982a, Phys. Rev. A **25**, 2434.
Iyetomi, H., and S. Ichimaru, 1982b, to be published.
Iyetomi, H., K. Utsumi, and S. Ichimaru, 1981a, Phys. Rev. B **24**, 3226.
Iyetomi, H., K. Utsumi, and S. Ichimaru, 1981b, J. Phys. Soc. Jpn. **50**, 3769.
Iyetomi, H., K. Utsumi, and S. Ichimaru, 1981c, J. Phys. Soc. Jpn. **50**, 3778.
Jancovici, B., 1977, J. Stat. Phys. **17**, 357.
Jindal, V. K., H. B. Singh, and K. N. Pathak, 1977, Phys. Rev. B **15**, 252.
Kalia, R. K., P. Vashishta, and S. W. de Leeuw, 1981, Phys. Rev. B **23**, 4794.
Kalman, G., 1978, in *Strongly Coupled Plasmas,* edited by G. Kalman (Plenum, New York), p. 141.
Keiser, G., and F. Y. Wu, 1972, Phys. Rev. A **6**, 2369.
Kimball, J. C., 1973, Phys. Rev. A **7**, 1648.
Kimball, J. C., 1976, Phys. Rev. B **14**, 2371.
Kleinman, L., 1967, Phys. Rev. **160**, 585.
Kleinman, L., 1968, Phys. Rev. **172**, 383.
Kloos, T., 1973, Z. Phys. **265**, 225.
Kohn, W., and L. J. Sham, 1965, Phys. Rev. **140**, 1133 A.
Krane, K. J., 1978, J. Phys. F **8**, 2133.
Kubo, R., 1957, J. Phys. Soc. Jpn. **12**, 570.
Kugler, A. A., 1975, J. Stat. Phys. **12**, 35.
Landau, L. D., and E. M. Lifshitz, 1959, *Fluid Mechanics* (Pergamon, London).
Langreth, D. C., 1969, Phys. Rev. **181**, 753.
Lantto, L. J., 1980, Phys. Rev. B **22**, 1380.
Lee, D. K., and F. H. Ree, 1972, Phys. Rev. A **6**, 1218.
Lieb, E. H., and H. Narnhofer, 1975, J. Stat. Phys. **12**, 291.
Lieb, E. H., and H. Narnhofer, 1976, J. Stat. Phys. **14**, 465.
Lindhard, J., 1954, K. Dan. Vidensk. Selsk. Mat.-Fys. Medd. (8) **28**, 1.
Lowy, D. N., and G. E. Brown, 1975, Phys. Rev. B **12**, 2138.
Lundqvist, B. I., 1968, Phys. Konden. Mater. **7**, 117.
Mandal, S. S., B. K. Rao, and D. N. Tripathy, 1978, Phys. Rev. B **18**, 2524.
Martin, P. C., 1967, Phys. Rev. **161**, 143.
Mazenko, G., 1974, Phys. Rev. A **9**, 360.
Mermin, N. D., 1965, Phys. Rev. **137**, 1441 A.
Mermin, N. D., 1970, Phys. Rev. B **1**, 2362.
Metropolis, N., A. W. Rosenbluth, M. N. Rosenbluth, A. H. Teller, and E. Teller, 1953, J. Chem. Phys. **21**, 1087.
Minoo, H., C. Deutsch, and J. P. Hansen, 1976, Phys. Rev. A **14**, 840.
Misawa, S., 1968, Prog. Theor. Phys. **39**, 1426.
Mitler, H. E., 1977, Astrophys. J. **212**, 513.
Mitra, S. K., and S. Sjödin, 1978, J. Phys. C **11**, 2655.
Monnier, R., 1972, Phys. Rev. A **6**, 393.
Morf, R. H., 1979, Phys. Rev. Lett. **43**, 931.
Mori, H., 1965a, Prog. Theor. Phys. **33**, 423.
Mori, H., 1965b, Prog. Theor. Phys. **34**, 399.
Morita, T., 1960, Prog. Theor. Phys. **23**, 829.
Mukhopadyay, G., and A. Sjölander, 1978, Phys. Rev. B **17**, 3589.
Mukhopadhyay, G., R. K. Kalia, and K. S. Singwi, 1975, Phys. Rev. Lett. **34**, 950.
Nagano, S., and S. Ichimaru, 1980, J. Phys. Soc. Jpn. **49**, 1260.
Ng, K. C., 1974, J. Chem. Phys. **61**, 2680.
Niklasson, G., 1974, Phys. Rev. B **10**, 3052.
Norman, G. E., and A. N. Starostin, 1970, Teplofiz. Vys. Temp. **8**, 413 [High Temp. Phys. (USSR) **8**, 381].
Nozières, P., and D. Pines, 1958, Phys. Rev. **111**, 442.
Nozières, P., and D. Pines, 1959, Phys. Rev. **113**, 1254.
O'Neil, T., and N. Rostoker, 1965, Phys. Fluids **8**, 1109.
Overhauser, A. W., 1968, Phys. Rev. **167**, 691.
Pathak, K. N., and P. Vashishta, 1973, Phys. Rev. B **7**, 3649.
Percus, J. K., 1964, in *The Equilibrium Theory of Classical Fluids,* edited by H. L. Frisch and J. L. Lebowitz (Benjamin, New York), II-33.
Percus, J. K., and G. J. Yevick, 1958, Phys. Rev. **110**, 1.
Pines, D., 1964, *Elementary Excitations in Solids* (Benjamin, New York).
Pines, D., 1966, in *Quantum Fluids,* edited by D. F. Brewer (North-Holland), p. 257.
Pines, D., and P. Nozières, 1966, *The Theory of Quantum Liquids* (Benjamin, New York), Vol. I.
Platzman, P. M., and P. Eisenberger, 1974, Phys. Rev. Lett. **33**, 152.
Pollock, E. L., and J. P. Hansen, 1973, Phys. Rev. A **8**, 3110.
Priftis, G. D., and J. Boviatsis, 1981, Phys. Stat. Sol. B **104**, 673.
Puff, R. D., 1965, Phys. Rev. **137**, 406 A.
Raether, H., 1980, *Excitations of Plasmons and Interband Transitions by Electrons* (Springer, Berlin).
Rice, S. A., and P. Gray, 1965, *The Statistical Mechanics of Simple Liquids* (Interscience, New York).
Rosenfeld, Y., and N. W. Ashcroft, 1979, Phys. Rev. A **20**, 1208.
Ross, M., and D. Seale, 1974, Phys. Rev. A **9**, 396.
Salpeter, E. E., 1954, Aust. J. Phys. **7**, 373.
Salpeter, E. E., 1973, Astrophys. J. Lett. **181**, L83.
Salpeter, E. E., and H. M. Van Horn, 1969, Astrophys. J. **155**, 183.
Sander, L. M., J. H. Rose, and H. B. Shore, 1980, Phys. Rev. B **21**, 2739.
Schatzman, E., 1958, *White Dwarfs* (North-Holland, Amsterdam).
Schatzman, E., 1978, in *Strongly Coupled Plasmas,* edited by G. Kalman (Plenum, New York), p. 407.
Schatzman, E., 1980, J. Phys. (Paris) Suppl. **41**, C2-89.
Schneider, T., 1971, Physica **52**, 481.
Schneider, T., R. Brout, H. Thomas, and J. Feder, 1970, Phys. Rev. Lett. **25**, 1423.
Shaw, R. W., 1970, J. Phys. C **3**, 1140.
Singwi, K. S., 1976, in *Linear and Nonlinear Electron Transport in Solids,* edited by J. T. Devreese and V. E. van Doren (Plenum, New York), p. 163.
Singwi, K. S., A. Sjölander, M. P. Tosi, and R. H. Land, 1970, Phys. Rev. B **1**, 1044.
Singwi, K. S., and M. P. Tosi, 1981, in *Solid State Physics,* edited by H. Ehrenreich, F. Seitz, and D. Turnbull (Academic, New York), Vol. 36, p. 177.
Singwi, K. S., M. P. Tosi, R. H. Land, and A. Sjölander, 1968, Phys. Rev. **176**, 589.
Sjödin, S., and S. K. Mitra, 1977, J. Phys. A **10**, L163.
Sjögren, L., and A. Sjölander, 1978, Ann. Phys. (N.Y.) **110**, 122.
Sjölander, A., 1978, in *Strongly Coupled Plasmas,* edited by G. Kalman (Plenum, New York), p. 61.

Slattery, W. L., G. D. Doolen, and H. E. DeWitt, 1980, Phys. Rev. A **21**, 2087.
Springer, J. F., M. A. Pokrant, and F. A. Stevens, 1973, J. Chem. Phys. **58**, 4863.
Stevens, F. A., and M. A. Pokrant, 1973, Phys. Rev. A **8**, 990.
Stevenson, D. J., 1975, Phys. Rev. B **12**, 3999.
Stevenson, D. J., 1980, J. Phys. (Paris) Suppl. **41**, C2-53.
Stevenson, D. J., and N. W. Ashcroft, 1974, Phys. Rev. A **9**, 782.
Stevenson, D. J., and E. E. Salpeter, 1977, Astrophys. J. Suppl. **35**, 221.
Strum, K., 1976, Z. Phys. B **25**, 247.
Sturm, K., 1977, Z. Phys. B **28**, 1.
Sturm, K., 1978a, Solid State Commun. **25**, 797.
Sturm, K., 1978b, Z. Phys. B **29**, 27.
Tago, K., K. Utsumi, and S. Ichimaru, 1981, Prog. Theor. Phys. **65**, 54.
Taylor, R., 1978, J. Phys. F **8**, 1699.
Takeno, S., and F. Yoshida, 1979, Prog. Theor. Phys. **62**, 883.
Toigo, F., and T. O. Woodruff, 1970, Phys. Rev. B **2**, 3958.
Toigo, F., and T. O. Woodruff, 1971, Phys. Rev. B **4**, 371.
Totsuji, H., 1978, Phys. Rev. A **17**, 399.
Totsuji, H., and S. Ichimaru, 1973, Prog. Theor. Phys. **50**, 753.
Totsuji, H., and S. Ichimaru, 1974, Prog. Theor. Phys. **52**, 42.
Totsuju, H., and H. Kakeya, 1980, Phys. Rev. A **22**, 1220.
Tripathy, D. N., and S. S. Mandal, 1977, Phys. Rev. B **16**, 231.
Utsumi, K., and S. Ichimaru, 1980a, Phys. Rev. B **22**, 1522.
Utsumi, K., and S. Ichimaru, 1980b, Phys. Rev. B **22**, 5203.
Utsumi, K., and S. Ichimaru, 1981a, Phys. Rev. B **23**, 3291.
Utsumi, K., and S. Ichimaru, 1981b, Phys. Rev. B **24**, 3220.
Van Horn, H. M., 1967, Phys. Rev. **157**, 342.
Van Horn, H. M., 1980, J. Phys. (Paris) Suppl. **41**, C2-97.
Van Horn, H. M., and E. E. Salpeter, 1967, Phys. Rev. **157**, 751.
van Leeuwen, J. M. J., J. Groeneveld, and J. De Boer, 1959, Physica **25**, 792.
Vashishta, P., and K. S. Singwi, 1972, Phys. Rev. B **6**, 875.
Vlasov, A. A., 1938, Zh. Eksp. Teor. Fiz. **8**, 291.
Vosko, S. H., L. Wilk, and M. Nusair, 1980, Can. J. Phys. **58**, 1200.
Wallenborn, J., and M. Baus, 1978, Phys. Rev. A **18**, 1737.
Widom, B., 1963, J. Chem. Phys. **39**, 2803.
Wigner, E. P., 1934, Phys. Rev. **46**, 1002.
Wigner, E. P., 1938, Trans. Faraday Soc. **34**, 678.
Yasuhara, H., 1972, Solid State Commun. **11**, 1481.
Yasuhara, H., 1974, J. Phys. Soc. Jpn. **36**, 361.
Yoshida, F., S. Takeno, and H. Yasuhara, 1980, Prog. Theor. Phys. **64**, 40.
Zabolitzky, J. G., 1980, Phys. Rev. B **22**, 2353.
Zacharias, P., 1975, J. Phys. F **5**, 645.
Ziman, J. M., 1961, Philos. Mag. **6**, 1013.
Zwanzig, R., 1961, in *Lectures in Theoretical Physics,* edited by W. Brittin and L. Dunham (Interscience, New York), Vol. 3, p. 135.
Zwanzig, R., and M. Bixon, 1970, Phys. Rev. A **2**, 2005.